UNIVERSIDADE DE LISBOA

INSTITUTO SUPERIOR TÉCNICO

FEEDSTOCK RECYCLING OF PLASTIC WASTE

Rita Duarte Kol de Carvalho

Thesis to obtain the Master of Science Degree in

Chemical Engineering

Supervisor: Professor Maria Amélia Nortadas Duarte de Almeida Lemos

Co-supervisor: Professor Francisco Manuel da Silva Lemos

Examination Committee

President: Professor Carlos Manuel Faria de Barros Henriques

Supervisor: Professor Maria Amélia Nortadas Duarte de Almeida Lemos

Vogal: José Manuel Félix Madeira Lopes

July 2019

[This page was left in blank.]

Acknowledgments

I would like to start the acknowledgments to Professor Maria Amélia Lemos and Professor Francisco Lemos. I am very grateful for the opportunity to work on this Thesis and I would like to thank the Professors for all the support and knowledge they provided me with. I would also like to thank them for the opportunity and confidence they deposited in me to participate at the International Conference on Chemical Kinetics (ICCK). It was a great experience not only at academic and professional level, but also at a personal level.

I would also like to thank my family, especially my mother Vanda Duarte, for all the support, patience and daily encouragement and my father Nuno Kol de Carvalho, who supported and motivated me and was always present despite the distance.

I would also thank my boyfriend Daniel Almeida for all the support, constant motivation, patience and daily kind words. And for always making me believe that I could do it.

My next acknowledgement goes to my colleague Patrícia Pereira for all the mutual help, motivation and encouragement throughout this work and during ICCK.

I would like to thank Dr. Eng. Bruna Rijo as well, for all the help and knowledge shared during this work.

My next acknowledgements goes to Tiago Godinho and John Torres, who were not only my colleagues at the laboratory but also at ICCK. I thank them for all the support and help. To my colleague at the laboratory Marta Martins goes also a big thank for all the help and daily conversations.

I would also like to thank Professor Teresa Carvalho and Francisca Rey for the sample preparation.

Finally, I would like to thank the financial support that permitted my participation in ICCK by Fundação para a Ciência e a Tecnologia (FCT) and Centro de Recursos Naturais e Ambiente (CERENA).

[This page was left in blank.]

Abstract

The thermal pyrolysis of polystyrene (PS) and acrylonitrile-butadiene-styrene (ABS) from waste of electrical and electronic equipment (WEEE) was investigated by thermogravimetric analysis coupled with differential scanning calorimetry (TG/DSC). The experiments were performed under dynamic and isothermal conditions in inert atmosphere. Virgin PS with two different molecular weight distributions were studied and compared to waste PS. The thermal degradation of the waste plastics under air was studied as well.

The TG results showed that the decomposition of waste PS occurs at higher temperatures than that of virgin PS. Waste polystyrene showed two degradation peaks, while virgin PS presented only one. Waste ABS decomposes in two degradation peaks as well. The TG results were used to study the kinetics of the decomposition of virgin PS and of waste plastic. The degradation of virgin PS is well described by a one component degradation model. The degradation of waste PS and ABS is well described by a two pseudo-component degradation model.

The pyrolysis of PS in a bench-scale reactor was also studied and compared with virgin polystyrene. The products were analysed using gas chromatography. In terms of liquid yield, both PS samples produce in majority hydrocarbons in the range of C_7 to C_9, which may be used as feedstock for the chemical industry. C_8 hydrocarbons are produced in higher quantity and are mostly constitute by styrene. These results show the possibility of the introduction of waste PS in a Circular Economy approach.

Keywords: Circular Economy, Thermal Pyrolysis, WEEE plastic, Polystyrene, Acrylonitrile-butadiene-styrene, Kinetic model

[This page was left in blank.]

Resumo

A pirólise térmica de poliestireno (PS) e acrilonitrila-butadieno-estireno (ABS) proveniente dos resíduos de equipamento elétrico e eletrónico (REEE) foi analisada recorrendo à análise simultânea de termogravimetria (TG) e análise de calorimetria diferencial de varrimento (DSC). Os ensaios foram realizados em condições dinâmicas e isotérmicas sob azoto. A degradação térmica sob ar destes dois plásticos também foi analisada. Duas amostras de poliestireno virgem com diferentes massas molares foram estudados e comparados com o resíduo de PS.

Os resultados do TG mostram que o resíduo PS se degrada a temperaturas mais altas que o PS virgem. O PS virgem apresenta um único pico de degradação enquanto o resíduo apresenta dois. O resíduo ABS também apresenta dois picos de degradação. Os resultados do TG foram usados para estudar a cinética de degradação dos plásticos. O modelo considerando a degradação de um único componente descreve adequadamente os dados experimentais das duas amostras de PS virgens. A degradação dos resíduos ABS e PS é bem descrita com um modelo que considera a degradação de dois pseudo-componentes.

A pirólise do PS virgem e resíduo foi também estudada num reator de bancada. Os produtos foram analisados através de cromatografia gasosa. Em termos de produtos líquidos, ambas as amostras PS produzem essencialmente hidrocarbonetos na gama do C_7 a C_9, que poderão ser usados como matéria-prima na indústria química. Em maior quantidade são produzidos hidrocarbonetos C_8 principalmente estireno. Assim, o resíduo de PS poderá ser introduzido no conceito de economia circular.

Palavras-chave: Economia Circular, Pirólise térmica, REEE plásticos, Poliestireno, Acrilonitrila-butadieno-estireno, Modelos cinéticos

[This page was left in blank.]

1. Table of content

List of Figures

List of Tables

[This page was left in blank.]

List of Equations

[This page was left in blank.]

Abbreviations

ABS - Acrylonitrile Butadiene Styrene

DSC – Differential Scanning Calorimetric

DTG – Differential Thermogravimetry

EEE – Electric and Electronic Equipment

EPS - Expanded Polystyrene

EU – European Union

GC – Gas Chromatography

HIPS - High-Impact Polystyrene

MSW – Municipal Solid Waste

MW – Molecular Weight

PBB - Polybrominated Biphenyls

PCR – Post-Consumer Recycled

PBDE - Polybrominated Diphenyl oxide

PE – Polyethylene

PET - Polyethylene terephthalate

PP - Polypropylene

PS – Polystyrene

PS1 – Virgin polystyrene with MW ~192 000

PS2 - Virgin polystyrene with MW ~350 000

TBBPA - Tetrabromobisphenol A

TBPE - 1,2 – Bistribromophenoxyethane

TDI - Toluene diisocyanates

TGA – Thermogravimetric Analysis

Tmax – Maximum temperature of degradation

Tonset – Initial temperature of weight loss

OPS – Oriented polystyrene

SAN - Styrene-acrylonitrile

SBR – Styrene-butadiene rubber

UPR - Unsaturated polyester resins

VOC - Volatile Organic Compounds

WEEE – Waste of Electric and Electronic Equipment

XPS - Extruded Polystyrene

[This page was left in blank.]

1. Introduction

1.1 Motivation and Objective

The world population is observing in the front line the environmental impact of plastic waste generation. “Ocean of plastic” is a concern nowadays and the society is becoming more aware of the excessive consumption of plastic. Due to plastic’s versatility and attractive qualities for a wide range of consumer and industrial application, the world plastic production has increased in the last 20 years nearly 200-fold. Linked with the increasing production is the plastic waste generation that is turning the plastic waste management into a critical issue. The waste of electrical and electronic equipment (WEEE) is currently considered to be one of the fastest growing waste streams in Europe, growing at 3 – 5 % per year. [1] In 2015, the quantity of WEEE amounted to 9.5 million tonnes, of which 1.2 million tonnes were plastic materials. [2] The European recycling industry is capable to recycle over 50 % of the plastic materials derived from WEEE into Post-Consumer Recycled (PCR) plastics. The remaining plastic materials can be used for incineration with energy recovery. [2] The challenge of recycling WEEE plastics lies on the complicated recycling process due to the existence of diverse plastic materials and additives, like flame retardants, colouring compounds, antioxidants, UV stabilizers, among others. [2,3] In this context, feedstock recycling, also known as chemical recycling is an attractive option for plastic waste management due to its particularity of converting plastic waste into valuable feedstock for the chemical industry. This technique allows also the treatment of mixed and unwashed plastic waste. Plus, it favours the introduction of plastic waste into a Circular Economy approach that focus on the minimization of waste by replacing the end-of-life concept of waste. [4]

Pyrolysis is a process that can be used in feedstock recycling and is a process of chemical and thermal decomposition of a material at high temperatures and in the absence of oxygen, leading to smaller molecules. The products generated by pyrolysis, such as solids (char), liquid (oil) and non-condensable gases, can be used as fuels, petrochemicals and monomers. [4,5]

In this context, the objective of this Thesis is to study the pyrolysis of ABS and PS plastics present in waste of electrical and electronic equipment, with four specific goals:

- Study of the thermal degradation of PS and ABS using the TG/DSC analysis.
- Estimation of the reaction kinetic parameters using a mechanistic model.
- Characterization of the products obtained by the thermal pyrolysis performed in a bench-scale reactor.
- Evaluation of the introduction of waste PS in a Circular Economy approach.

1.2 Organization of the Thesis

The Thesis is organized into five chapters, starting with an introduction of this Thesis, a literature review of the critical aspects for the development of the work, the experimental methodology used, discussion of the results, conclusion and future perspectives.

[This page was left in blank.]

2. Literature Review

2.1 Plastics

2.1.1 Plastic classification

Plastics is the term commonly used to describe synthetic or natural materials made from polymers.[4] Polymers are macromolecules that are composed of smaller units, monomers, which react together to form a long chain. These monomers can be identical and in this case the polymer is named by prefixing “poly” to the name of the monomer from which it is derived, for example, the polymer from styrene is polystyrene.

Polymers may be produced synthetically from simple starting materials by addition polymerisation or condensation polymerization [6] In addition polymerisation, monomers react to form a polymer, and no side products are formed. [6] Some examples produced by this type of technique are: polyethylene and polystyrene, among others. In condensation polymerisation usually, elimination of water occurs. One example are polyamides.

Plastics are divided into two categories: thermoplastics and thermosets. The thermoplastics can be heated and reformed repeatedly. Some examples of thermoplastics are polypropylene (PP), polyethylene (PE), polyethylene terephthalate (PET), polystyrene (PS) and acrylonitrile-butadiene-styrene (ABS). The other group, the thermosets, cannot be reheated. Once these plastics are formed, reheating will cause the material to decompose rather than melt. Some thermosets plastics are polyurethane (PUR) and epoxy resins. [7]

Plastic show some common characteristic properties, such as[4]:

- An amorphous, i.e. non-crystalline structure related to the disorder among polymer chains;
- Low thermal conductivity;
- High electrical resistance;
- Low softening temperatures;
- Viscous-elastic behaviour.

2.1.2 Plastic Production

Worldwide the plastic production has increased since 1950 from 2 million tonnes [8] to 348 million tonnes in 2017 [7]. China is the country representing the major production (29 %) followed by the rest of Asia (21 %) and with Europe (EU) in third place (18 %), (see Figure 2.1). Within Europe, with a total demand for plastics of 51.2 million tonnes in 2017[8], Germany was the country with the highest plastic demand, followed by Italy and France, Figure 2.1.

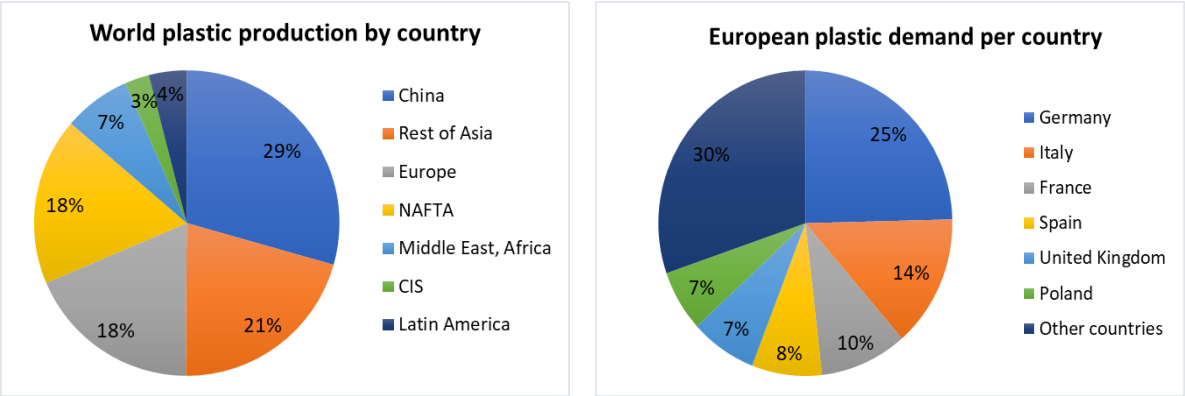

Figure 2.1 - World plastic production by country (total of 348 million tonnes in 2017) and European plastic demand per country (total of 51.2 million tonnes in 2017). [8]

Within the European market, the market sector that had in 2017 the highest demand for plastic is the packaging market, with 40 % of the total plastic demand. The building & construction market sector and automotive sector are the followers, representing 20 % and 10 %, respectively, of the total demand. The total quantity of plastics used to produce electric and electronic products amounted in 2017 ca. 3 million tonnes, representing 6 % of the total demand for plastics in Europe, Figure 2.2.

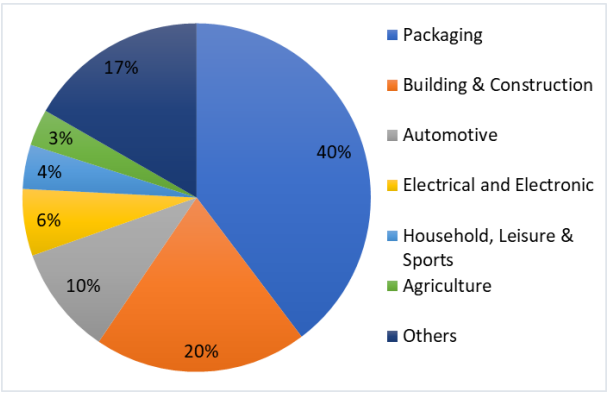

Figure 2.2 – Distribution of the European plastic demand by market sector, in 2017, for a total of 51.2 million tonnes. [7]

2.1.3 Plastic Waste Management

Linked with the increase of plastic production is the increase of plastic waste. The waste stream of electric and electronic equipment waste is currently considered to be one of the fastest growing waste streams in the EU, growing at 3 – 5 % per year. [1] WEEE embraces diverse forms of electric and electronic equipment that are at the end of their lives or have been discarded by their owners.[9] In 2015 in Europe, the quantity of waste from electric and electronic equipment amounted to some 9.5 million tonnes per year.[2] About 1.2 million tonnes were plastic material, composed in majority by high-impact polystyrene (HIPS) (27 %) and acrylonitrile-butadiene-styrene (ABS) (24 %), Figure 2.3.

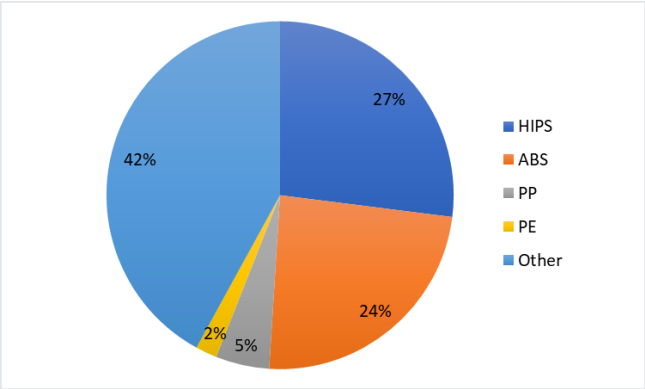

Figure 2.3 - Composition of WEEE (total of 1.2 million tonnes in 2015 in Europe). HIPS = high impact polystyrene; ABS = acrylonitrile – butadiene – styrene; PP = polypropylene; PE = polyethylene; Others include polystyrene, HIPS and ABS with flame retardants, polycarbonate ABS, polyvinyl chloride, poly(phenyl oxide), etc. [2]

There are four options available in the management of WEEE plastics: landfilling, mechanical recycling, energy recycling and feedstock recycling[9]:

- Landfilling refers to roughly bury waste under layers of earth. However, it has some disadvantages as excessive land utilization, soil and groundwater contamination, air pollution, disruption of wildlife and emission of harmful greenhouse gases.[9]
- Mechanical recycling involves reprocessing of WEEE plastic to form new similar plastic product with nearly the same or less performance level than the original products. Mechanical reformation of plastic involves a series of steps that include sorting, grinding, washing, drying and granulation. The granules can be moulded to various forms via extrusion and other techniques.[9,10]
- Incineration is a conventional technique to recover energy from waste plastics, involving combustion of the material in the presence of oxygen or air to recover energy that can be used for heating or electric power generation. However, based on the type and composition of the plastic waste, it can lead to the emission of toxic volatile organic compounds (VOCs),among other contaminants. [11]
- Chemical recycling is known as tertiary recycling with basic idea of converting plastics into fuels, original monomers or other valuable chemicals. [9,10]

The European recycling industry is capable to recycle over 50 % of the plastic materials derived from WEEE into Post-Consumer Recycled (PCR) plastics. The remaining plastic materials can be used for incineration with energy recovery. The challenge of recycling WEEE plastics lies on the complicated recycling process due to the existence of diverse plastic materials and the presence of additives that are often hazardous and can change the material properties such as colour, melting point, flammability and density. These additives may be pigments (e.g., TiO_2, ZnO, Cr_2O_3, Fe_2O_3, Cd), flame retardants (often brominated organics, such as polybrominated diphenyl oxide (PBDE), polybrominated biphenyls (PBB), 1,2 - Bistribromophenoxyethane (TBPE) and Tetrabromobisphenol A (TBBPA)[12,13]), antioxidants, UV stabilizers or plasticizers (e.g. compounds of Ba, Cd, Pb, Sn and Zn).[2,14–16] It is difficult to achieve to the separation of sufficiently pure polymers that are suitable for further treatment.

2.1.4 Polystyrene and Acrylonitrile-butadiene-styrene

Polystyrene (PS) plastic is a transparent thermoplastic. It is available as a typical solid plastic, with applications in medical devices, CD cases, as well as in the form of a rigid foam material. The foam form of PS is used most often in the packaging industry.[17] Polystyrene is hard and brittle with low impact strength.[18]

Polystyrene is typically a synthetic aromatic hydrocarbon homopolymer produced by the polymerization of styrene, Figure 2.4.

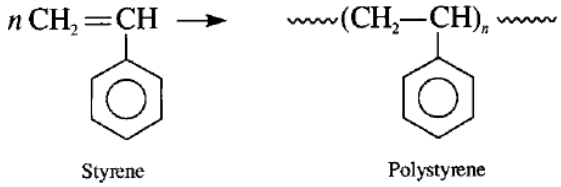

Figure 2.4 - Polymerization of styrene leads to polystyrene.[6]

Three major types of polystyrene include polystyrene foam, regular polystyrene plastic and polystyrene film. Amongst the different types of foam are expanded polystyrene (EPS) and extruded polystyrene (XPS). Some types of polystyrene plastics are copolymers. Often the homopolymer PS is modified by adding a polybutadiene rubber phase to improve the impact resistance, known in this form as high impact polystyrene (HIPS).[19] Polystyrene films can be stretched into oriented polystyrene (OPS). [18]

HIPS is a composite material consisting of a PS phase and a dispersed polybutadiene (PB) rubber phase. Polybrominated compounds and antimony trioxide (Sb_2O_3) are synergistic flame retardant combinations that are frequently added to HIPS.[19,20]

To facilitate the identification of the plastics used at different applications, for recycling purposes, they are classified by “Plastic Identification Codes”. The polystyrene identification code is shown in Figure 2.5.

Figure 2.5 - Polystyrene recycling identification code. [10]

Acrylonitrile-butadiene-styrene (ABS) is a synthetic copolymer thermoplastic produced by the polymerization of styrene, acrylonitrile and polybutadiene, Figure 2.6. The properties of ABS are based on the proportions of the three monomers. Typically, the composition is about 50 % styrene and the rest is balanced between butadiene and acrylonitrile. ABS has good mechanical properties, chemical resistance, good processing characteristics and relatively low cost. ABS is used in cases for electrical devices, parts for automotive, aircraft applications, toys, furniture, etc. [21–23]

On the other hand, the high flammability of ABS limits its application where a controlled reaction to fire is required. In these cases, flame retardant additives are added to ABS. The most used flame retardant are halogenated compounds. [24]

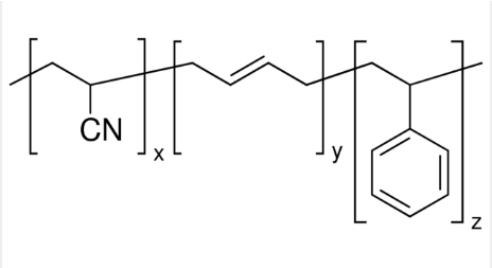

Figure 2.6 - Structure of ABS. x – acrylonitrile, y – butadiene, z - styrene.[22]

Its plastics identification code is depicted in Figure 2.7.

Figure 2.7 - ABS recycling identification code.[25]

Table 2.1 presents the main properties of both polymers, PS and ABS.

Table 2.1 - PS and ABS properties.

Polymer	Density (g/mL) KG/M3	Glass transition temperature (ºC)	Specific Heat Capacity (J/gºC)	Melt temperature (ºC)	Thermal conductivity (W/mK)
PS[26,27]	0.0130-1.18	83.0 - 100	1.2-1.5	170 - 280	0.170
ABS[28]	0.882-3.50	105 – 109	1.96 – 2.13	149 – 323	0.128-0.187

2.2 Chemical Recycling

Chemical, or feedstock recycling is an innovative technology where post-consumer plastic waste is converted into valuable chemical that can be used as fuel or raw materials by the chemical industry. These technology includes pyrolysis, gasification, chemical depolymerization, catalytic cracking & reforming and hydrocracking [29]

Pyrolysis is a process of chemical and thermal decomposition, generally leading to smaller molecules. It can be conducted at various temperature levels, reaction times, pressures and in the presence or absence of reactive gases or liquids, and of catalysts. The thermal decomposition of plastics can be proceeded at low (< 400 ºC), medium (400-600 ºC) or high temperature (> 600 ºC). Most commonly the pressure is atmospheric. The pyrolysis leads to gases, liquid products called pyrolytic oil and a small amount of solid carbonaceous residue called char, which can be applied as fuel, petrochemicals and monomers. [4]

Pyrolysis processes involve breaking bonds and are often endothermic. The onset of the pyrolysis reaction is strongly influenced by the presence of additives, such as stabilizers, plasticizers and pigments. The required reaction time is determined principally by the reaction temperature. The formation of primary products, e.g. monomers, is favoured by short times, the formation of more thermodynamically stable products (H_2, CH_4, aromatics, carbon) by long ones. [4] The product yield can vary depending on the polymer type and the operation conditions. [9] High temperature (>600 ºC) favour

the production of simple small gaseous molecules; low temperature (<400 ºC) leads to more viscous liquid products.[4]

The major factors of influence determining the product distribution resulting from the plastic pyrolysis are summarized in Table 2.2.

Table 2.2 - Factors affecting pyrolysis products distribution.[4]

Factor of influence	Effect
Chemical composition of the resin	The primary products from pyrolysis are directly related with the chemical structure and composition of the polymer, and also to the mechanism of its decomposition (thermal or catalytic).
Temperature and heating rate	High operation temperatures and heating rates enhance bond breaking and favour the production of small molecules.
Time	Longer residence times favours a secondary conversion of the primary products, yielding more coke, tar, as well as thermally stable products.
Reactor type	Determines the quality of heat transfer, mixing, gas and liquid phase residence times and the escape of primary products. Most used are: semibatch/batch, fixed bed and fluidized bed.
Operating atmosphere	The presence of reactive gases, such as air, influences the mechanism of degradation.
Operating pressure	Low pressure favours the production of primary products.
Use of catalysts	Influences kinetics and mechanism of degradation, and hence, the product distribution.
Presence of additives	The additives generally evaporate or decompose. Some may influence kinetics and mechanism.

The thermal degradation of plastics, including kinetics factors and mechanism, can be investigated using different techniques, such as thermogravimetry linked with differential scanning calorimetry (see Chapter 2.5 Thermogravimetry analysis (TGA) and differential scanning calorimetry (DSC)). From the TG analysis it is possible to determine the behaviour of the sample with respect to time, temperature and heating rate and to determine the optimum temperature range for degradation. This information is useful for the design of reactor where the thermal decomposition of the solid takes place.

2.3 Pyrolysis of PS

2.3.1 Thermogravimetric analysis

Various thermogravimetric studies on the thermal degradation of polystyrene were performed by other authors. Table 2.3 summarizes the results of these thermogravimetric studies. Regarding the decomposition under inert atmosphere, different researchers conclude that virgin polystyrene decomposes with one single peak. [30–32] The onset temperature varies between 276.00 ºC and 340.85 ºC and the maximum degradation temperature between 379.85 ºC and 413.85 ºC. [30–32] When applying different heating rates still one decomposition peak is visible and only the maximum degradation temperature increases with the heating rate. [31,33]

Singh *et al.* observed that the waste plastic shows an earlier loss of mass and a reduction in the maximum degradation temperature, when compared to virgin plastic and this is likely to be related to the presence of additives. They reported as well that individual plastics have a short degradation temperature range when compared to waste plastic. The presence of foreign materials also leads to an

increase in residue. [33] Kiran *et al.* reported that waste PS decomposes with one peak, with an onset temperature of 388 ºC and a maximum degradation temperature of 419 ºC. [34]

Katančić *et al.* reported that HIPS without additives decomposes in one step. The maximum degradation temperature observed by these authors was 421 ºC.[35]

Jakab *et al.* studied the thermal degradation of HIPS containing brominated flame retardants and trioxide antimony as synergist. The results showed that the brominated flame retardant decompose at the same temperature range as HIPS in the absence of Sb_2O_3. The presence of Sb_2O_3 changes the thermal decomposition of HIPS considerably indicating that the synergist Sb_2O_3 initiates the decomposition of brominated flame retardants and PS. The additives decompose during the first step and the majority of PS in the second step. [19] Peng *et al.* studied the thermal decomposition of a TV housing plastic sample, composed of flame-retarded HIPS containing PBDE and observed two stages for the decomposition of the sample. C-C and C-H bonds of HIPS are more stable than C-Br bonds of brominated flame retardants and therefore the C-Br bond should break first when heated. [20]

Experiments under air have shown that virgin PS decomposes with one peak. The onset temperature varies between 237.55 ºC and 308.85 ºC and the maximum degradation temperature between 372.85 ºC and 409.85 ºC. [30–32]

Table 2.3 - Results of the thermogravimetric studies made by others researches for polystyrene.

Sample	Degradation steps	T profile (ºC)	Atmosphere, Flow Rate (mL/min)	Heating rate (ºC/min)	Sample mass (mg)	T on set (ºC)	T max (ºC)	Residue (wt%)	Reference
Virgin PS	1	35-700	N_2, 20	10	5	299.85	379.85	*	[31]
Virgin PS	1	RT-700	N_2, 20	10	5	276.00	*	*	[32]
Virgin PS	1	25-700	N_2, 20	10	5	340.85	413.85	*	[30]
Virgin PS	1	35-700	Air, 20	10	5	237.55	372.85	*	[31]
Virgin PS	1	RT-700	Air, 20	10	5	245.00	*	*	[32]
Virgin PS	1	RT-700	Air, 20	10	5	308.85	409.85	*	[30]
Waste PS	1	RT-700	N_2, *	10	*	388	419	0	[34]
HIPS	1	25-550	N_2, 100	5	10	*	421	1.1	[35]

*Information not found.

2.3.2 Degradation mechanism

The mechanism of the degradation of PS is generally described as a radical depolymerization, leading mostly to styrene monomers as products. [33,36] The degradation of polystyrene initiates by scission of polymer chains to form radicals. The radical then undergo a propagation reaction which is accompanied by intramolecular or intermolecular transfer of radicals. [37,38] The styrene monomer is produced via beta-scission of a chain end formed by the initial chain scission (end-chain mechanism), while dimer and trimer are evolved via radical transfer followed by beta-scission. [33,39,40]

An overview of the mechanism for thermal degradation of PS can be visualized in Figure 2.8. The described steps are presented below Figure 2.8.

Initiation	
Random scission:	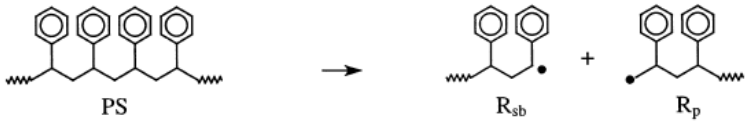
Chain-end scission:	
Propagation	
Intermolecular abstractions:	
Intramolecular abstractions:	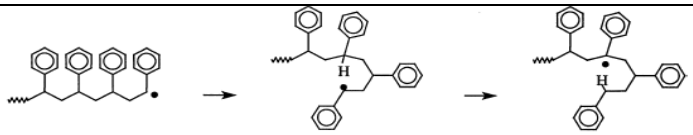
β-scission:	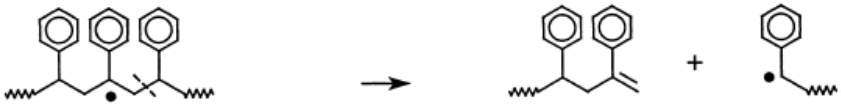
Termination	
Recombination:	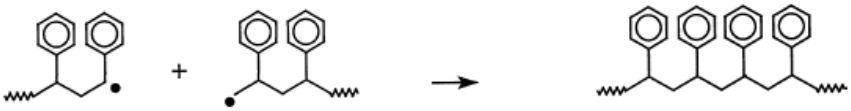
Disproportionation reactions of radicals:	

Figure 2.8 - Reaction mechanism of polystyrene.[33,38]

The steps in Figure 2.8 can be described as[33,38]:

- Initiation - The reaction starts with a C-C- bond cleavage of the polymer chain to form radicals. Two types of initiation reactions can be identified:
  - Random scission: forming of a primary radical (R_p) and a secondary benzyl radical (R_{sb}) with a strong benzylic resonance.

- Chain-end scission: forming of a secondary benzyl radical (R_{sb}) and a resonantly stabilized allyl benzene radical (R_a).

- Propagation - The propagation reaction consists of the sequence of H-abstraction and beta-decomposition reactions. There are two types of H-abstraction reactions:
  - Intermolecular abstractions – the radicals abstract the hydrogen from a different molecule. The intermolecular abstraction is only considered on the tertiary carbon atom because the resonantly stabilized benzylic radical formed is very stable.
  - Intramolecular abstractions – the radicals R_{sb} and R_p can form numbered rings intermediates from R_{sb} and R_p, which are also called as backbiting reactions.
  - β-scission:The tertiary benzylic radical R_t undergoes a scission of the C-C bond in beta-position to form a secondary benzylic radical and a polymer species with an unsaturated end.

- Termination **-** The termination reactions can be:
  - Recombination reactions
  - Disproportionation reactions of radicals, which produced unsaturated ends.

2.3.3 Pyrolysis reactor and products yield

Experiments have been performed in laboratory scale reactors that provide a preliminary insight into pyrolysis. The product yields have been reported by several authors which are summarized in Table 2.4. Achilias *et al.* obtained for the pyrolysis of virgin polystyrene at 510 ºC in a fixed bed reactor 91.8% liquid product, 2.5 % gas and 5.7 % char.[41]

The pyrolysis of waste polystyrene has also been studied, in a fixed bed reactor at different temperatures, producing 65.71 % oil, 25.69 % gas and 8.60 % residue at 300 ºC.[42] As the temperature increased, the yield of oil and gases increases and of residue decreases. [42,43] However, the liquid yield reaches a peak at a certain operating temperature and then decreases.[42] At lower temperature (350 ºC[43] and 300 ºC[42]), for both virgin and waste polystyrene, the degradation is not complete, which results in high amount of residue. Sogancioglu *et al.* observed that the maximum liquid yield is obtained at 500 ºC. [33,42]. Encinar and González used a fluidized bed reactor to study the pyrolysis of waste polystyrene (10 g) at 800 ºC with a heating rate of 10 ºC/min, which produced 95.79 % oil, 3.40 % gas and 1.81 % char. [44] The composition of the product obtained differed when changing the heating rate. As the heating rate increases, the yield of gases increases and the yield of oil and wax decreases.[44]

MSW PS has also been pyrolyzed. Williams and Slaney reported that MSW PS produced 71 % liquid, 2 % gas and 27 % residue at 500 ºC, using a batch reactor. [45] At 700 ºC, using a fixed bed reactor, Wiliams and Williams obtained a liquid yield of 83.8 %.[46] Achillias *et al.* observed that MSW PS had a lower liquid yield (77.8 %) comparing to virgin PS (91.8 %) at 510 ºC, using a fixed bed reactor. [41] Singh *et al.* observed that the liquid yield of MSW increases with temperature – from 70 % at 450 ºC to 600 at 80.5 %.[33]

It has been found that styrene is the main oil product of the thermal degradation of virgin polystyrene [33,36] Zhang *et al.* and Lee *et al*. reported styrene, dimer, α-methylstyrene, toluene, ethylbenzene as main liquid products.[47,48]

Kiran *et al.* observed that the main products of waste polystyrene pyrolysis were styrene, toluene, naphthalene and xylene. [34] William and Stanley reported that the oil products of MSW PS pyrolysis are: styrene, toluene, alpha-methyl styrene, ethylbenzene, benzene, cumene, dimers, trimers, tetramers, indene derivatives, naphthalene derivatives, phenanthrene and anthracene. [45] For the main products styrene and dimers it was observed that as the temperature increases, the styrene yield decreases from 81.54 % at 400 ºC to 55.14 % at 800 ºC, while the yield of dimers increases from 6.65 % at 400 ºC to 16.20 % at 800 ºC.[45]

Jakab *et al.* reported that the presence of brominated flame retardants and Sb_2O_3 highly affect the product distribution of HIPS: less styrene monomer, dimer and trimer are evolved and the formation of various other products (for example 2 -phenyl naphthalene and 1,3,5 – triphenyl benzene) is enhanced. [19]

The gaseous products of waste PS decomposition are found to be pentane, 2-methyl-1-pentene, 1-pentene, 1-heptene, hexane, benzene, toluene, octane, styrene and ethylbenzene. [42] Williams and Williams reported that the gaseous products of MSW PS pyrolysis are mostly methane, ethane, ethene, propane, propene, butane and butene. [46]

Table 2.4 - Products distribution of the PS pyrolysis obtained by other authors. L = liquid; R = residue; G = gas.

				Product Yield (wt%)			
Sample	**Pyrolysis Temperature (ºC)**	**Sample mass (g)**	**Type of reactor**	**L**	**R**	**G**	**Reference**
Virgin PS	510 (at * ºC/min)	1.5	Fixed bed	91.8	5.7	2.5	[41]
Virgin PS	350 (at * ºC/min)	2	*	59	40	1	[43]
	550 (at * ºC/min)	2		92	7	1	
Waste PS[a]	800 (at 10ºC/min)	10	Fluidized bed	95.79	1.81	3.40	[44]
Waste PS[a]	300 (at 5ºC/min)	*	Fixed bed	65.71	8.60	25.69	[42]
	400 (at 5ºC/min)	*		66.45	7.02	26.53	
	500 (at 5ºC/min)	*		67.23	6.21	26.56	
	600 (at 5ºC/min)	*		64.85	6.36	28.79	
	700 (at 5ºC/min)	*		67.12	4.95	27.93	
Waste PS[b]	500 (at 5ºC/min)	30-40	Batch-autoclave	71	27	2	[45]
Waste PS[b]	700 (25 ºC/min)	3	Fixed bed	83.8	3.5	3.4	[46]
Waste PS[b]	510 (at * ºC/min)	1.5	Fixed bed	77.8	18.6	3.6	[41]
Waste PS[b]	450	*	Semi-batch	70	14	16	[33]
	500			84	8	8	
	550			82.5	6	11.5	
	600			80.5	5	14.5	

*Information not found.

[a]Not specified from which type of waste.

[b]PS from MSW.

2.4 Pyrolysis of ABS

2.4.1 Thermogravimetric analysis

Various thermogravimetric studies on the thermal degradation of ABS were performed by other authors. Table 2.5 summarizes the results of the thermogravimetric studies. It has been reported that virgin ABS show only one decomposition peak [3,24,49–52], at different heating rates.[21,52]. Diverse authors performed the thermal degradation of ABS under nitrogen atmosphere, at 600 ºC with a heating rate of 10 ºC/min and the results show that the onset temperature varies between 372.5 ºC and 385.5 ºC and the maximum degradation temperature between 410.7 and 423.8 ºC.[3,49,50] It has been observed that with the increasing of the heating rate, the TG curve shifts to higher temperatures. [21,53] Liu *et al.* explained that the poor thermal conductivity of particles limits the heat transfer inside the materials at higher heating rates. [21] Some authors obtained for 20 ºC/min a onset temperature of 387 ºC [51] and 402 ºC [24], and a maximum degradation temperature of 433 ºC [51] and 440 ºC[24]. Suzuki and Wilkie verified that the onset temperature is 340 ºC [52].

Other researchers observed that, based on the different characterizing conditions, the degradation of ABS can occur with either one or two peaks, with a first maximum temperature of 443 ºC and a second one of 623 ºC. [54,55]

Feng *et al.* has reported that the thermal degradation of virgin ABS results in a negligible quantity of residue at the end, while the introduction of additives, like flame retardants, leaves more residue at the end of the pyrolysis process. The maximum temperature degradation tends to decrease with the presence of these compounds. [24]

ABS found in WEEE generally include brominated compounds as flame retardants and antimony trioxide as a synergist. [53,56] Some researchers have studied the thermal degradation of this type of ABS and the TG analyses shows two degradation peaks, where the second peak has a higher weight loss associated. The two decomposition regions seem to result from the existence of the flame retardants and the synergist. [53,56] The first peak is likely to be the decomposition of the additive and the second the decomposition of ABS itself. [56]

The thermal decomposition of ABS containing brominated flame retardant has also been studied by Bhaskar *et al.* and it showed that the bromine compound decreases the onset temperature of the virgin ABS decomposition from 400 ºC to 350 ºC. [57]

Experiments under air have shown that virgin ABS shows either one or two decomposition peaks. The decomposition with only one peak showed an onset temperature of 370 ºC [58] and 371 ºC [51]. The maximum temperature reported by Song *et al*. is of 423 ºC. [51] The decomposition with two peaks under air showed a first maximum degradation temperature of 445 ºC and a second of 554 ºC. [55] Around 470 ºC a plateau has been observed. [51,58] The transitory residue present at this plateau volatilised completely at 600 ºC. It indicates that oxidative dehydrogenation is an important process in the char formation of ABS in the presence of oxygen. [58]

Table 2.5 - Results of the degradation of ABS found in literature.

Sample	Additives	Degradation steps	Temperature Profile (ºC)	Atmosphere, Flow Rate (mL/min)	Heating rate (ºC/min)	Sample mass (mg)	T on set (ºC)	T max1 (ºC)	T max2 (ºC	Residue (%wt)	Reference
Virgin ABS		1	40-600	N_2, 20	10	*	380	416	-	*	[49]
Virgin ABS		1	40-600	N_2, 50	10	5	372.5	410.7	-	0.9	[50]
Virgin ABS		1	RT – 600	N_2, 40	10	20	385.5	423.8	-	*	[3]
Virgin ABS		2	RT-1000	N_2, 25	10	5-10	*	443	623	0.3	[55]
Virgin ABS		1	RT-600	N_2, *	20	*	387	433	-	1.9	[51]
Virgin ABS		1	35 – 800	N_2, 35	20	10	402	440	-	0	[24]
Virgin ABS		1	RT-600	N_2, 30	20	40	340		-	4	[52]
Virgin ABS		2	RT-1000	Air, 25	10	5-10	*	445	554	0.6	[55]
Virgin ABS		1	RT-600	Air, *	20	*	371	423	-	0.22	[51]
Virgin ABS		1	RT-600	Air, 90	10	100	370	*	-	0	[58]
Waste ABS	Yes[a]	2	30 – 600	N_2, 100	10	10-20	*	350	450	*	[53]
ABS	Yes[b]	2	RT-600	N_2, 400	25	2	350	*	*	*	[57]

*Information not found.

[a] Brominated flame retardants and antimony trioxide.

[b] Bromine.

2.4.2 Degradation mechanism

According to the literature is was mostly found that a radical process with random scission seems to be the most appropriate reaction mechanism to describe the thermal degradation of ABS.[3] However, some authors also observed that the degradation is a radical process through both end-chain and random scissions.[55,58] Dewon *et al.* reported that there are many different possible theories on the degradation behaviour of ABS, however, the mechanism may be described in term of a radical depolymerization. [59]

2.4.3 Pyrolysis reactor and products yield

Experiments have been performed in laboratory scale reactors to study the pyrolysis of ABS. The product yields have been reported by several authors which are summarized in Table 2.6. A batch reactor has been used to study the pyrolysis of virgin ABS, producing 63.5 % oil, 7.8 % gas and 28.7 % of residue at 440 ºC. [60] Munteanu *et al*. used a semi-batch reactor and obtained at 450 ºC 65 % of oil, 8 % of gas and 27 % of residue was produced [61], while Brebu *et al*. reported 72 % oil, 5 % gas and 24 % residue at the same temperature. [62] Zhou *et al.* reported a yield at 500 ºC of 84.9 % oil, 7.9 % gas and 7.2 % residue, using a batch reactor. [63]

The pyrolysis of ABS containing brominated flame retardant has also been studied using a semi-batch reactor at 450 ºC. Bhaskar *et al.* reported a production of 39 % liquid, 4 % gas and 57 % residue [57], while Mitan *et al*.[64] had the following yields: 23.6 % liquid, 4.3 % gas and 72.1 % residue. Brebu *et al*. observed that the presence of brominated flame retardants decreases the oil yield when comparing to virgin ABS, namely from 72 % to 34 %, and increases the residue from 24 % to 61 %. [62]

The pyrolysis of waste ABS found in WEEE has been also studied in a fluidized bed reactor at different temperatures. At 484 ºC it produces 77.42 % oil, 2.97 % gas and 19.61 % residue. [53] The oil yield increases with increasing temperature from 437 to 484 ºC, where it reaches a maximum, and then the yield decreases with increasing temperature. [53]

At lower temperatures (360 ºC [60] and 437 ºC[53], for both virgin and waste ABS, respectively), the degradation is likely to be incomplete, yielding a high quantity of residue and low quantity of liquid products. [53]

According to the literature, the hydrocarbons found in the oil product of virgin ABS decomposition are mostly butylene, cyclohexane, benzene, toluene, ethylbenzene, styrene, isopropylbenzene, *alpha*-methylstyrene and 1,3- diphenylpropane.[60] Some researches published that the recovered oil products are mainly composed of styrene monomer and benzene. [21,65] Bozi *et al.* observed that styrene is the most significant decomposition products, but dimers and trimers composed of styrene and acrylonitrile monomer segments are also main components of the pyrolysis oil. [66]

The main products found in the oil derived from the pyrolysis of virgin ABS containing brominated flame retardants and trioxide antimony are ethylbenzene, styrene and toluene. [67]

The gaseous products of virgin ABS decomposition are found to be HCN, NH_3 and a high quantity of hydrocarbons such as methane, ethylene, ethane, propylene, propane, unsaturated and saturated C_4 and C_5,and traces of benzene, toluene, ethylbenzene and styrene. [60]

Table 2.6 - Products distribution of the ABS pyrolysis obtained by other authors. L = liquid; R = residue; G = gas.

				Product Yield (wt%)			
Sample	**Pyrolysis Temperature (ºC)**	**Sample mass (g)**	**Type of reactor**	**L**	**R**	**G**	**Reference**
Virgin ABS	360 (at 3ºC/min)	10	Semi-batch	23.7	72.9	3.4	[60]
	380 (at 3ºC/min)			38.9	56.9	4.2	
	400 (at 3ºC/min)			49.5	43.3	7.2	
	420 (at 3ºC/min)			56.0	37.5	6.5	
	440 (at 3ºC/min)			63.5	28.7	7.8	
Virgin ABS	450 ºC (x)	10	Semi-batch	72	24	5	[62]
Virgin ABS	450 ºC(10 ºC/min)	8	Semi-batch	65	27	8	[61]
Virgin ABS	500 (at 10ºC/min)	10	Batch	84.9	7.2	7.9	[63]
ABS[a]	450 ºC (10 ºC/min)	10	Semi-batch	39	57	4	[57]
ABS[a]	450 ºC (x)	10	Semi-batch	34	61	5	[62]
ABS[b]	450 ºC (x)	10	Semi-batch	23.6	72.1	4.3	[64]
Waste ABS[b]	437 (at * ºC/min)	300	Fluidized bed	64.14	34.74	1.12	[53]
	468 (at * ºC/min)			75.87	20.91	3.21	
	484 (at * ºC/min)			77.42	19.61	2.97	
	510 (at * ºC/min)			73.98	22.62	3.4	

[a] containing bromide compound as flame retardant.

[b] containing brominated flame retardants and antimony trioxide.

(x) complex temperature program.

2.5 Thermogravimetry analysis (TGA) and differential scanning calorimetry (DSC)

Thermogravimetry analysis (TGA) and differential scanning calorimetry (DSC) are commonly used methods to investigate the thermal stability of polymers. TGA is a technique in which the mass of a substance is monitored as a function of temperature or time as the sample is subjected to a controlled temperature program in a controlled atmosphere. The TGA thermal curve shows the weight loss that occurred during the temperature profile. From these results it is possible to measure the onset temperature, T onset, which corresponds to the initial temperature of weight loss, as well as the maximum temperature of degradation, which corresponds to the point of inflection of the TG curve. The DTG (derivative thermogravimetry) has a minimum which corresponds to the maximum degradation temperature, Tmax.[4,68]

The onset temperature can be graphically obtained from the TG curves as the intersection between the starting mass line and the maximum gradient tangent to the TG curve, Figure 2.9. [69,70] The temperature at maximum mass loss rate is represented in the DTG.[70]

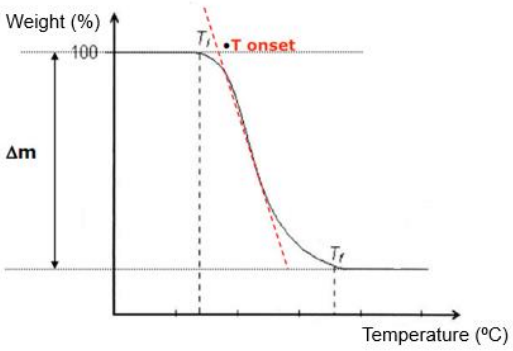

Figure 2.9 - Representation of a TG curve. Adapted [71].

DSC is a technique in which the difference in the amount of heat required to increase the temperature of a sample and reference is measured as a function of temperature. The DSC curve, Figure 2.10, allows to identify the temperature range of degradation of the sample as well as to measure the specific heat and enthalpies of phase transition and chemical processes. [4,68] Endothermic peaks can correspond to melting, loss of mass of the sample (evaporation of water, additives or volatile products from the reaction of decomposition), while exothermic peaks are usually associated with processes like crystallization, polymerization reactions, oxidation, oxidative degradation or adsorption. [71]

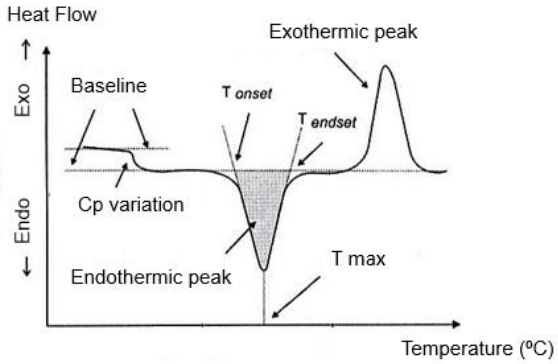

Figure 2.10 - Representation of a DSC curve. Adapted [71].

2.6 Kinetic models

Munteanu *et al.* assumed that the cleavage of bonds in random scission processes follows a first order kinetics.[61] Achillias *et al.* found that the kinetic parameters vary with the heating rate and the type of temperature profile (dynamic or isothermal). As the heating rate increases, the activation energy and the kinetic constant decrease.[41]

2.6.1 PS

Several authors have studied the kinetics of the degradation mechanism of polystyrene using different models. Table 2.7 summarizes the results of the kinetic parameters obtained by other researches for the thermal decomposition of polystyrene.

The reported activation energies for virgin PS vary between 190 and 262 kJ/mol under dynamic conditions. [30,72–75]. Jellinek reported that the activation energy is independent on the molecular weight [76] and Funt and Magill observed the same behaviour for molecular weights above 360 000 g/mol [77].

Katančić *et al*. reported an activation energy between 261 and 268 kJ/mol for virgin HIPS. [35]

Peng *et al.* observed two decomposition stages for HIPS containing flame retardant and reported an activation energy of 149.87 kJ/mol for the first stage and 219.98 kJ/mol for the second. It can be inferred that the first activation energy reflects the thermal degradation of low-thermostability compounds, while the second reflect compounds of high thermostability. [20]

Kiran *et al.* reported an activation energy of 269 kJ/mol for waste PS. [34] Encinar and González observed that under isothermal conditions the activation energy of waste PS is 136.64 kJ/mol and under dynamic conditions is 231.90 kJ/mol. [44]

Table 2.7 - Kinetic parameters obtained by different authors for the decomposition of polystyrene. n=reaction order, Ea=activation energy.

Plastic	Conditions	Model	n	Ea (kJ/mol)	Reference
Virgin PS	Dynamic conditions, different heating rates	Kissinger method	*	195.00	[30]
Virgin PS	Dynamic conditions, 5 ºC/min	Model fitting method	1	199.20	[73]
Virgin PS	Dynamic conditions, different heating rates	First-order reaction model	1	217.90	[74]
Virgin PS	Dynamic conditions, different heating rates	Friedmann method	*	190.00	[75]
Virgin PS	Dynamic conditions	*	2.1	262	[72]
HIPS	Dynamic conditions	One step model	*	261-268	[35]
HIPS[a]	Dynamic conditions	*	0.11 1.2	149.87 219.98	[20]
Waste PS	Dynamic conditions	Freeman-Caroll method	*	269	[34]
Waste PS	Dynamic conditions, 10 ºC/min	First-order reaction model	1	231.90	[44]
Waste PS	Isothermal conditions	First-order reaction model	1	136.64	[44]

*Information not found.

[a] Containing brominated flame retardant and Sb_2O_3.

2.6.2 ABS

The kinetics of the degradation mechanism of ABS has also been studied by different authors. Table 2.8 summarizes the results of the kinetic parameters obtained by others researches for the thermal decomposition of ABS. The reported activation energies for virgin ABS vary between 121.6 and 332 kJ/mol under dynamic conditions [44,61,78] and between 118.31 and 134.18 under isothermal conditions.[44,55]

Table 2.8 - Kinetic parameters obtained by different authors for the decomposition of ABS. n=reaction order, Ea=activation energy.

Plastic	Conditions	Model	n	E_a (kJ/mol)	Reference
Virgin ABS	Dynamic conditions, different heating rates	Friedman method		178.90	[78]
Virgin ABS	Dynamic conditions, 10 ºC/min	First-order reaction model	1	121.6	[44]
Virgin ABS	Dynamic conditions	*	0.8-1.5	142-332	[61]
Virgin ABS	Isothermal conditions	Freeman and Carroll method		134.18	[55]
Virgin ABS	Isothermal conditions	First-order reaction model	1	118.31	[44]

*Information not found.

2.7 Market demand

Toluene, styrene and *alpha*-methylstyrene are some of the main products of the thermal pyrolysis of polystyrene[34,79] and ABS[60,67] . It is interesting to understand the market demand of these products.

Toluene is used to manufacture benzene, p-xylene for polyethylene terephthalate (PET) resins, and toluene diisocyanates (TDI) for polyurethane applications, and is widely used as a solvent. Toluene is also frequently used as an octane booster in gasoline.[80] About 47% of all toluene was consumed to make on-purpose benzene, mixed xylenes, and p-xylene in 2017. The major consumers of toluene are China, United States and South Korea (data for 2017). Although Western Europe, North America, South America, and Japan may experience small or no capacity increases (or even declines), overall world capacity will increase during 2017–22. [81]

The major markets of styrene are polystyrene, acrylonitrile-butadiene-styrene (ABS)/styrene-acrylonitrile (SAN) resins, styrene-butadiene copolymer latexes, styrene-butadiene rubber (SBR) elastomers and latexes, and unsaturated polyester resins (UPR). In 2017 the major consumer of styrene was China, followed by Western Europe. Overall, styrene consumption is forecast to grow at an average rate of only 2% per year in 2017–22. [82]

Alpha-methylstyrene finds a variety of applications across a diverse set of industries including plastics, adhesives, and chemicals among others. In plastics industry, *alpha*-methylstyrene is used to manufacture ABS. Until 2026 it is expected that the growing demand from the chemical industry will drive the growth of the global *alpha*-methylstyrene market. [83]

3. Experimental Procedures and Apparatus

This chapter describes the methods and techniques used to study the degradation of ABS and PS. Firstly, it covers a description of the plastic materials. Secondly, the experimental conditions performed in the thermogravimetric and differential scanning calorimetric analysis. Finally, it includes a description of the reactor system used for the pyrolysis of polystyrene and of the gas chromatographs used to analyse the gaseous and liquid pyrolysis products.

3.1 Plastic materials

The materials used for the experiments were waste ABS coming from a food blender and waste PS derived from an outer casing from a television (Figure 3.1). The plastics were collected in Portugal by *Ambigroup Reciclagem*. The samples were prepared at the *Geolab* of *Instituto Superior Técnico*[1] as follows: the collected equipment was manually dismantled; chipped on a guillotine to fit the *Retsch 2000* mill feed; in the mill, the plastics were fragmented to a calibre of less than 8 mm and thereafter the two plastics were classified by dry screening in the particle sizes <2 mm and 4-5.6 mm (Figure 3.1).

Two virgin polystyrene samples with different molecular weight (MW) were purchased from *Sigma-Aldrich*, namely pellets of polystyrene with MW~192 000 - designated as PS1 - and pellets of polystyrene with MW ~350 000, Mn ~170 000 and density of 1.04 g/mL at 25 ºC - designated as PS2 – (Figure 3.2).

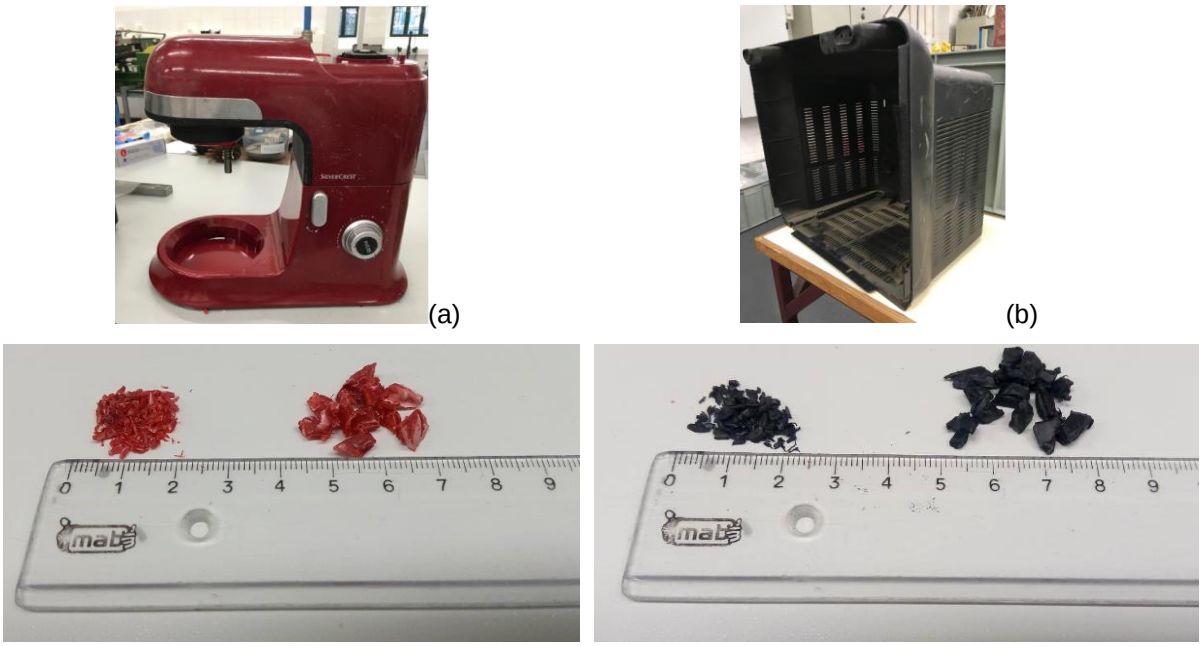

Figure 3.1 – Images of the waste plastic sample. (a) - ABS food blender, (b) - PS television outer casing, (c)- 2mm and (4-5,6) mm pieces of ABS, (d) – 2 mm and (4- 5,6) mm pieces of PS.

[1] Prepared by Francisca Rey.

PS1

PS2

Figure 3.2 – Images of the virgin polystyrene: PS1 and PS2.

3.1.1 Proximate Analysis

The proximate analysis was carried out using the TG/DSC equipment described in Chapter 3.2. The samples were first pyrolyzed under nitrogen up to 900 ºC with a heating rate of 10 ºC/min. The volatile matter was calculated using Equation 3.1. The remaining residue was combusted under air to determine the fixed carbon and ash content, using Equation 3.2 and Equation 3.3.

Equation 3.1 - Volatile Matter.

$$Volatile\ Material\ (\%) = \frac{Initial\ mass - Mass\ after\ pyrolysis}{Initial\ mass} \times 100$$

Equation 3.2 - Fixed Carbon.

$$Fixed\ carbon\ \ (\%) = \frac{Mass\ after\ pyrolysis - Mass\ after\ combustion}{Initial\ mass} \times 100$$

Equation 3.3 - Ash.

$$Ash\ (\%) = 100 - \%\ Volatile\ Material - \%\ Fixed\ Carbon$$

3.1.2 Ultimate Analysis

The chemical composition of the plastics in terms of C, H, N and S was determined by an elemental analysis executed by *Laboratório de Análises* of *Instituto Superior Técnico*.

3.2 Thermogravimetric (TG) and Differential Scanning Calorimetric (DSC) analysis

3.2.1 Sample preparation

All the TG/DSC experiments were conducted in a Perkin-Elmer STA 6000 simultaneous thermal analyser. A continuous nitrogen flow rate of 20 mL/min was used to purge all the air from the system and to act as protector of the equipment. All the samples were prepared using an analytical balance (with an error of ± 0.1 mg) and placed in an alumina TG crucible.

For the TG/DSC analysis waste ABS and PS samples with grain size < 2 mm were used. In all experiments around 20.3 ± 1.8 mg of waste plastic samples were prepared. Regarding the virgin polystyrene samples of 33.4 mg of PS1 and 27.7 mg of PS2 was used.

3.2.2 Temperature Profile

Experiments at dynamic and isothermal conditions were performed under nitrogen with a continuous flow rate of 20 mL/min.

For the dynamic conditions, the temperature was raised to 900 ºC with heating rates of 5, 10, 20, 50, 100 and 200 ºC/min. The temperature profile was as followed: 10 min equilibration at 40 ˚C, temperature raise from 40 ºC to 900 ºC at different heating rates, holding for 10 min at 900 ˚C and then cooling to room temperature (Figure 3.3).

The experiments under isothermal conditions were performed with a heating rate of 10 ºC/min and a holding time of 1 h. The temperature profile was as follow: 10 min equilibration at 40 ºC, temperature raise from 40 ºC to desired temperature at 10 ºC/min, holding for 60 min at that temperature and then cooling to room temperature (Figure 3.4).

A combustion experiment was performed to study the behaviour of the samples under air. The samples were heated at 10 ºC/min until 700 ºC for PS and 900 ºC for ABS under a flow rate of 20 mL/min of air. To analyse the composition of the remaining residue at the end of the pyrolysis experiments as well as to clean the TG crucible, additional combustions experiments were performed for ABS and PS, respectively. A flow rate of 20 mL/min of air was applied and the temperature ranged from 40 ºC to 700 ºC at a heating rate of 100 ºC/min.

For each experiment baseline experiments were conducted without samples to compensate for the apparent weight change of the empty crucible. The apparent weight change occurring during an experiment with an empty crucible is caused by several factors, such as changes in buoyancy, convection effects within the furnace, crucible geometry, radiation effects and the atmosphere in the furnace.[84]

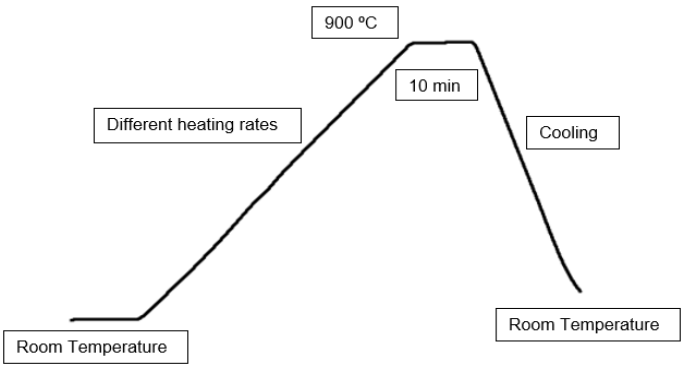

Figure 3.3 - Temperature Profile for the TG at dynamic conditions.

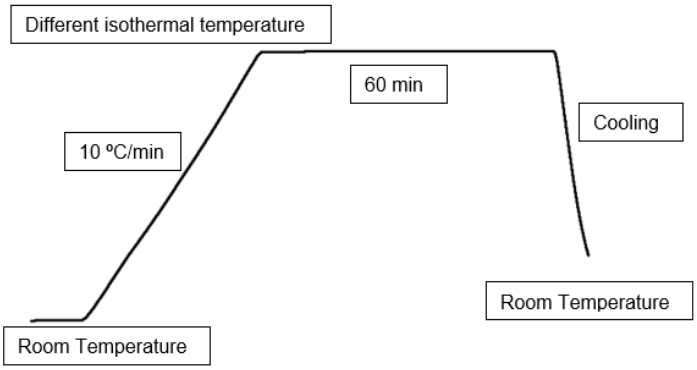

Figure 3.4 - Temperature Profile for the TG at isothermal conditions.

3.2.3 Equipment

The TG/DSC apparatus consists of three components:

1. Sensitive recording balance.
2. Furnace and associated controller/atmosphere management.
3. Computer with special data system and recorder.

The TG/DSC instruments are presented in Figure 3.5.

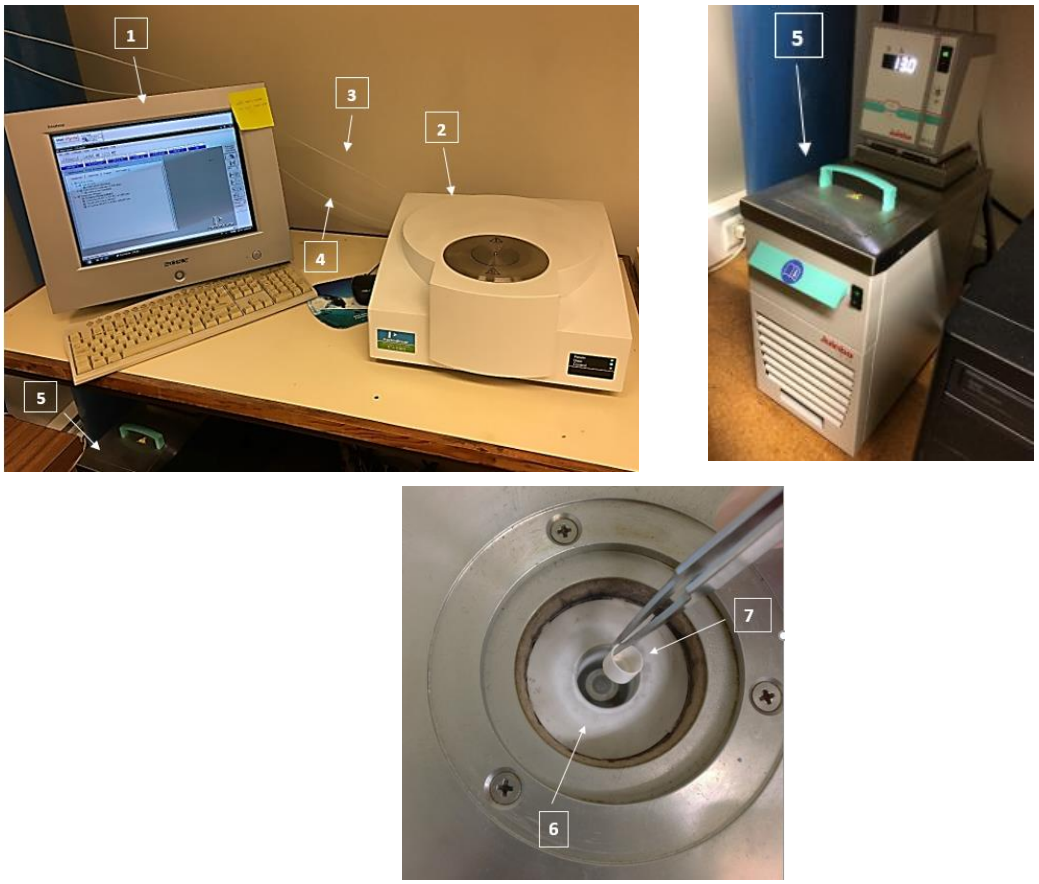

Figure 3.5 - TG/DSC equipment. 1 - Computer; 2 - TG/DSC equipment; 3 – N_2 line; 4- reconstituted air line; 5 - Refrigerator; 6 – Furnace; 7 – TG alumina crucible.

3.3 Pyrolysis Reactor

3.3.1 Sample preparation

For all the experiments approximately 10 g of virgin and waste polystyrene was placed in the reactor. For waste PS a granulometry of 4-5.6 mm was used.

3.3.2 Procedure

The pyrolysis experiments were carried out using a bench-scale reactor in semi-batch operation at atmospheric pressure. The reactor works as a reactive distillation system. The reactor was initially flushed with nitrogen for 10 minutes to inertize the system. The samples were heated at 10 ºC/min to different set point temperatures (400, 450 and 500 ºC) and maintained 90 minutes at that temperature, Figure 3.6.

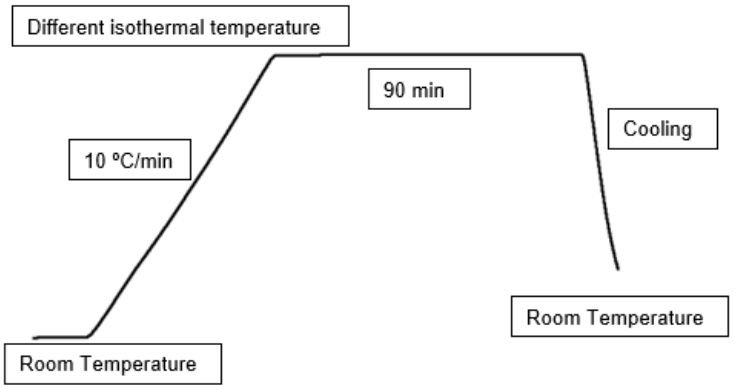

Figure 3.6 - Temperature profile used in the reactor.

A Schlenk-type glass vessel of around 0.1 L was placed in a furnace. The reactor is equipped with a thermocouple to monitor the temperature inside the reactor. The reactor was insulated with glass wool and aluminium foil to reduce heat losses. The gaseous products rise and condense in the liquid collector when it comes in contact with ambient temperature. The liquid collector is connected with a condenser to promote the condensation of the liquid products. The coolant feeding to the condenser was controlled by a thermostat at 20 ºC to control the exit of the products in the gaseous phase. The products that are gases at atmospheric temperature exit by the top of the condenser and are collected in a gas collector. All the products generated from the pyrolysis (solid, liquid and gas phase) were collected and analysed.

The quantity of solids (residue inside the reactor) and the liquid phase were weighted using an analytical balance with an error of ± 0,1 mg to calculate the pyrolysis yield (see Chapter 3.4.1.).

3.3.3 Equipment

The reaction system is presented in Figure 3.7. It consists of the following components:

1. *TermoLab* Furnace from *Fornos Elétricos, Lda*
2. Reactor
3. Liquid collector
4. Condenser
5. Flask of gas collection
6. Thermostatic Bath

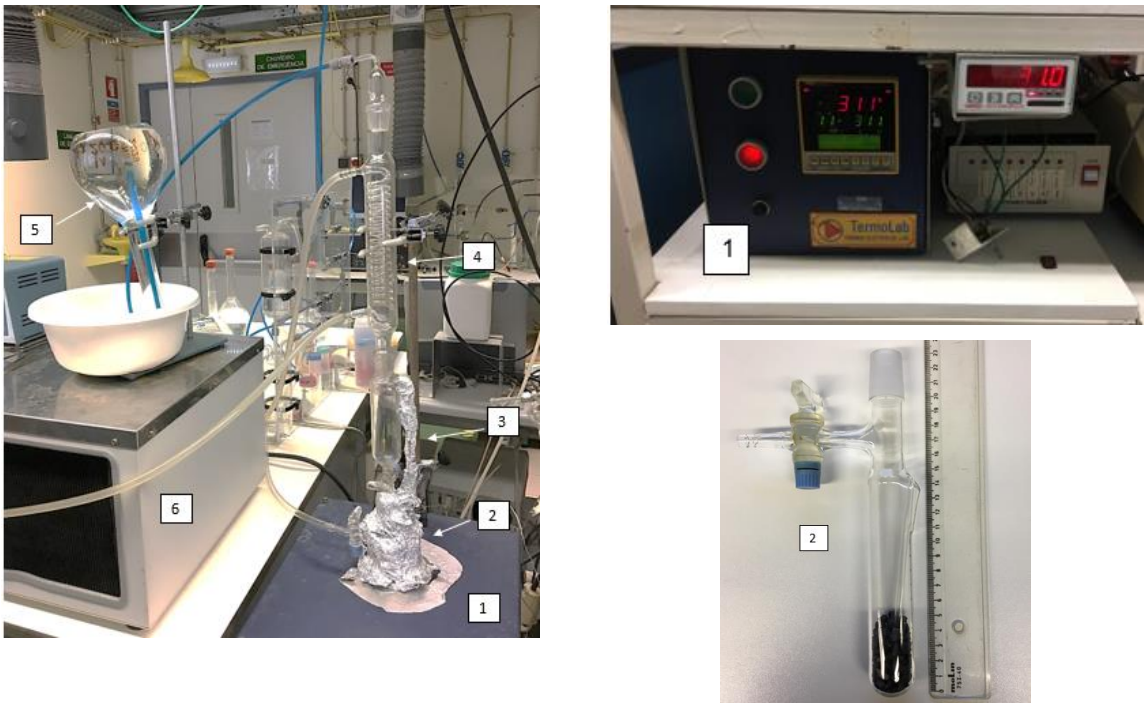

Figure 3.7 – Experimental pyrolysis reactor. 1 – Furnace, 2 -Reactor, 3 – Liquid collector, 4 – Condenser, 5– Flask of gas collection, 6 – Thermostatic Bath.

3.4 Product Analysis

3.4.1 Yield

The yields of the solid and liquid products were calculated using Equation 3.4 and Equation 3.5, respectively. The solid yield is the ratio between the mass of solid weighted at the end of the reaction, m_{solid}, and the initial sample weight, $m_{polymer}$. The liquid yield is the ratio between the weighted mass of liquid collected in the liquid collector, m_{liquid}, and the initial sample weight, $m_{polymer}$. The gas liquid is obtained by difference, assuming no mass losses, Equation 3.6.

Equation 3.4 - Solid yield.

$$Yield_{solid}(\%) = \frac{m_{solid}}{m_{polymer}}\ x\ 100$$

Equation 3.5 - Liquid yield.

$$Yield_{liquid}(\%) = \frac{m_{liquid}}{m_{polymer}}\ x\ 100$$

Equation 3.6 - Gas yield.

$$Yield_{gas}(\%) = 100 - Yield_{liquid}(\%) - Yield_{solid}(\%)$$

3.4.2 Gas Chromatography

The products obtained on pyrolysis of the polymer in gaseous and liquid phases were analysed by gas chromatography (GC).

3.4.2.1 Gas chromatography – Gas phase product

The chromatograph used to analyse the gaseous products was *Shimadzu GC-9A* gas chromatograph (Figure 3.8). The chromatograph works at 2 bar and is equipped with a 50 -meter capillary column PLOT (KCl/Al_2Cl_3), a flame ionization detector where the outlet gas was analysed, and a split/splitless injector (with a splitting ratio of 100/1) was used. Further GC specification are given in attachment (I – Gas chromatography, Table I. 1). The gas chromatograph (GC) was coupled to a Shimadzu C-R3A integrator that was used to analyse the chromatographic signal and to integrate the peak. The gases introduced in FID ignite under a flowrate of hydrogen and air of the 0.6 kg/cm^2 and 0.5 kg/cm^2, respectively.

Figure 3.8 – Shimadzu GC-9A chromatograph.

The temperature profile of the chromatograph is presented in Figure 3.9.

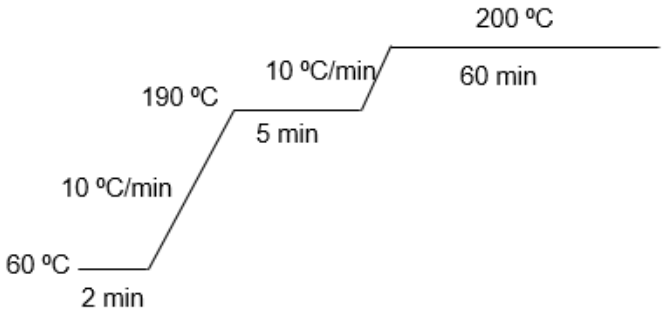

Figure 3.9 - Temperature Profile of the chromatograph.

To identify the products, pure hydrocarbons were injected to obtain their retention times as reference (see Annex II). The products were grouped based on their respective GC retention times. The percentage of area of the various products obtained was calculated from Equation 3.7, where A_i is the area of the peaks corresponding to the product i and A_{total} is the sum of the area of all the peaks in the chromatogram.

Equation 3.7 - Area.

$$Area\ (\%) = \left(\frac{A_i}{A_{total}}\right) x100$$

3.4.2.2 Gas chromatography – Liquid phase product

For the liquid phase, the chromatograph used was a *Perkin-Elmer 680* gas chromatograph (Figure 3.10) equipped with a flame ionization detector (FID) and an SFE BP1 capillary column 30 m long x 0.25 mm width. The injector and detector were kept at 250 ºC, and nitrogen was used as carrier gas. The flow rates used in the detector were 45 cm^3/min of hydrogen and 450 cm^3 /min of air, measured at atmospheric pressure and room temperature. Further GC specification are in attachment (I – Gas chromatography, Table I. 1).

The temperature profile and products analysis were performed the same way as explained in Chapter 3.4.2.1. for the *Shimadzu GC-9A* gas chromatograph.

Figure 3.10 - Perkin- Elmer 680 chromatograph.

3.4.3 Solid analysis

The solid obtained from the thermal pyrolysis was analyzed using the TG/DSC analysis. The samples were heated under inert atmosphere from room temperature to 700 ºC at 10 ºC min and maintained during 10 min at 700 ºC.

4. Results and discussion

This chapter includes in first place the material characterization obtained by the proximate and ultimate analysis.

Secondly, it covers the TG/DSC results and discussion for the thermal degradation of virgin PS, waste PS and waste ABS. The analysis includes the influence of the heating rate in a non-isothermal way and the influence of the temperature in isothermal conditions. The TG/DSC analysis was used further to determine the experimental conditions of the bench-scale reactor, such as temperature, heating rate and residence time and to study a kinetic model capable of describing the decomposition of both plastics.

Different kinetic models were studied for PS and ABS decomposition allowing the estimation of the kinetic parameters.

The results of the thermal pyrolysis performed for waste and virgin PS in a bench-scale reactor is analyzed in terms of yields. The obtained products are characterized by gas chromatography.

4.1 Proximate Analysis

The samples were heated up to 900 ºC under nitrogen in the TG/DSC apparatus, as described in Chapter 3.1.1. After the pyrolysis the remaining residue was burnt to determine the fixed carbon and ash values.

Table 4.1 presents the proximate analysis of both virgin polystyrenes. PS1 has 99.83 % volatile matter. PS2 has 99.04 % volatile matter.

Table 4.1 - Proximate Analysis of both virgin polystyrenes.

	PS1	**PS2**
Initial Mass (mg)	33.54	27.78
Mass after pyrolysis (mg)	0.06	0.27
Volatile Matter (%)	99.83	99.04
Fixed Carbon (%)	*	*
Ash (%)	*	*

*The remaining quantity of residue was very low (less than 1 %). The combustion was not performed.

For waste PS and ABS three sets of experiments were performed for both plastics. The corresponding TG and DTG curves for waste PS are shown in Figure 4.1. The average values and standard deviations are shown in Table 4.2. The results show that waste PS has around 95 % of volatile matter, 4 % fixed carbon and less than 1 % non-volatile inorganics.

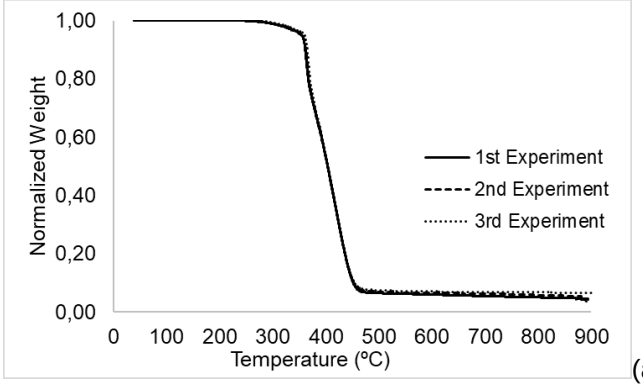

(a)

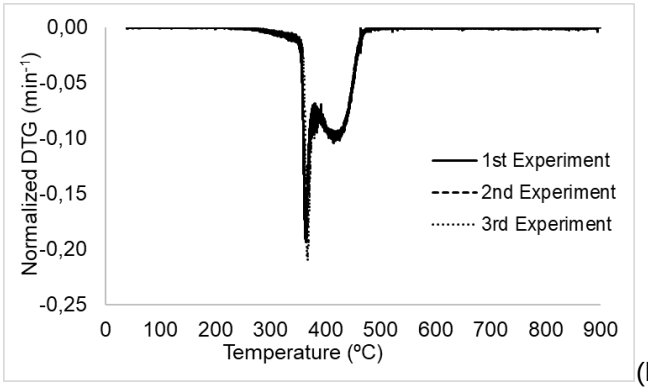

(b)

Figure 4.1 – TG and DTG curve for the 3 experiments - waste PS.

Table 4.2 - Proximate Analysis of waste PS.

	Experiment 1	Experiment 2	Experiment 3	Standard deviation	Average values
Initial Mass (mg)	19.73	19.83	19.87	-	-
Mass after pyrolysis (mg)	0.83	0.73	1.31	-	-
Mass after combustion (mg)	0.08	0.07	0.13	-	-
Volatile Matter (%)	95.78	96.34	93.43	1.26	95.18
Fixed Carbon (%)	3.80	3.29	5.91	1.13	4.34
Ash (%)	0.42	0.37	0.66	0.13	0.48
Total (%)	100.00	100.00	100.00	-	100.00

The corresponding TG and DTG curve of waste ABS are shown in Figure 4.2. Table 4.3 presents the average values and standard deviations results of the proximate analysis of waste ABS. ABS waste has around 96 % of volatile matter, 3 % of fixed carbon and less than 1% ash.

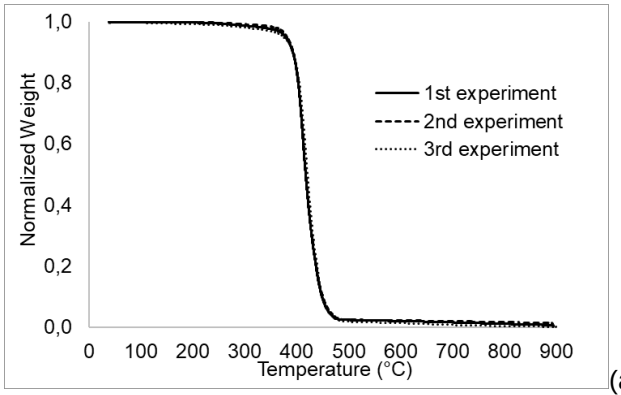

(a)

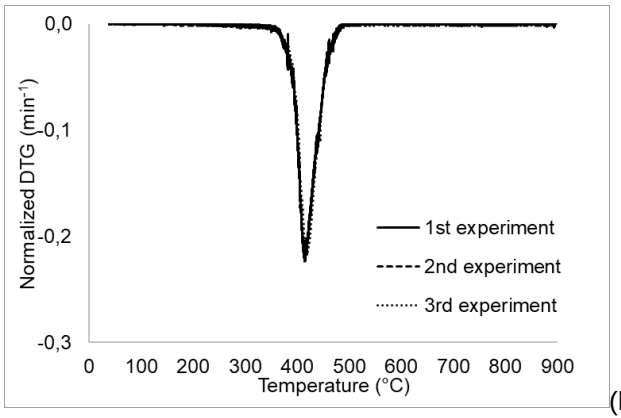

(b)

Figure 4.2 - TG and DTG curve for the 3 experiments - waste ABS

Table 4.3 - Proximate Analysis of waste ABS.

	Experiment 1	Experiment 2	Experiment 3	Standard deviation	Average values
Initial Mass (mg)	22.05	21.82	19.47	-	-
Mass after pyrolysis (mg)	0.08	0.23	1.17	-	-
Mass after combustion (mg)	*	0.02	0.00	*	-
Volatile Matter (%)	99.64	98.93	94.01	2.46	96.47
Fixed Carbon (%)	*	0.96	5.99	2.51	3.48
Ash (%)	*	0.11	0.00	0.05	0.05
Total (%)	*	100.00	100.00	-	100.00

*The remaining quantity of residue was very low (less than 1 %). The combustion was not performed.

4.2 Ultimate Analysis

Two ultimate analysis for waste PS and ABS were performed. The average values and the respective standard deviation for the ultimate analysis are presented in Table 4.4. For PS the content in nitrogen is under the limit of detection and for both plastics the content in sulphur is also under the limit of detection.

The results show that PS has 77.63 % carbon and 6.79 % hydrogen atoms, making a total of 84.42 %. The remaining unknown composition of 16 % may be related with the presence of additives, since typically, for virgin polystyrene, the sum of carbon and hydrogen atoms makes up to 99.8%. [36]

ABS is composed of 5.63 % nitrogen, 84.42 % carbon and 7.84 % hydrogen atoms, making up to 97.89 % of the total composition. The remaining unknown composition may be related with the presence of additives, since, for virgin ABS the sum of carbon, hydrogen and nitrogen atoms makes up to 99.03 %.[21]

Table 4.4 - Ultimate Analysis.

Sample	N (%)	C (%)	H_2 (%)	S (%)	Total (%)
PS	< 0.5	77.63	6.79	< 2	84.42
Standard deviation	-	0.08	0.04	-	-
ABS	5.63	84.42	7.84	< 2	97.89
Standard deviation	0.05	0.01	0.12	-	-

4.3 Virgin PS versus waste PS

Figure 4.3 presents the TG, DSC and DTG results for the decomposition of waste PS and virgin polystyrene at a heating rate of 10 ºC/min.

From the TG curve it is possible to estimate the temperature at which the polymer starts to degrade, which corresponds to the onset temperature. The weight loss starts when the polymer bonds start to break with the input of energy and volatile lighter products evaporate from the TG crucible. The recorded weight will decrease as more energy is given to the sample and more products will evaporate. The TG results (Figure 4.3a and Table 4.5) show that the onset temperature of PS1 is 386.34 ºC and of PS2 388.72 ºC. The onset temperature of waste PS is 355.19 ºC, showing that waste plastic starts to degrade at lower temperatures than virgin polystyrene, which is likely related with the presence of additives, that decompose at lower temperatures than polystyrene. [33]

The DSC coupled with the DTG curve gives information about the phenomena that occur during the experiment. An endothermic peak related with weight loss will correspond to the decomposition of the polymer, since it consumes energy to break the bonds and volatile lighter products will evaporate. On the other hand, endothermic peaks at lower temperatures with no weight loss associated is related with the melting of the plastic, since it will consume energy to melt, but no mass will evaporate.

The DSC curve (Figure 4.3b) shows one endothermic peak for both virgin plastics in the temperature range of 370 ºC and 450 ºC, which has been observed by other authors as well. [30–32] In contrast, the DSC curve for waste PS shows two endothermic peaks between 350 ºC and 500 ºC. The DTG curve confirms that during this endothermic peak a maximum weight loss occurs, indicating that this temperature range corresponds to the decomposition of the plastic. The maximum degradation temperature of PS1 is 417.71 ºC and of PS2 414.88 ºC (Table 4.5). Waste PS has two maximum degradation temperatures of 364.73 ºC and 417.78 ºC (Table 4.5). The first maximum degradation temperature is lower than of virgin PS and this first peak is likely to be related to the degradation of additives. [33] The second degradation temperature is close to the maximum degradation temperature of virgin PS, indicating that this second peak is likely the degradation of polystyrene itself. [19]

The heat consumed during the pyrolysis process will depend on the number of broken bonds. The results presented in Table 4.5 show the heat consumed during pyrolysis: 449.17 J/g for waste PS, 677.54 J/g for PS1 and 535.26 J/g for PS2.

The presence of foreign materials in the waste leads to an increased residue [33]: Waste PS has 4.22 % remaining residue at the final of pyrolysis, while PS1 has 0.17 % and PS2 0.96 % (Table 4.5).

Comparing both virgin PS with different molecular weight, it is possible to see that the decomposition behaviour is similar, presenting only slightly differences: the starting temperature is 2.4 ºC earlier for the plastic with lower MW; the maximum degradation temperature differs in 3 ºC and the final remaining residue is less than 1 % for both virgin plastics. Thus, the molecular weight of the polymer seems to not affect significantly the thermal behaviour of the polymer in accordance with what has been observed by Marcilla and Beltrán as well.[74]

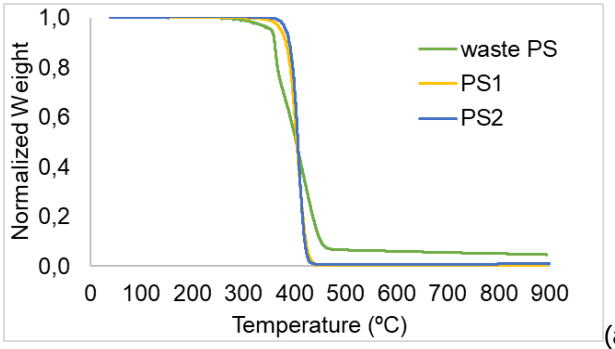

(a)

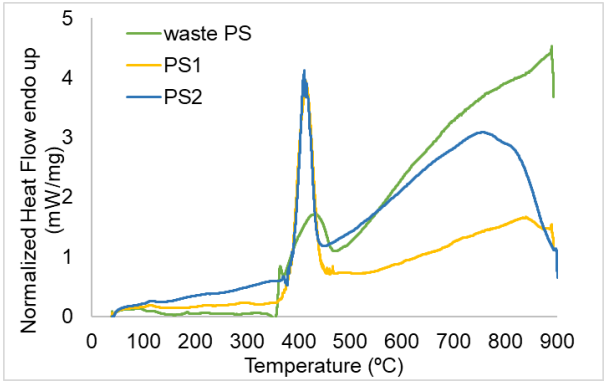

(b)

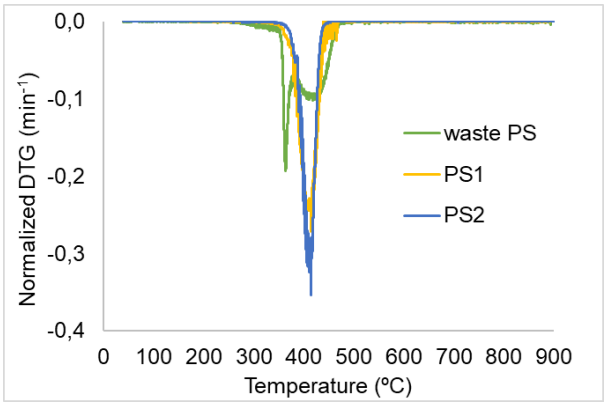

(c)

Figure 4.3 – TG(a), DSC (b) and DTG (c) curve for the thermal degradation of waste PS, PS1 and PS2.

Table 4.5 - TG results (onset temperature, maximum degradation temperature, residue and heat transferred) for waste PS, PS1 and PS2.

Plastic	Initial Mass (mg)	Tonset (ºC)	Tmax1 (ºC)	Tmax2 (ºC)	Heat transferred (J/g)*	Residue (%)
Waste PS	19.73	355.19	364.73	417.78	449.17*	4.22
PS1	33.54	386.34	417.71	-	677.54	0.17
PS2	27.78	388.72	414.88	-	535.26	0.96

*Corresponds to the heat consumed by the global pyrolysis process.

4.4 TG/DSC analysis - dynamic conditions

4.4.1 PS

The waste polystyrene was heated up to 900 ºC at 10 ºC/min. The TG, DSC and DTG curves are presented in Figure 4.4. The TG curve shows that the polystyrene starts to degrade at 355.19 ºC.

The DSC curve (Figure 4.4b) shows two endothermic peaks between 350 ºC and 500 ºC, approximately. The first endothermic peak is sharp, while the second is more an endothermic curve. The DTG curve (Figure 4.4b) confirms the existence of two decomposition peaks. Usually the first peak is related with the decomposition of additives and brominated flame retardants[19,33] since the C-Br bounds are weaker than C-C bonds [20], and the second to the decomposition of the polymer. The first maximum temperature, at which the maximum weight loss occurs, is 364.73 ºC and the second maximum temperature is 417.78 ºC.

The DSC signal does not show any melting peaks indicating that polystyrene is possibly amorphous.

The comparison of the obtained results with literature shows that two decomposition peaks were observed only for the decomposition of HIPS containing brominated flame retardants and trioxide antimony as synergist by Jakab *et al.* [19] and by Peng *et al*.[20]. Kiran *et al.* reported one decomposition peak for waste PS. [34] The obtained onset temperature is lower than the one obtained by Kiran *et al.* [34] The second maximum temperature observed for the waste PS in study is close to the one reported by Kiran *et al.* (419 ºC). [34]

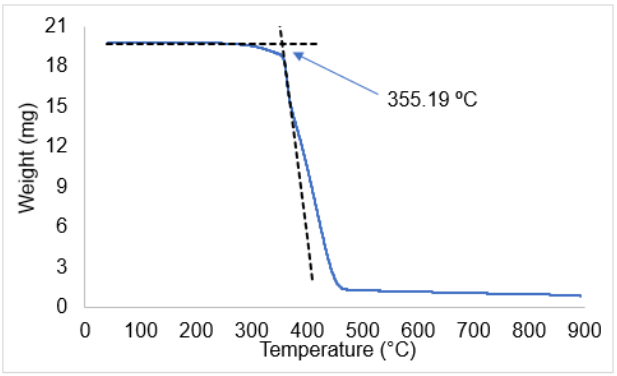

(a)

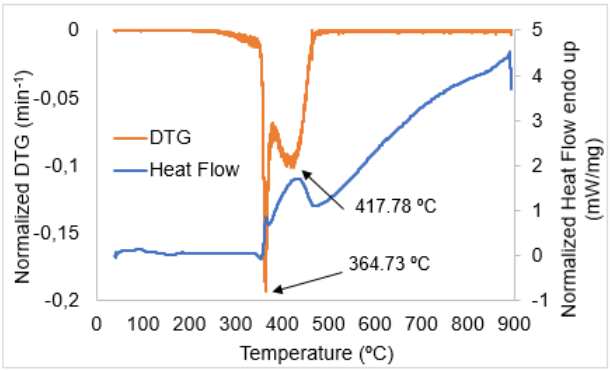

(b)

Figure 4.4 – TG curve (a), DSC vs DTG curves (b) for waste polystyrene degradation at 10 ºC/min.

The effect of the heating rate on the thermal decomposition of waste polystyrene was studied by conducting experiments at different heating rates (5, 10, 20, 50, 100 and 200 ºC/min). TG, DSC and DTG curves for the degradation of waste PS at different heating rates are shown in Figure 4.5.

The TG and DTG curve for the PS degradation (Figure 4.5a and c) show that the onset and maximum degradation temperatures shift to higher temperatures with the increase of the heating rate. This behaviour is likely related with kinetic effects and possible heat transfer limitations. As the heating rate increases, there is less time for heat to transfer inside the particles, which will leads to a decomposition at apparently higher temperatures. [85] The onset temperature increases in fact with the heating rate from 339.92 ºC at 5 ºC/min to 393.09 ºC at 100 ºC/min.

The DSC signal (Figure 4.5b) shows an endothermic curve in the temperature range of 40 ºC to approximately 350 ºC that becomes more pronounced as the heating rate increases.This endothermic curve doesn't have weight loss associated (Figure 4.7a).

The DSC curve (Figure 4.5b) shows that the endothermic peaks in the temperature range 350 ºC to 500 ºC, approximately, shifts to higher temperatures as the heating rates increases. The DTG curve (Figure 4.5c) confirms that during this temperature range a maximum weight loss occurs, indicating that these endothermic peaks correspond to the decomposition of the plastic. The maximum degradation temperatures (Tmax 1 and Tmax 2) increase with the heating rate (Table 4.6) and tend to stabilize (Figure 4.6).

The DSC curve (Figure 4.5b) shows an exothermic peak for higher heating rates (50, 100 and 200 ºC) after the degradation peak of the polymer. However, these peaks are not accompanied by significant mass loss, as confirmed by Figure 4.7 for the experiment at 50 ºC/min. To analyze the reproducibility of the experiments, this experiment was performed a second time (see Section 4.4.1.1). The second experiment performed didn't present any exothermic peak. This result indicates that the exothermic peak can be related with the position of the TG crucible in the furnace and with the asymmetry of the TG crucible, which can induce variations on the heat flow. [86]

The heat consumed by the pyrolysis process varies between 478.35 J/g (at 5ºC/min) and 413.55 J/g (at 100 ºC/min).

From 5 to 20 ºC/min the percentage of residue increases from 2.66 % to 4.58 % (Table 4.6). However the amount of residue does not show a regular pattern for higher heating rates (50, 100 and 200 ºC/min), which is likely related with thermal transpiration and air buoyancy effects that induce changes in the apparent weight. This has been observed in the reproductibility experiments, too (see Section 4.4.1.1).

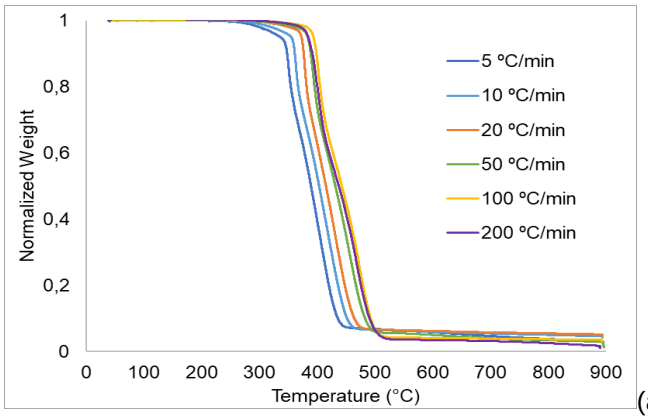

(a)

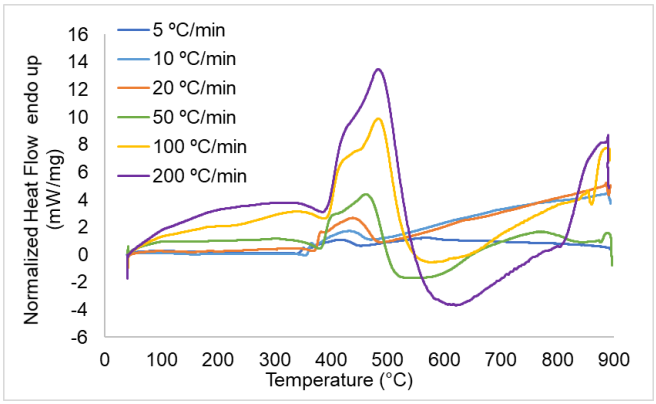

(b)

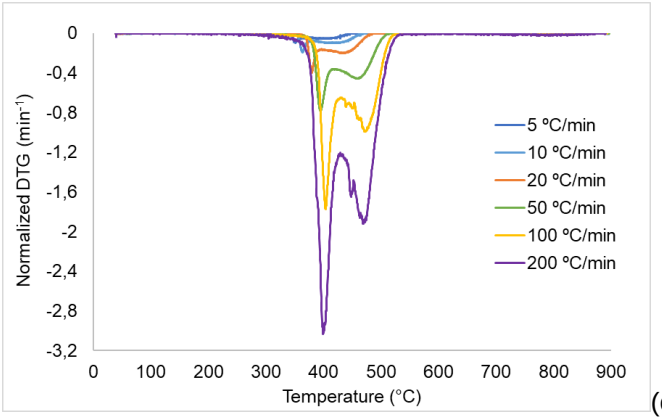

(c)

Figure 4.5 - TG (a), DSC (b) and DTG (c) curve for PS degradation at different heating rates.

Table 4.6 - Heating rate, onset temperature, maximum temperatures of degradation and percentages of residue for waste PS degradation at different heating rates.

Plastic	Heating rate (ºC/min)	Tonset (ºC)	Tmax1 (ºC)	Tmax2 (ºC)	Heat transferred (J/g)	Residue (%)
PS	5	339.92	351.24	409.79	478.35	2.66
	10	355.19	364.73	417.78	449.17	4.22
	20	372.27	379.81	437.57	464.34	4.58
	50	382.88	395.64	460.96	455.40	1.22
	100	393.09	403.38	473.88	413.55	3.00
	200	386.22	400.51	473.35	357.30	0.99

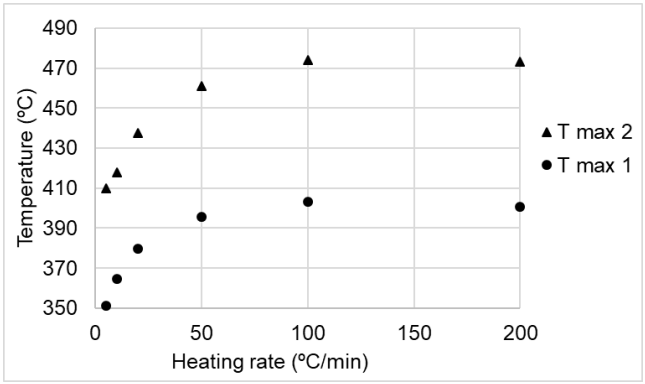

Figure 4.6 - Maximum degradation temperatures as function of the heating rate for the waste PS decomposition.

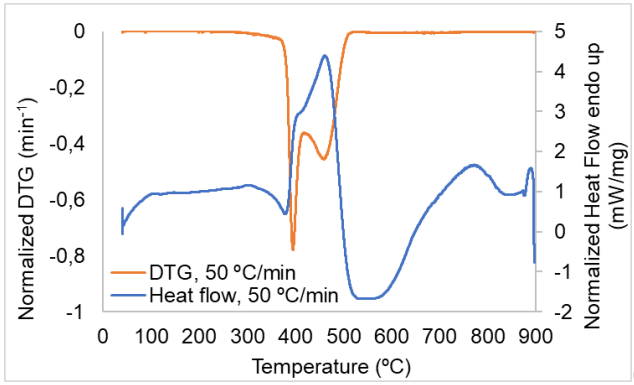

(a)

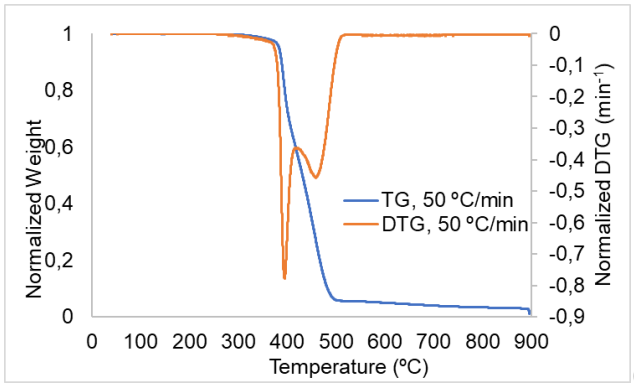

(b)

Figure 4.7 - DTG and DSC curves (a), TG and DTG curves (b) for PS degradation.

4.4.1.1 Reproducibility

The reproducibility of the experiments is important to understand not only the confidence of the obtained results but also the variability of the samples. There are different aspects that can influence the reproducibility of the experiments, namely:

- The initial mass of the sample. Some authors observed that the initial sample weight can slightly influence the conversion of reaction. However, for values lower than 45 mg, the conversion is almost independent of the initial mass.[44]
- The position of the TG crucible in the furnace induce variation on the consumed heat flow because of the non-uniformity of hot zones in the furnace [86]
- The possible unevenness of the temperature throughout the sample, particularly if it has a low thermal conductivity[86] , which is the case of plastics[4]

- The TG crucible geometry. [86]
- The crucible material. [86]

To analyse the reproducibility of the experiment, the thermal decomposition until 900 ºC at 50 ºC/min was performed a second time. Figure 4.8 presents the results of the TG, DSC and DTG analysis. The TG and DTG results (Figure 4.8a and c) show that the weight loss curve is very similar within the two experiments, indicating that the samples does not show significant variability, although a difference in the final amount of residue can be observed. The average values and the respective standard deviations were calculated (Table 4.7). The onset temperature is 384.08 ± 1.20 ºC; the first maximum degradation temperature is 395.14 ± 0.50 ºC; the second Tmax is 458.53 ± 2.43 ºC; the heat transferred during pyrolysis is 433.05 ± 22.36 J/g and the conversion 97.03 ± 1.75 %.

The DSC curve (Figure 4.8b) shows a large similarity until 500 ºC. From that temperature on, the exothermic peak present in the first experiment doesn't appear in the second experiment. Some aspects that can influence this result are the position of the TG crucible in the furnace, which can induce variations on the heat flow and the asymmetry of the TG crucible, but also the variability of the sample itself.

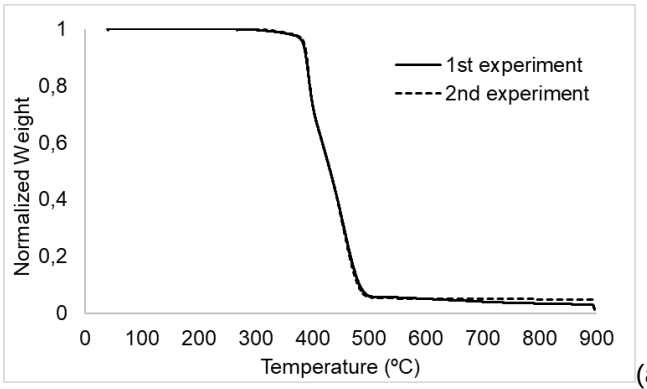

(a)

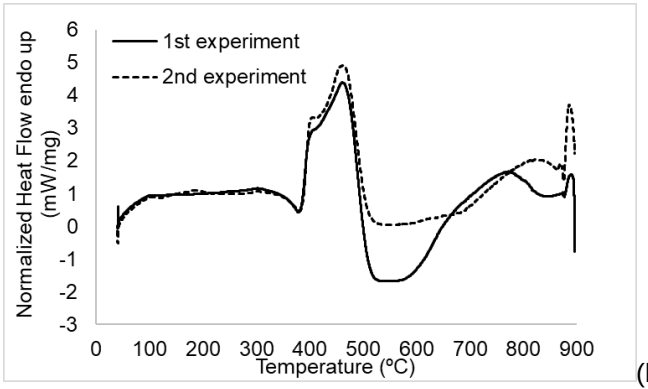

(b)

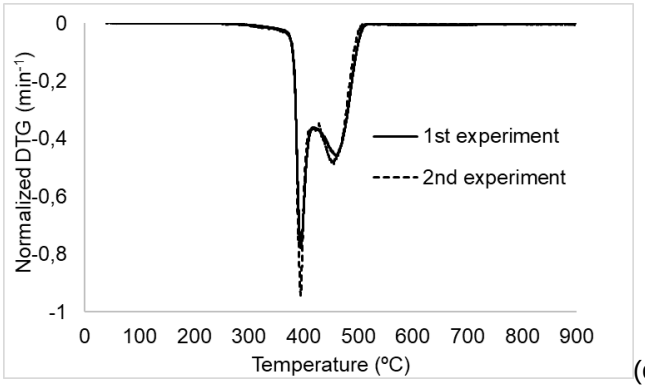

(c)

Figure 4.8 - Reproducibility of the experiments for the polystyrene experiments. Thermal decomposition until 900 ºC at 50 ºC/min. TG curve (a), DSC curve (b) and DTG curve (c).

Table 4.7 - Results of the reproducibility for the polystyrene experiments. Thermal decomposition until 900 ºC at 50 ºC/min.

	Initial Weight (mg)	Tonset (ºC)	Tmax1 (ºC)	Tmax2 (ºC)	Heat transferred (J/g)	Conversion (%)
1st experiment	19.49	382.88	395.64	460.96	455.40	98.78
2nd experiment	19.87	385.29	394.64	456.10	410.69	95.27
Average	19.68	384.08	395.14	458.53	433.05	97.03
Standard deviation	0.19	1.20	0.50	2.43	22.36	1.75

4.4.2 ABS

The waste ABS was first heated up to 900 ºC at 10 ºC/min. The TG, DSC and DTG results are presented in Figure 4.9. The TG curve (Figure 4.9a) shows that ABS starts to degrade at 393.24 ºC. From the DSC and DTG (Figure 4.9b) it is possible to see a well-defined endothermic peak followed by a “shoulder” between 380 ºC and 500 ºC, approximately, which corresponds to the decomposition of the plastic. The first maximum temperature is 415.89 ºC and the second is 437.55 ºC.

The onset temperature is higher than the ones found in literature for virgin ABS [3,49,50] and for ABS contaminated with brominated flame retardants [57].

The maximum degradation temperatures are lower than the ones obtained by Yang *et al.* for virgin ABS. Yang *et al.* observed two degradation peaks for virgin ABS and reported a first maximum degradation temperature of 445 ºC and a second of 554 ºC. [55] Jung *et al.* obtained for waste ABS containing brominated flame retardants and antimony trioxide different maximum degradation temperatures than ABS in study, namely a first T_{max} of 350 ºC and a second of 450 ºC. [53] The differences to the literature can be related with the operational conditions and/or with composition of the plastic itself, due to the different percentages of acrylonitrile, butadiene and styrene and because of the additives.

The DSC signal does not show melting peaks indicating that ABS is possibly amorphous.

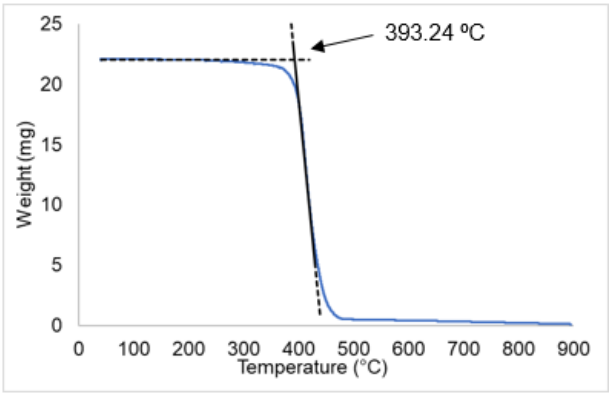

(a)

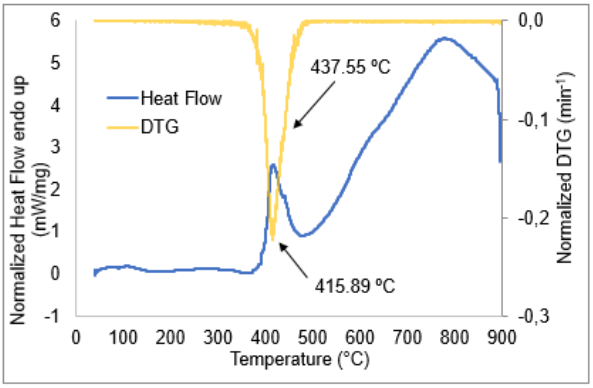

(b)

Figure 4.9 - TG curve (a), DSC vs DTG curves (b) for the ABS degradation at 10 ºC/min.

The effect of the heating rate on the thermal decomposition of ABS was studied by conducting experiments at different heating rates (5, 10, 20, 50, 100 and 200 ºC/min). TGA, DSC and DTG curves for the degradation of waste ABS at these different heating rates are shown in Figure 4.10 .The main observation and conclusion are the same as for waste PS, namely that the onset and maximum degradation temperature increase with the heating rate (see Chapter 4.4.1).

With the increase of the heating rate the onset temperature of waste ABS increases from 384.29 ºC at 5 ºC/min to 419.52 ºC at 100 ºC/min (Table 4.8). The onset temperature at 20 ºC/min is found to be similar to literature for virgin ABS, differing 1 ºC. [24]

The first endothermic curve in the DSC signal (Figure 4.10b) between 40 ºC and approximately 390 ºC becomes more pronounced as the heating rate increases. There is no mass loss involved (Figure 4.12).

The DSC curve shows that the two endothermic peaks in the temperature range of 390 to 500 ºC, approximately, shift to higher temperatures as the heating rates increases. The DTG curve (Figure 4.10c) confirms that during this temperature range a maximum weight loss occurs, indicating that these endothermic peaks correspond to the decomposition of the plastic. The maximum degradation temperatures (Tmax 1 and Tmax 2) increase with the heating rate (Table 4.8 and Figure 4.11)

The DSC signal (Figure 4.10b) shows an exothermic curve for higher heating rates, namely for 100 ºC/min and 200 ºC/min. Figure 4.12 confirms that this exothermic curve is not accompanied by any significant weight loss.

From 5 to 50 ºC/min the residue increases from 0.10 % to 1.03 % (Table 4.8) and becomes approximately constant for higher heating rates.

The heat consumed by the pyrolysis process increases with the heating rate from 391.93 J/g at 5 ºC/min to 502.30 J/g at 20 ºC/min. At higher heating rates (50, 100 and 200 ºC/min), the heat consumed during pyrolysis tends to decrease (Table 4.8).

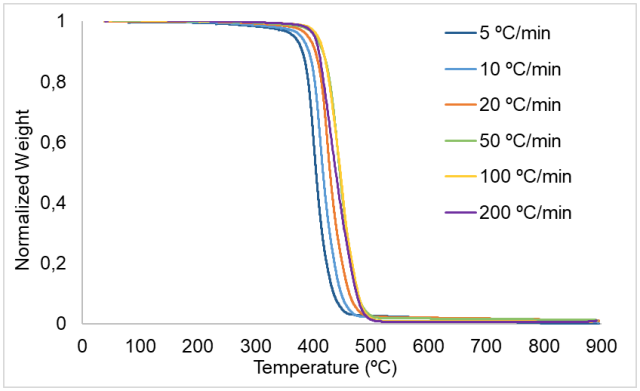

(a)

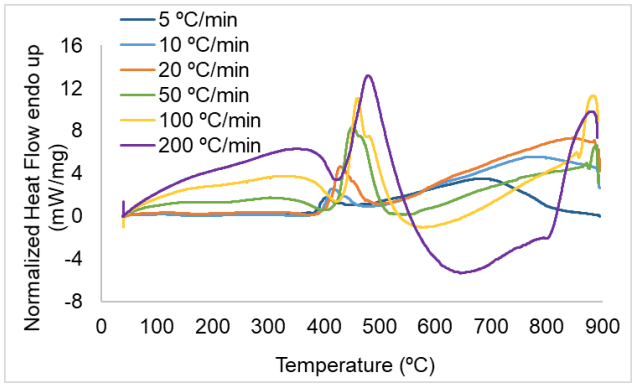

(b)

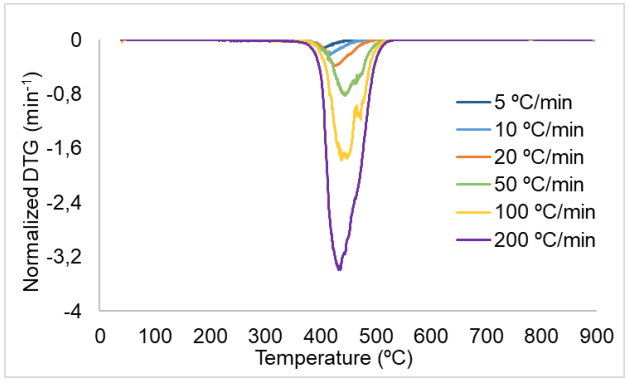

(c)

Figure 4.10 - TG (a), DSC(b) and DTG(c) curves for ABS degradation at different heating rates.

Table 4.8 – Heating rate, onset temperature, maximum temperature and percentage of residue for ABS decomposition at different heating rates.

Plastic	Heating rate (ºC/min)	T onset (ºC)	Tmax1 (ºC)	Tmax2 (ºC)	Heat transferred (J/g)	Residue (%)
ABS	5	384.29	403.99	*	391.93	0.10
	10	393.24	415.89	437.55	489.24	0.36
	20	401.34	427.59	453.34	502.30	0.90
	50	419.54	445.00	461.72	489.10	1.03
	100	419.52	449.80	472.44	286.57	0.85
	200	405.44	436.07	*	233.68	1.05

* no clear peak.

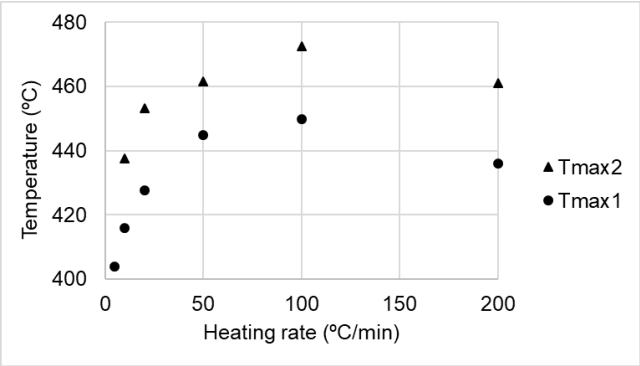

Figure 4.11 - Maximum weight loss temperatures as function of the heating rate for the waste ABS decomposition.

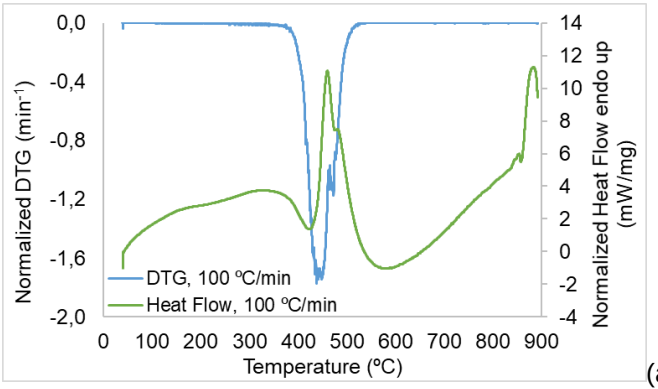

(a)

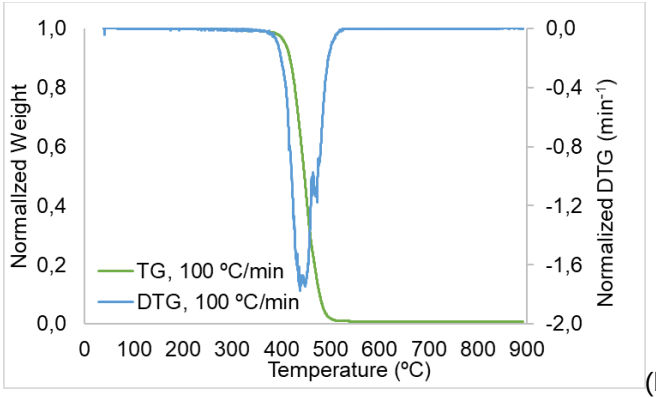

(b)

Figure 4.12 -DTG and DSC curves (a); TG and DTG curves (b) for ABS degradation with a heating rate of 100 ºC/min.

4.5 TG/DSC analysis - isothermal conditions

4.5.1 PS

Isothermal experiments were performed at different temperatures to analyse the degradation of waste polystyrene at these conditions. The TGA, DSC and DTG results are present in Figure 4.13.

The TG curve (Figure 4.13a) shows that the plastic starts to degrade at around 350 ºC for all isothermal experiments. As the temperature increases, the conversion increases. The conversion values are summarized in Table 4.9. After the isothermal run, at 300 ºC only 9.37 % of the initial sample weight was converted. At 400 ºC the conversion is approximately 92.60 % and from this temperature on the conversion tends to stabilize, reaching 96 % at 500 ºC (Figure 4.14). This observation can be confirmed by the DTG curve (Figure 4.13b). As the temperature increases, the weight loss rate increases. From 400 ºC to 500 ºC two peaks are visible. The DSC curve (Figure 4.13d) shows for the isothermal at 400 ºC to 500 ºC two endothermic peaks at the same time range where the maximum weight loss occurs, which are related with the degradation of the plastic.

The weight loss during the heating ramp increases with temperature, which is expected since the time to react during the heating increases, for the same heating rate (Table 4.9).

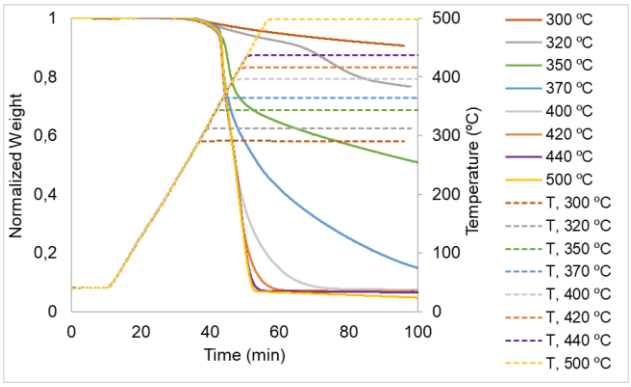

(a)

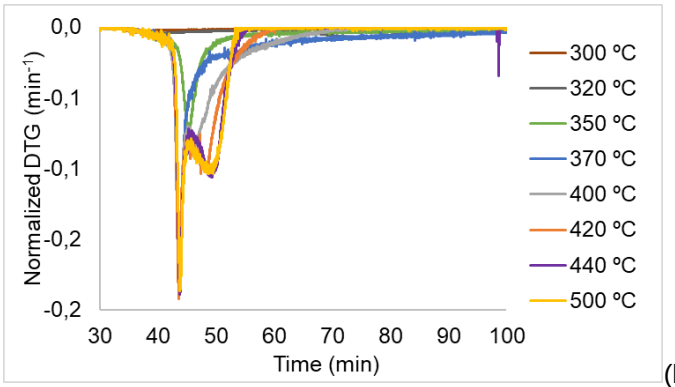

(b)

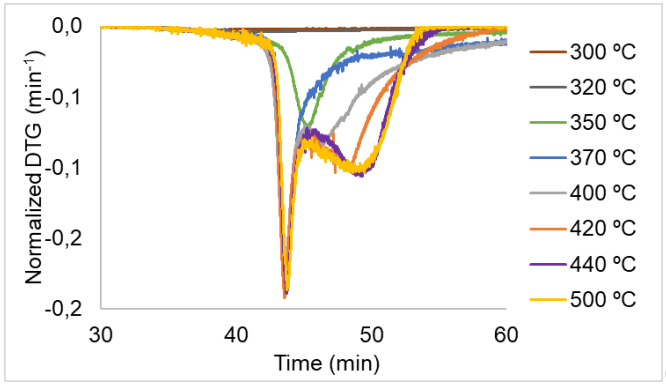

(c)

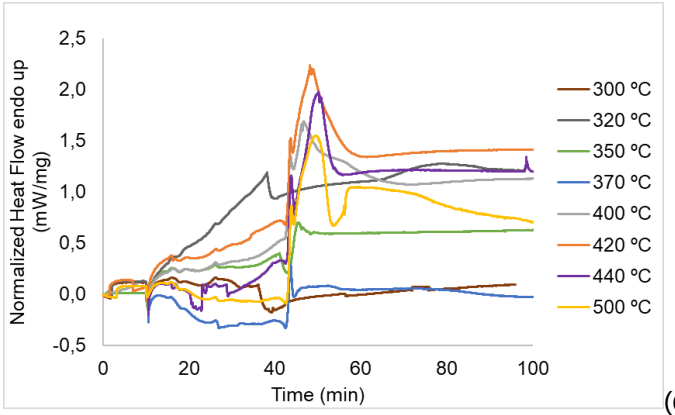

(d)

Figure 4.13 - TG curve (a), DTG curve (b), close-up of DTG curve (c) and DSC curve (d) of waste polystyrene degradation under isothermal conditions.

Table 4.9 - Data obtained from the isothermal experiments for PS.

Plastic	Isothermal temperature (ºC)	Weight loss during heating (%)	Weight loss at the isothermal (%)	Total conversion after isothermal run (%)
PS	300	0.45	8.95	9.37
	320	0.98	22.48	23.37
	350	3.62	45.88	49.46
	370	5.30	80.88	86.12
	400	39.46	53.10	92.60
	420	57.44	35.67	93.20
	440	75.76	17.73	93.57
	500	93.34	2.68	96.00

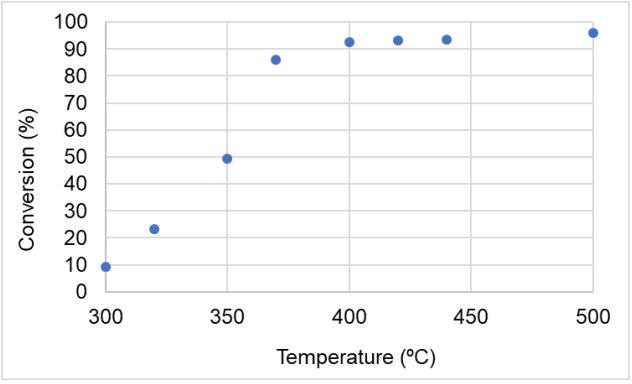

Figure 4.14 - Conversion as function of temperature.

4.5.2 ABS

Isothermal experiments were also performed at different temperatures to analyse the degradation of ABS at these conditions. The TGA, DSC and DTG results are present in Figure 4.15.

The TG curve (Figure 4.15a) shows that the plastic starts to degrade at around 390 ºC for all the isothermal experiments. As the temperature increases, the conversion increases (Figure 4.16). At 380 ºC approximately 84 % of the initial mass was converted, while at 500 ºC the conversion reaches 98.52 % (Table 4.10).

The weight loss during the heating ramp increases with temperature, which is expected since the time to react during the heating increases, for the same heating rate (Table 4.10).

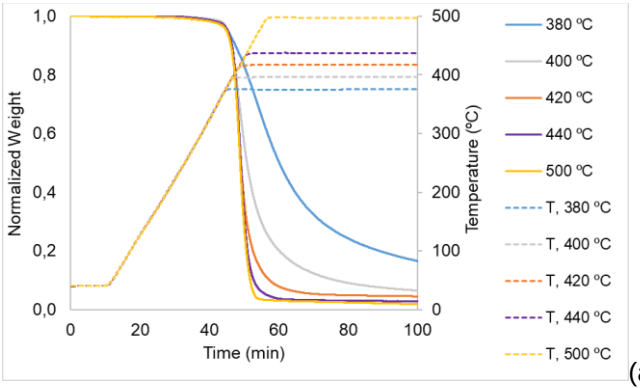

(a)

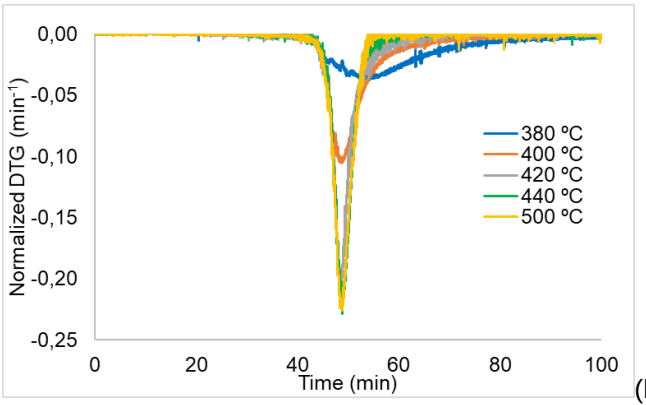

(b)

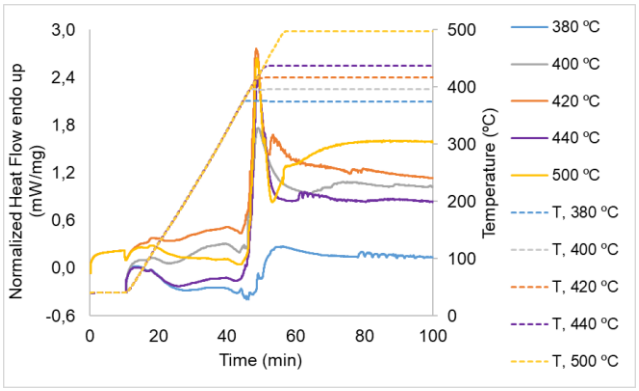

(c)

Figure 4.15 - TGA(a), DTG(b) and DSC(c) curves for ABS degradation at isothermal conditions.

Table 4.10 - Data obtained from the isothermal experiments for ABS.

Plastic	Isothermal temperature (ºC)	Weight loss during heating (%)	Weight loss at the isothermal (%)	Total conversion after isothermal run (%)
ABS	380	3.26	81.16	84.43
	400	8.00	85.99	93.98
	420	28.60	66.92	95.58
	440	67.60	29.69	97.28
	500	96.59	1.85	98.52

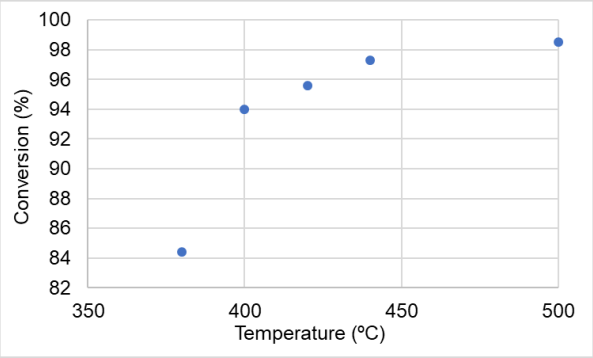

Figure 4.16 - Conversion vs temperature for ABS degradation at isothermal conditions.

4.6 Combustion

4.6.1 PS

The degradation of waste polystyrene under air was analysed. The TGA, DSC and DTG results are presented in Figure 4.17.

The TG curve (Figure 4.17a) shows that the degradation under air presents a different behaviour from 450 ºC on, comparing to the degradation in nitrogen. The DSC signal (Figure 4.17b) confirms that at approximately 450 ºC an exothermic peak appears, followed by a second one at 500 ºC. The DTG curve (Figure 4.17c) shows an extra weight loss peak at 500 ºC. Comparing the DSC and DTG curves together (Figure 4.18) it is possible to see that the first two weight loss peaks are related with the degradation of the plastic. The first exothermic peak occurs during the degradation of the plastic. The second exothermic peak is associated with the third weight loss peak, indicating that an oxidative degradation takes place.

The temperature range of degradation under nitrogen conditions is approximately from 350 to 500 ºC, while under air conditions it is shortened, ending at approximately 450 ºC. The heat transferred during the global thermal degradation of the polystyrene under air conditions is lower than under nitrogen: 335.94 J/g and 449.17 J/g, respectively (Table 4.11).

The onset temperature under air is 353.43 ºC and under nitrogen 355.19 ºC (Table 4.11). The onset temperature reported in literature for the degradation of virgin PS under air conditions is in the range of 237.55 to 308.95 ºC[30–32]. The onset temperature of waste PS is higher than the reported in literature for virgin PS.

The maximum degradation temperature is 364.73 ºC under inert atmosphere and 361.74 ºC for combustion, (Table 4.11). Values for virgin PS found in literature had a maximum temperature in the range of 372.85 to 409.85 ºC, under air.[30–32]

The combustion of the plastic leads to less remaining residue (Table 4.11) when compared with inert atmosphere, namely 0.83 % and 4.22%, respectively, because the non-volatile heavy hydrocarbons are degraded.

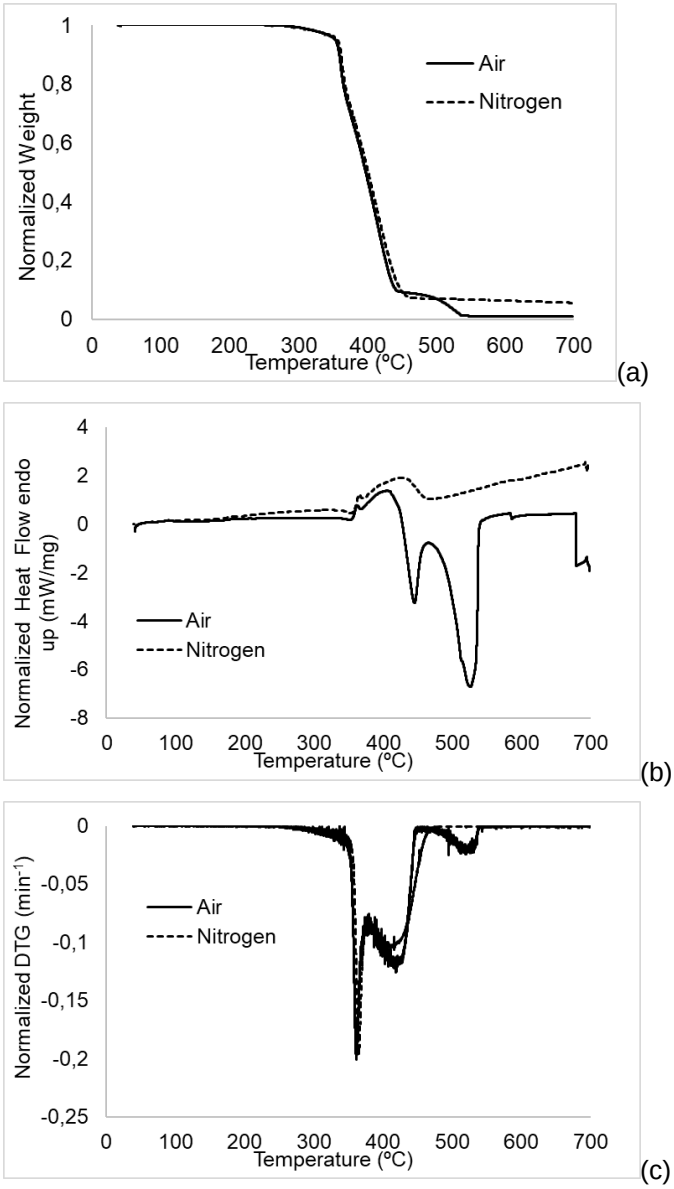

Figure 4.17 - TG (a), DSC (b) and DTG (c) curves for PS decomposition under air and nitrogen atmosphere.

Table 4.11 - Results of PS decomposition under air and nitrogen atmosphere.

Plastic	Atmosphere	Initial Mass (mg)	T onset (ºC)	T max1 (ºC)	T max2 (ºC)	Heat transferred (J/g)	Residue (%)
PS	Air	19.25	353.43	361.74	*	335.94	0.83
	Nitrogen	19.85	355.19	364.73	417.78	449.17	4.22

*difficult to determine.

**Corresponds to the heat consumed by the global thermal degradation process.

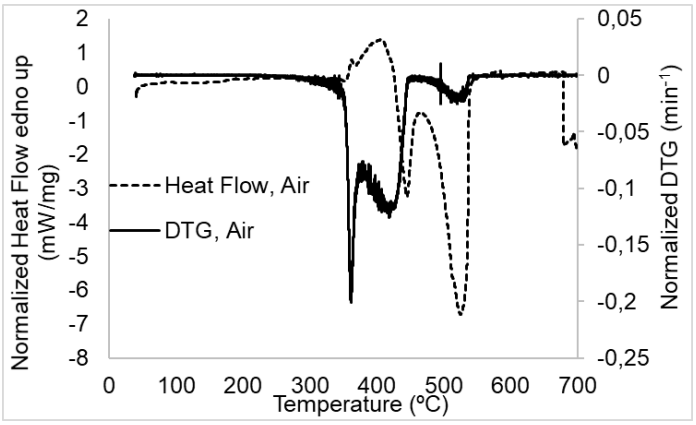

Figure 4.18 - DSC curve vs DTG curve for the degradation of PS under air conditions.

4.6.2 ABS

The degradation of waste ABS under air was also analysed and the TG, DTG and DSC curves are presented in Figure 4.19.

The TG curve (Figure 4.19a) shows that the degradation under air presents a different behaviour for temperatures above 450 ºC, when comparing to the degradation under nitrogen. The DSC signal (Figure 4.19b) confirms that at approximately 550 ºC an exothermic peak appears. The DTG curve (Figure 4.19c) shows one extra weight loss peak at 550 ºC for the degradation of ABS under air. Comparing both TG and DTG curve (Figure 4.20) it is possible to see that the exothermic peak that appears at 550 ºC is associated with the extra weight loss peak, indicating that an oxidative degradation takes place. Interesting to notice is that after the first endothermic peak, a plateau between 450 and 500 ºC is formed, which may indicate that a stable residue is formed due to the presence of oxygen, which will then degrade at 550 ºC. This observation has been reported in literature, too. [87]

The temperature range of degradation under air conditions is wider than under nitrogen atmosphere.

Under inert atmosphere the onset temperature is 393.24 ºC and under air it decreases to 391.26 ºC (Table 4.12). In literature the onset temperature for the degradation of virgin ABS under air is around 370 ºC. [51,58] The onset temperature of waste ABS is higher than the reported for virgin ABS.

The first and second maximum degradation temperature obtained under air is 417.47 ºC and 560.82 ºC, respectively (Table 4.12).

The remaining residue decreases under air when compared to the process under nitrogen, namely from 0.36 % to 0.11%, probably because non-volatile heavier hydrocarbons are degraded. [48]

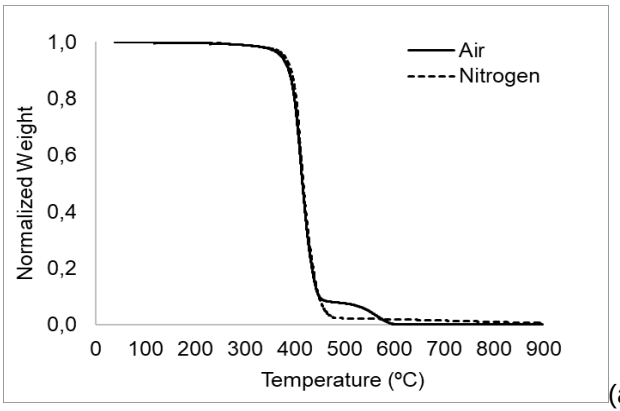

(a)

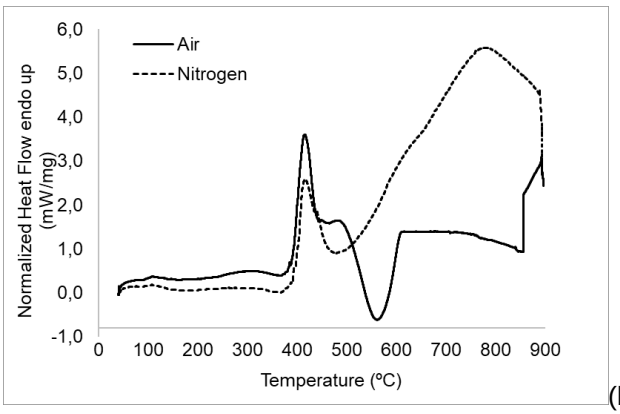

(b)

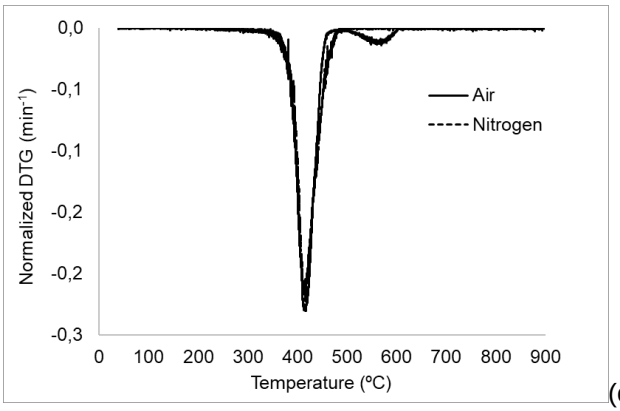

(c)

Figure 4.19 - TG (a), DSC (b) and DTG (c) curves for ABS decomposition under air and nitrogen atmosphere.

Table 4.12 - Results of ABS decomposition under air and nitrogen atmosphere.

Plastic	Atmosphere	Initial Mass (mg)	T onset (ºC)	T max1 (ºC)	Tmax 2 (ºC)	Heat transferred (J/g)*	Residue (%)
ABS	Air	21.61	391.26	417.47	560.82	964.01	0.11
	Nitrogen	22.05	393.24	415.89	437.55	489.24	0.36

*Corresponds to the heat consumed by the global thermal degradation process.

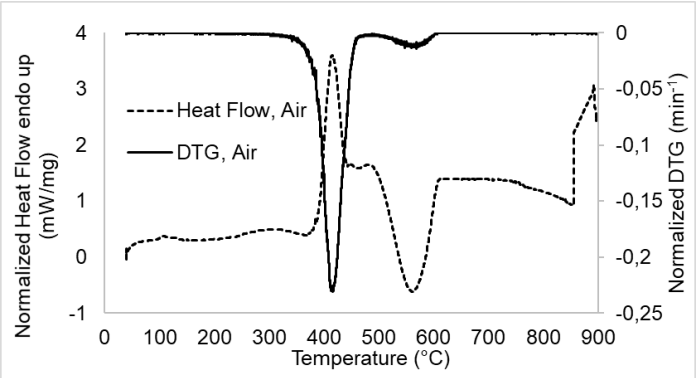

Figure 4.20 - DSC curve vs DTG curve for the degradation of ABS under air conditions.

4.7 Kinetic model

Different kinetic models were built and analysed for PS and ABS decomposition using the TG/DTG data.

The reaction rate can be described by Equation 4.1, where $k(T)$ is the temperature-dependent kinetic constant, n is the reaction order (for this work was considered as 1) and W is the fractional weight of the sample at the time t.

Equation 4.1 - Reaction rate.

$$\frac{dW}{dt} = -k(T)W^n$$

The kinetic constant $k(T)$ is described by the Arrhenius Equation (Equation 4.2), where k_0 is the pre-exponential factor, s^{-1}; E_a is the activation energy, J/mol; R is the gas constant, J/(molK) and *T* the sample temperature, K. A kinetic constant reference, $k_{ref}(T_{ref})$ (Equation 4.3) is introduced to reduce the correlation between the pre-exponential factor and the activation energy during the fitting processes, where T_{ref} is a reference temperature chosen within the range of the experimental values (673,15 K was chosen for this work). The resulting kinetic constant is described by Equation 4.4.

Equation 4.2 - Kinetic constant.

$$k(T) = k_o e^{-\frac{E_a}{RT}}$$

Equation 4.3 - Kinetic constant reference.

$$k_{ref}(T_{ref}) = k_0 e^{-\frac{E_a}{RT_{ref}}}$$

Equation 4.4 - Kinetic constant as function of the kinetic constant reference.

$$k(T) = k_{ref}(T_{ref}) e^{-\frac{E_a}{R}\left(\frac{1}{T}-\frac{1}{T_{ref}}\right)}$$

To calculate the fraction weight, the Euler method was used. All the models were fitted to the experimental TG curve. The model parameters were estimated by a least-squares procedure, using the sum of the squares of the residues on the fractioned weight as the objective function to be minimized (Equation 4.5).

Equation 4.5 - Objective Function (O.F).

$$O.F = \sum_{all\ data\ points} (Fraction\ Weight_{experimental} - Fraction\ Weight_{computed})^2$$

The optimization procedure was carried out using the Solver tool from Microsoft ® Office Excel.

4.7.1 Discrimination of models

To discriminate the studied models the R squared and adjusted R squared coefficients were applied. The R squared quantifies how well a model fits the data. A perfect fit will result in an R^2 value of 1, a very good fit near 1 and a poor fit near 0.[88,89] The adjusted R^2 accounts for the number of parameters that are being used to fit the model to the experimental data, indicating if a higher number of parameters induces a better fit or not. [89]

R^2 is given by Equation 4.6. [88]

Equation 4.6 - R squared equation.

$$R^2 = 1 - \frac{SSE}{SS_{yy}}$$

where $SSE = \sum(y - \hat{y})^2$, $SS_{yy} = \sum(y - \bar{y})^2$, y is the actual experimental value, $\hat{y}$ is the predicted value of y, and $\bar{y}$ is the mean of the y values.

The adjusted R^2 is given by Equation 4.7. [89]

Equation 4.7 - Adjusted R squared equation.

$$Adjused\ R^2 = 1 - \frac{SSE/\ (np - K)}{SS_{yy}/(np - 1)}$$

where SSE is the sum-of-squares of the discrepancy between the y value of the curve and the predicted value of y; SS_{yy} is the sum-of-squares of the differences between the overall y mean and each y value; np is the number of data points, and K is the number of parameters fit.

The adjusted R^2 is smaller than the ordinary R^2 whenever the number of parameters (*K*) is greater than 1. [89] By adding useful variables, the adjusted R squared will increase, and the addition of useless variables decreases the adjusted R squared. [90]

4.7.2 Estimation of errors in the estimated kinetic parameters

The bootstrap is a resampling method that permits to quantify uncertainty by calculating standards errors and confidence intervals by sampling a dataset with replacement. The sample data is assumed to represent the population from which it was taken.[91] A bootstrap sample $x^* = (x_1{}^*, x_2{}^*, \dots, x_n{}^*)$ is obtained by randomly sampling *n* times, with replacement, from the original data points $x_1, x_2, \dots, x_n$. For example, with n=7 one possible bootstrap sample is $x^* = (x_5, x_7, x_5, x_4, x_7, x_3, x_1)$. [92]

In the case of the ABS and PS modelling, bootstrapping was performed by creating a bootstrap sample (new sample) with the same size as the original sample using the function *random* from *Excel*. The random number generated was used to establish a weight of 0, 1 or 2 to be applied to each experimental data point. Thus, a function was applied to the random number: if the number is lower than 1/3 than the number should stay; if It is lower than 2/3 it should be throwed away; and if it is not of these cases than it equals 2. These weights were used in calculation of the sum of the squares of the residuals; the *Solver* tool from *Excel* was used to estimate a new set of kinetic parameters by the same least-squares procedure.

To estimate the standard deviation of the estimated kinetic constants this procedure was carried-out 10 times, generating 10 resampled sets of data for each model.

4.7.3 Virgin PS

4.7.3.1 Understanding of the degradation mechanism

The TG/DSC results presented in Chapter 4.3 show one decomposition peak for virgin PS, which is in agreement with literature.[30–32] Therefore, the model studied considers a one-component decomposition (Equation 4.8). The reaction rate is given by Equation 4.9. The reaction order, *n*, is considered as 1.

Equation 4.8 - Reaction.

$$C_1 \xrightarrow{k1} prod.$$

Equation 4.9 - Reaction rate.

$$\frac{dW_{C1}}{dt} = -k_{ref,1} e^{-\frac{E_{a,1}}{R}\left(\frac{1}{T}-\frac{1}{T_{ref}}\right)} {W_{C1}}^{n_1}$$

The TG and DTG curve for the model and experimental data of PS1 are present in Figure 4.21. The model was fitted to the TG curve. The results show that the fitting is very good and thus the model describes the degradation mechanism of PS1.

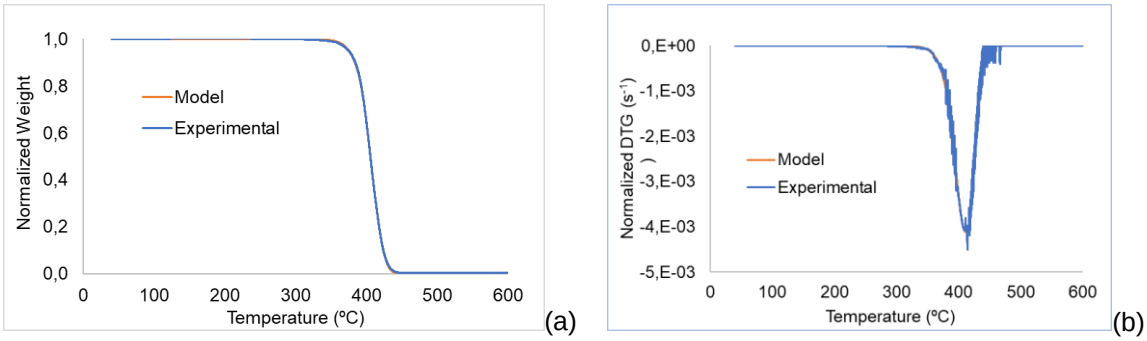

Figure 4.21 - Model vs experimental data for PS1. (a) - TG curve; (b) - DTG curve.

The TG and DTG curve for the model and experimental data of PS2 are present in Figure 4.22. The model was fitted to the TG curve. The results show that the fitting is very good and thus the model describes the degradation mechanism of PS2.

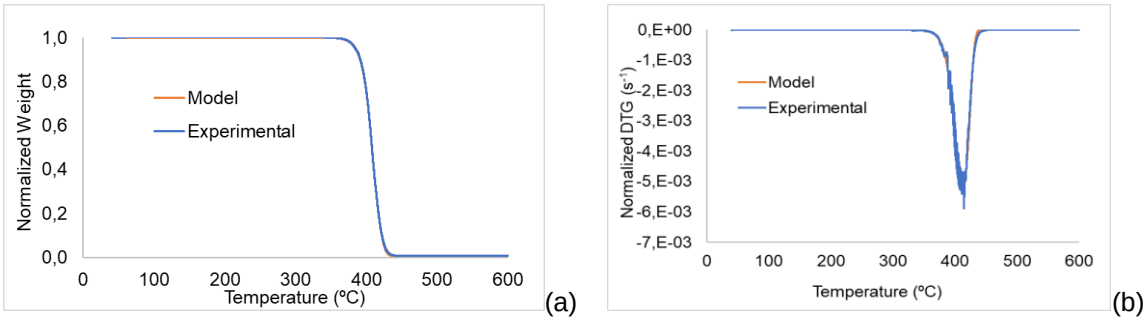

Figure 4.22 – Model vs experimental data for PS2. (a) - TG curve; (b) - DTG curve.

4.7.3.2 Discrimination of the model

To analyse the fitting of the model to the experimental data a non-linear regression was performed, and the R squared was calculate, as described in Chapter 4.7.1. The obtained R squared are 0.999967 for PS1 and 0.999899 for PS2 (Table 4.13). This result indicates that the fitting is good.

Table 4.13 - Discrimination of PS1 and PS2 model.

Polymer/Parameter	SSE	SS_{yy}	R^2
PS1	$1.87\ x\ 10^9$	$5.58\ x\ 10^{13}$	0.999967
PS2	$5.69\ x\ 10^9$	$5.66\ x\ 10^{13}$	0.999899

4.7.3.3 Kinetic parameters

The bootstrap method, explained in Chapter 4.7.2, was used to estimate the standard deviation of the estimated variables. Table 4.14 presents the average kinetic parameters obtained and their standard deviation. For PS1 an activation energy of 282.07 ± 0.04 kJ/mol was obtained and for PS2, a value of 375.00 ± 0.10 kJ/mol. Both virgin polystyrene samples showed larger activation energies,

although with the same order of magnitude, as those found in literature (between 190.00 and 217.9 kJ/mol) [30,73–75], which have used another methods to estimate the kinetic parameters (see Chapter 2.6.1).

The results indicate that the molecular weight has some influence on the activation energy, namely that polystyrene with a higher molecular weight presents a higher activation energy. Both virgin PS have different particle size, which might influence the kinetics.

Table 4.14 – Average kinetic parameters obtained for virgin PS1 and PS2. W= fractioned weight, n=reaction order, kref= reference kinetic constant (s^{-1}), Ea=activation energy (kJ/mol).

Polymer/Kinetic parameters	PS1	PS2
W_{C1}	1	1
n_1	1	1
$k_{ref,1}$ (1/s)	$5.02\ x\ 10^{-3} \pm 2.57x\ 10^{-7}$	$4.59\ x\ 10^{-3} \pm 8.76x\ 10^{-7}$
$E_{a,1}$ (kJ/mol)	282.09 ± 0.05	375.01 ± 0.10

4.7.4 Waste PS

4.7.4.1 Study of the possible model/Understanding of the degradation mechanism

The degradation pattern for the waste PS samples is somewhat more complicated than the one for the virgin PS samples. Different models were studied for the decomposition of polystyrene since its degradation mechanism is known to be very complex [93–95]. While the TG analysis showed only one decomposition peak for virgin PS, it showed two distinct decomposition peaks for the waste PS sample.

As a first approach, six models were studied, which tried to model the experimental TG and DTG curve under dynamic conditions at 10 ºC/min. This first attempt was elaborated with the intention of finding a model that better describes the decomposition of waste polystyrene.

Table 4.15 summarizes the models that were constructed. All the models were fitted to the experimental TG curve. For all the models it was considered the existence of a fixed quantity of residue that doesn't degrade and is maintained constant throughout the degradation.

- Model 1: Considers the degradation of one pseudo-component to a product.
- Model 2: Considers a two-component decomposition in parallel. The pseudo-components are independent from each other.
- Model 3: Considers three pseudo-components that decompose in parallel. The components are independent from each other.
- Model 4: Considers that a pseudo-component degrades in a parallel reaction to a product and an intermediate, which degrades as well with different kinetic parameters. This reaction model has been considered by other authors found in the literature. [74]
- Model 5: It considers a reaction in series, in which a pseudo-component decomposes to a product and an intermediate and the intermediate decomposes to a product as well.
- Model 6: It is a more complex version of model 5, considering a second pseudo-component and intermediate.

Table 4.15 - Kinetic models considered for the decomposition of waste polystyrene.

PS		
Model	**Reaction**	**Equations**
1	$C_1 \xrightarrow{k1} prod.$ $residue$	$\frac{dW_{C1}}{dt} = -k_{ref,1} e^{-\frac{E_{a,1}}{R}\left(\frac{1}{T}-\frac{1}{T_{ref}}\right)} {W_{C1}}^{n_1}$ $W_t = W_{C1} + W_{residue}$ $\frac{dW_t}{dt} = \frac{dW_{C1}}{dt}$
2	$C_1 \xrightarrow{k1} prod.$ $C_2 \xrightarrow{k2} prod.$ $residue$	$\frac{dW_{C1}}{dt} = -k_{ref,1} e^{-\frac{E_{a,1}}{R}\left(\frac{1}{T}-\frac{1}{T_{ref}}\right)} {W_{C1}}^{n_1}$ $\frac{dW_{C2}}{dt} = -k_{ref,2} e^{-\frac{E_{a,2}}{R}\left(\frac{1}{T}-\frac{1}{T_{ref}}\right)} {W_{C2}}^{n_2}$ $W_t = W_{C1} + W_{C2} + W_{residue}$ $\frac{dW_t}{dt} = \frac{dW_{C1}}{dt} + \frac{dW_{C2}}{dt}$
3	$C_1 \xrightarrow{k1} prod.$ $C_2 \xrightarrow{k2} prod.$ $C_3 \xrightarrow{k3} prod.$ $residue$	$\frac{dW_{C1}}{dt} = -k_{ref,1} e^{-\frac{E_{a,1}}{R}\left(\frac{1}{T}-\frac{1}{T_{ref}}\right)} {W_{C1}}^{n_1}$ $\frac{dW_{C2}}{dt} = -k_{ref,2} e^{-\frac{E_{a,2}}{R}\left(\frac{1}{T}-\frac{1}{T_{ref}}\right)} {W_{C2}}^{n_2}$ $\frac{dW_{C3}}{dt} = -k_{ref,3} e^{-\frac{E_{a,3}}{R}\left(\frac{1}{T}-\frac{1}{T_{ref}}\right)} {W_{C3}}^{n_3}$ $W_t = W_{C1} + W_{C2} + W_{C3} + W_{residue}$ $\frac{dW_t}{dt} = \frac{dW_{C1}}{dt} + \frac{dW_{C2}}{dt} + \frac{dW_{C3}}{dt}$
4	$C_1 \xrightarrow{k1} I^*$ $C_1 \xrightarrow{k2} prod.$ $I^* \xrightarrow{k3} prod.$ $residue$	$\frac{dW_{C1}}{dt} = -k_{ref,1} e^{-\frac{E_{a,1}}{R}\left(\frac{1}{T}-\frac{1}{T_{ref}}\right)} (xW_{C1})^{n_1} - k_{ref,2} e^{-\frac{E_{a,2}}{R}\left(\frac{1}{T}-\frac{1}{T_{ref}}\right)} ((1-x)W_{C1})^{n_2}$ $\frac{dW_I}{dt} = k_{ref,1} e^{-\frac{E_{a,1}}{R}\left(\frac{1}{T}-\frac{1}{T_{ref}}\right)} (xW_{C1})^{n_1} - k_{ref,3} e^{-\frac{E_{a,3}}{R}\left(\frac{1}{T}-\frac{1}{T_{ref}}\right)} {W_I}^{n_3}$ $W_t = W_{C1} + W_I + W_{residue}$ $\frac{dW_t}{dt} = \frac{dW_{C1}}{dt} + \frac{dW_I}{dt}$
5	$C_1 \xrightarrow{k1} prod. + I^*$ $I^* \xrightarrow{k2} prod.$ $residue$	$\frac{dW_{C1}}{dt} = -k_{ref,1} e^{-\frac{E_{a,1}}{R}\left(\frac{1}{T}-\frac{1}{T_{ref}}\right)} {W_{C1}}^{n_1}$ $\frac{dW_I}{dt} = k_{ref,1} e^{-\frac{E_{a,1}}{R}\left(\frac{1}{T}-\frac{1}{T_{ref}}\right)} (xW_{C1})^{n_1} - k_{ref,2} e^{-\frac{E_{a,2}}{R}\left(\frac{1}{T}-\frac{1}{T_{ref}}\right)} (W_I)^{n_2}$ $W_t = W_{C1} + W_I + W_{residue}$ $\frac{dW_t}{dt} = \frac{dW_{C1}}{dt} + \frac{dW_I}{dt}$

6	$C_1 \xrightarrow{k1} prod. + {I_1}^*$ ${I_1}^* \xrightarrow{k2} prod.$ $C_2 \xrightarrow{k3} prod. + {I_2}^*$ ${I_2}^* \xrightarrow{k4} prod.$ $residue$	$\frac{dW_{C1}}{dt} = -k_{ref,1} e^{-\frac{E_{a,1}}{R}\left(\frac{1}{T}-\frac{1}{T_{ref}}\right)} {W_{C1}}^{n_1}$ $\frac{dW_I}{dt} = k_{ref,1} e^{-\frac{E_{a,1}}{R}\left(\frac{1}{T}-\frac{1}{T_{ref}}\right)} (xW_{C1})^{n_1} - k_{ref,2} e^{-\frac{E_{a,2}}{R}\left(\frac{1}{T}-\frac{1}{T_{ref}}\right)} (W_I)^{n_2}$ $\frac{dW_{C2}}{dt} = -k_{ref,3} e^{-\frac{E_{a,3}}{R}\left(\frac{1}{T}-\frac{1}{T_{ref}}\right)} {W_{C2}}^{n_3}$ $\frac{dW_{I,2}}{dt} = k_{ref,3} e^{-\frac{E_{a,3}}{R}\left(\frac{1}{T}-\frac{1}{T_{ref}}\right)} (x_2 W_2)^{n_3} - k_{ref,4} e^{-\frac{E_{a,4}}{R}\left(\frac{1}{T}-\frac{1}{T_{ref}}\right)} (W_{I,2})^{n_4}$ $W_t = W_{C1} + W_I + W_{C2} + W_{I,2} + W_{residue}$ $\frac{dW_t}{dt} = \frac{dW_{C1}}{dt} + \frac{dW_I}{dt} + \frac{dW_{C2}}{dt} + \frac{dW_{I,2}}{dt}$

Figure 4.23 presents the fitting of the models to the experimental data, the first observation are the following:

- Model 1: The model shows only one peak, as expected. It is clearly inadequate to describe the observed results.
- Model 2: The model begins the decomposition at lower temperatures and has a slightly more intensive maximum. However, overall the model provides an adequate description of the experimental data.
- Model 3: It was built in an attempt to improve model 2. The TG curve shows that the fractioned weight of the 3rd pseudo-component is practically zero and neglectable.
- Model 4: The model doesn't adequately describe the initial weight loss neither the first degradation peak visible in the DTG curve.
- Model 5: The model doesn't describe the initial weight loss neither the first degradation peak visible in the DTG curve.
- Model 6: The TG curve shows that the fractioned weight of both intermediates is practically zero and despicable.

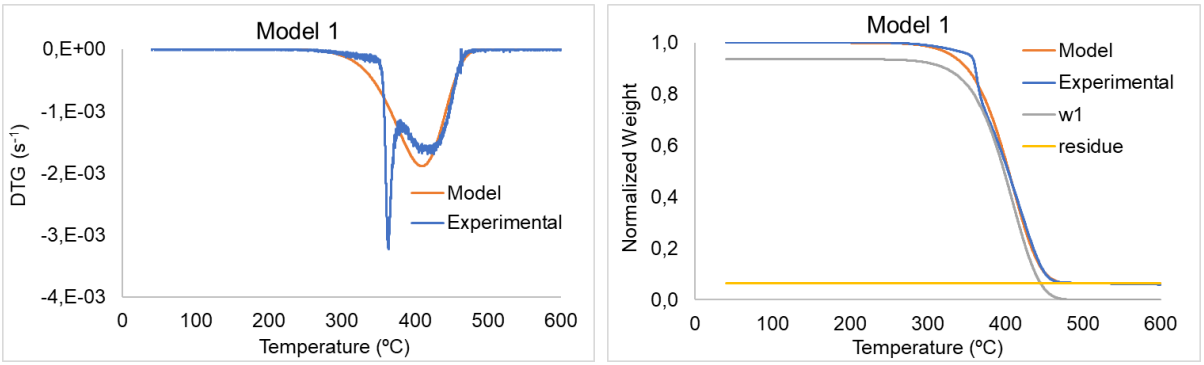

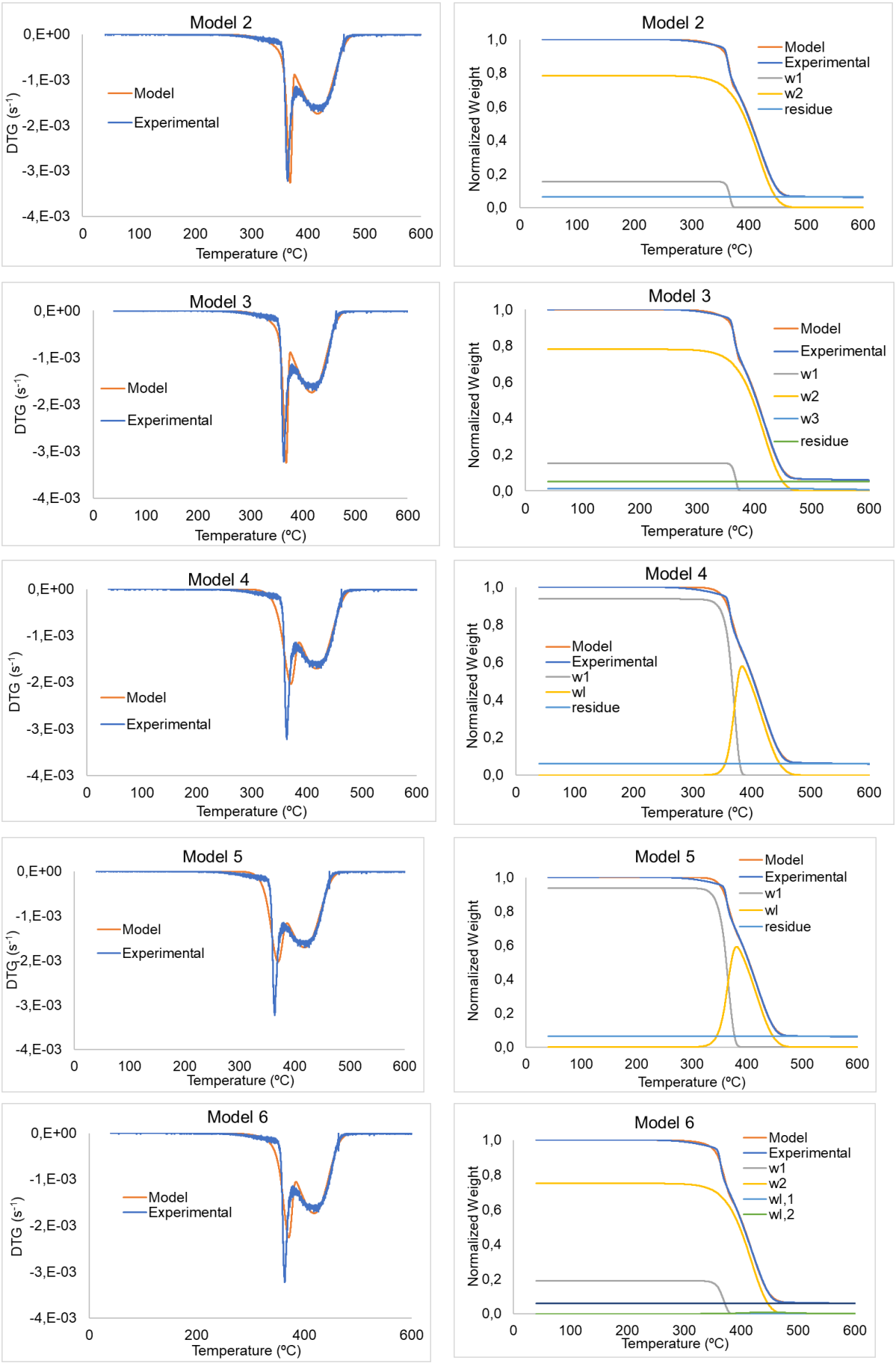

Figure 4.23 - Kinetic models for PS decomposition.

The first approach to the models shows that model 2, which considers a two pseudo-component degradation is the model that better describes the experimental data.

4.7.4.2 Discrimination of the model

The R^2 and adjusted R^2 of all models were calculated (Table 4.16). The result shows that model 2 and 3 have the highest R-squared and adjusted R-squared. Comparing both, model 3 has the highest adjusted R-squared. However, when fitting model 3 it was realized that the weight fraction of the third component was negligible and therefore this model was rejected. Hereupon, model 2 is the model that provides an overall better description of the experimental data.

Table 4.16 - Discrimination of waste PS models.

Model/Parameter	SSE	SS_{yy}	R^2	N	K	R^2 adjusted
Model 1	5.99×10^{10}	4.67×10^{13}	0.99871875	27271	3	0.99871865
Model 2	4.23×10^{9}	4.67×10^{13}	0.99990949	27271	6	0.99990948
Model 3	4.06×10^{9}	4.67×10^{13}	0.99991309	27271	9	0.99991306
Model 4	9.64×10^{9}	4.67×10^{13}	0.99979370	27271	8	0.99979365
Model 5	1.01×10^{10}	4.67×10^{13}	0.99978308	27271	6	0.99978304
Model 6	6.43×10^{9}	4.67×10^{13}	0.99986243	27271	12	0.99986238

4.7.4.3 Validation of the model for the different heating rates

The best fitting model, model 2, was applied for different heating rates in order to:

1. Ensure that a single set of kinetic parameters describes the experimental data.
2. Understand and validate the model at these conditions.

The results present in Figure 4.24 show that the model fits for the heating rates of 5 and 10 ºC/min. At 20 ºC/min and for higher heating rates some deviations between the model and the experimental data appears (see Annex IV.1, Figure I 2). This result may be related with limitation to mass and heat transfer that may become more pronounced at higher heating rates [44] and the model doesn't have these limitations into account, or to other kinetic effects that were not taken into consideration. The particle size may have also some effect on the heat transfer.

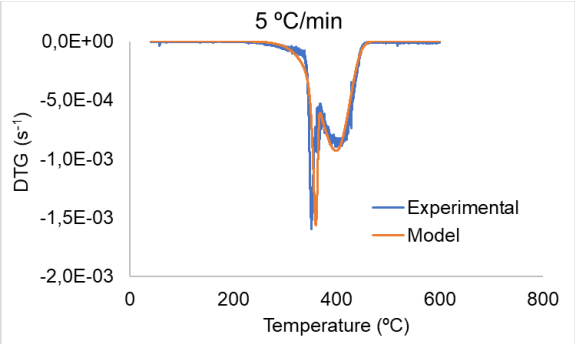

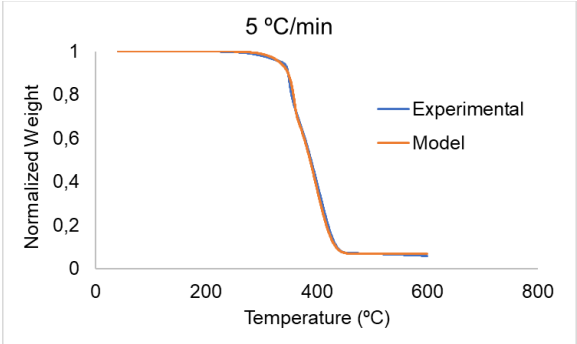

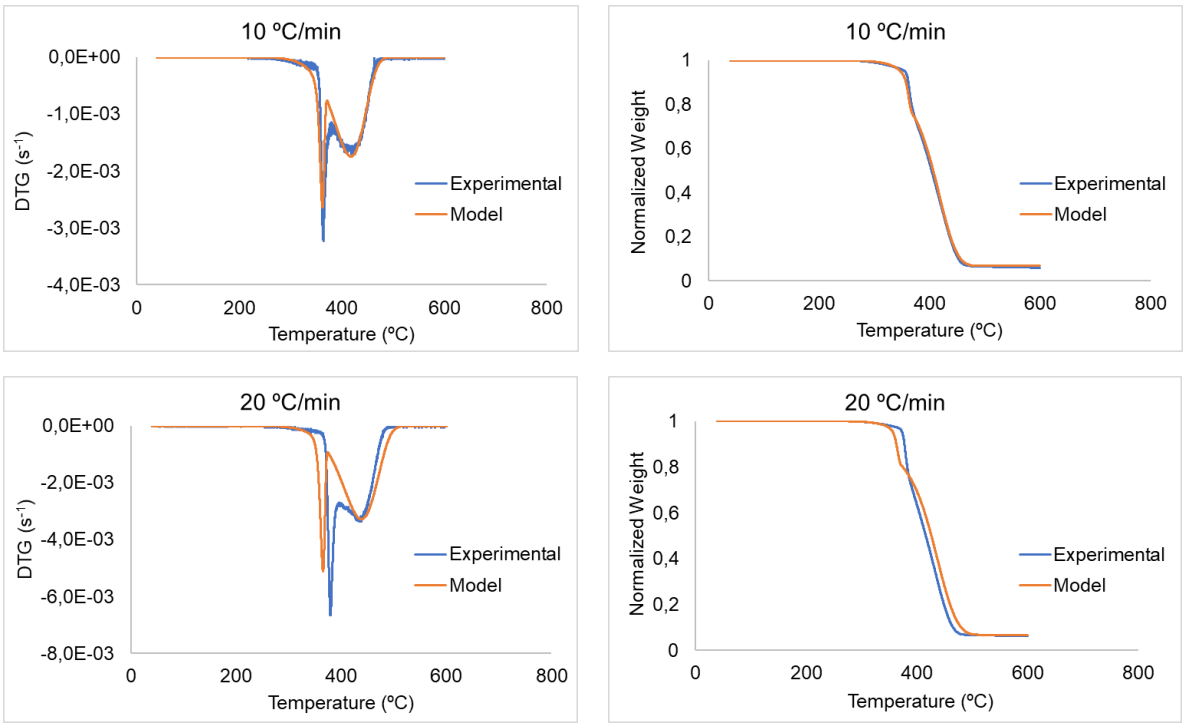

Figure 4.24 - Application of the model to different heating rates (for PS).

4.7.4.4 Validation of the model with isothermal experiments

Model 2 was applied to the different isothermal runs, with the same objective as when it was applied for different heating rates. The same set of kinetic parameters obtained in dynamic conditions is maintained. The results presented in Figure 4.25 show that the model describes the isothermals from 400 to 500 ºC. At lower temperatures, however, the deviation between the experimental data and the model are significant. At 350 ºC, before the onset temperature, the model, with the kinetic parameters, is not able to describe the peak.

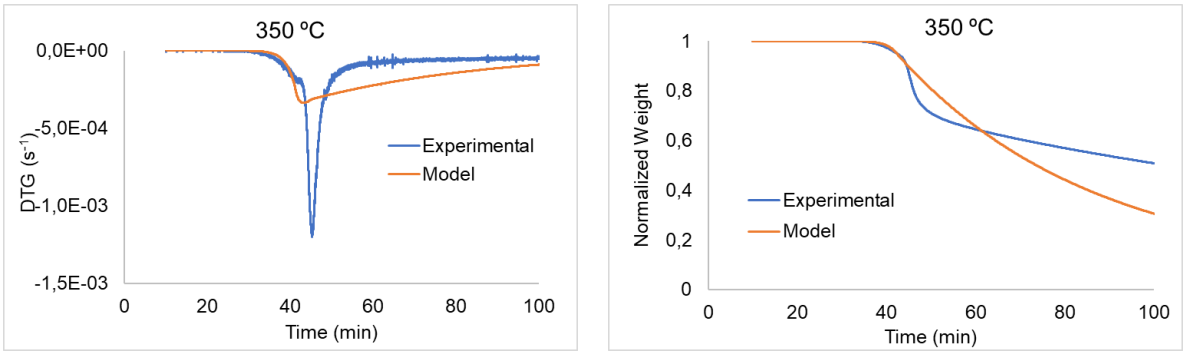

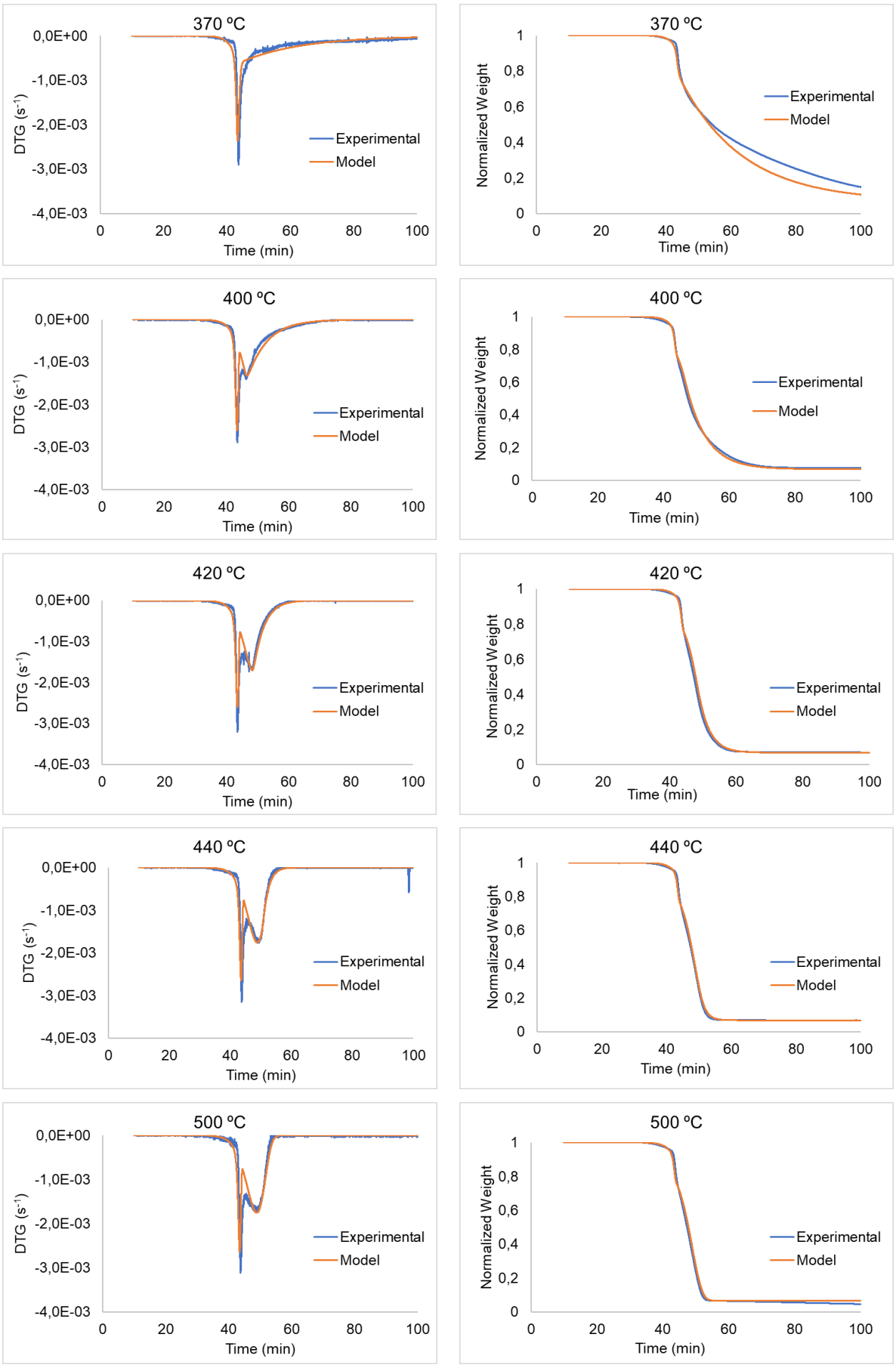

Figure 4.25 - Application of the model to the different isothermals (for PS).

4.7.4.5 Kinetic parameters

As mentioned before, model 2 was applied for dynamic and isothermal conditions with a single set of kinetic parameters. The kinetic parameters were estimated by making an overall fitting to the experimental data at dynamic conditions. The objective function minimized was the sum of the sum of the squares of the residues on the fractioned weight of the different heating rates.

The bootstrapping method, explained in Chapter 4.7.2, was used to estimate the standard deviation of the estimated variables. Table 4.17 presents the average kinetic parameters obtained and their standard deviation. Waste PS has a first activation energy of 814.73 ± 1.96 kJ/mol and a second of 128.14 ± 0.75 kJ/mol.

Table 4.17 - Average kinetic parameters obtained for waste PS. W= fractioned weight, n=reaction order, kref= reference kinetic constant (s^{-1}), Ea=activation energy (kJ/mol).

	Waste PS
W_{C1}	$0.14 \pm 2.60\ x\ 10^{-3}$
W_{C2}	$0.79 \pm 1.83x\ 10^{-3}$
$W_{residue}$	$0.07 \pm 7.84\ x\ 10^{-4}$
n_1	1.00
$k_{ref,1}$ **(s^{-1})**	283.95 ± 13.55
$E_{a,1}$ **(kJ/mol)**	814.73 ± 1.96
n_2	1.00
$k_{ref,2}$ **(s^{-1})**	$2.96\ x\ 10^{-3} \pm 2.90x\ 10^{-5}$
$E_{a,2}$ **(kJ/mol)**	128.14 ± 0.75

4.7.5 Waste ABS

4.7.5.1 Study of the possible model/Understanding of the degradation mechanism

Different models were studied for the decomposition of the waste ABS sample, since its degradation mechanism is known to be very complex. [59] The TG analyses for waste ABS showed two decomposition peaks.

As a first approach, three models were studied, which tried to model the TG and DTG curve for the experiments under dynamic conditions at 10 ºC/min. This first attempt was elaborated with the intention of finding a model that better describes the decomposition of waste ABS.

Table 4.18 summarizes the models that were constructed. For all the models it was considered the existence of a fixed quantity of residue that doesn't degrade and is maintained throughout the degradation.

- Model 1: Considers a one-component degradation.
- Model 2: Considers a two-component degradation. Both pseudo-components are independent from each other and degrade in parallel.
- Model 3: A reaction in series mechanism is considered, in which a single pseudo-component decomposes to a product and an intermediate and the intermediate decomposes to a product as well.

Table 4.18 - Kinetic models considered for the decomposition of waste ABS.

ABS		
Model	**Reaction**	**Equations**
1	$C_1 \xrightarrow{k1} prod.$ $residue$	$\frac{dW_{C1}}{dt} = -k_{ref,1} e^{-\frac{E_{a,1}}{R}\left(\frac{1}{T}-\frac{1}{T_{ref}}\right)} {W_{C1}}^{n_1}$ $W_t = W_{C1} + W_{residue}$ $\frac{dW_t}{dt} = \frac{dW_{C1}}{dt}$
2	$C_1 \xrightarrow{k1} prod.$ $C_2 \xrightarrow{k2} prod.$ $residue$	$\frac{dW_{C1}}{dt} = -k_{ref,1} e^{-\frac{E_{a,1}}{R}\left(\frac{1}{T}-\frac{1}{T_{ref}}\right)} {W_{C1}}^{n_1}$ $\frac{dW_{C2}}{dt} = -k_{ref,2} e^{-\frac{E_{a,2}}{R}\left(\frac{1}{T}-\frac{1}{T_{ref}}\right)} {W_{C2}}^{n_2}$ $W_t = W_{C1} + W_{C2} + W_{residue}$ $\frac{dW_t}{dt} = \frac{dW_{C1}}{dt} + \frac{dW_{C2}}{dt}$
3	$C_1 \xrightarrow{k1} prod. + {I_1}^*$ ${I_1}^* \xrightarrow{k2} prod.$ $residue$	$\frac{dW_{C1}}{dt} = -k_{ref,1} e^{-\frac{E_{a,1}}{R}\left(\frac{1}{T}-\frac{1}{T_{ref}}\right)} {W_{C1}}^{n_1}$ $\frac{dW_I}{dt} = k_{ref,1} e^{-\frac{E_{a,1}}{R}\left(\frac{1}{T}-\frac{1}{T_{ref}}\right)} (xW_{C1})^{n_1} - k_{ref,2} e^{-\frac{E_{a,3}}{R}\left(\frac{1}{T}-\frac{1}{T_{ref}}\right)} (W_I)^{n_2}$ $W_t = W_{C1} + W_I + W_{residue}$ $\frac{dW_t}{dt} = \frac{dW_{C1}}{dt} + \frac{dW_I}{dt}$

Figure 4.26 presents the fitting of the models to the experimental data, the first observation are the following:

- Model 1: The model doesn't describe well the beginning of the decomposition and the maximum degradation peak is not fitted.
- Model 2: The model provides a better description of the experimental data than model 1.
- Model 3: The TG curve shows that the beginning of the decomposition isn't perfectly fitted by the model.

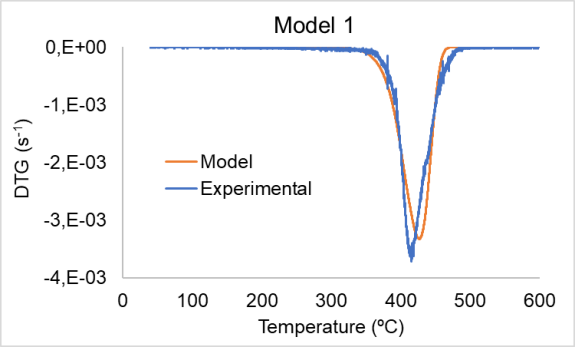

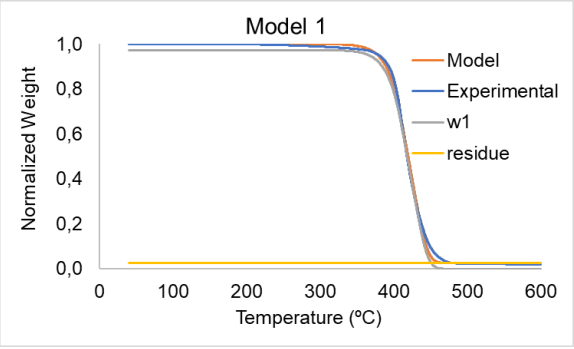

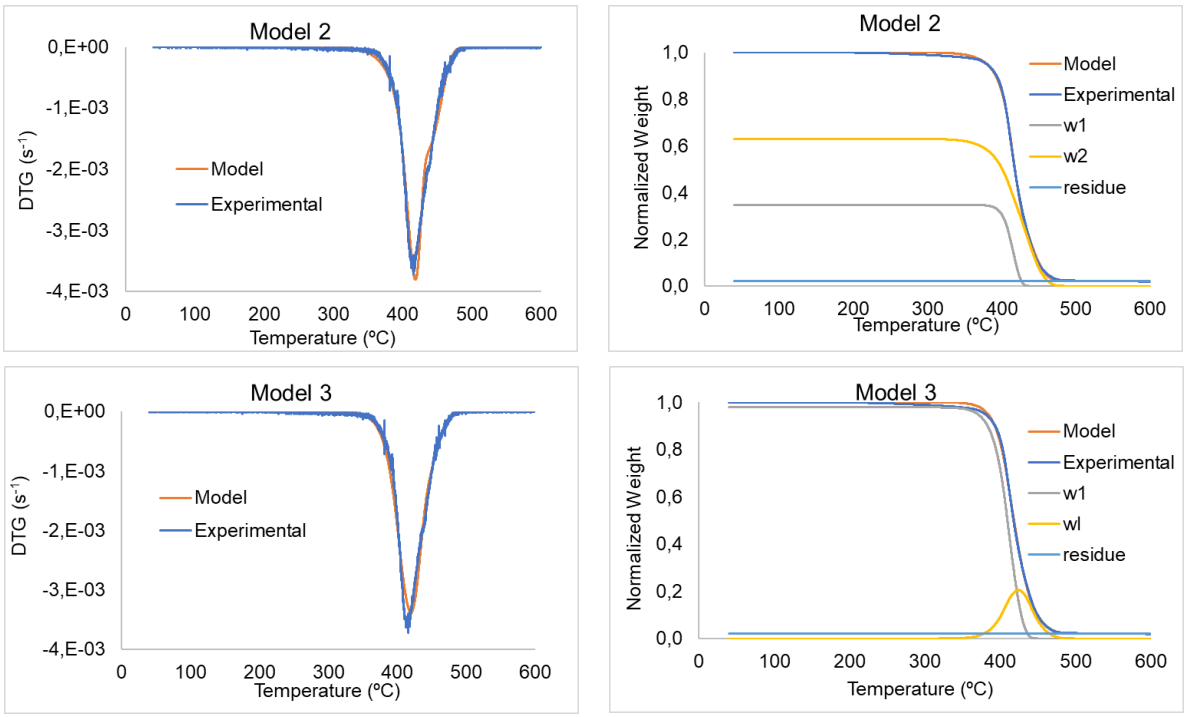

Figure 4.26 - Kinetic models for ABS decomposition.

The first approach to the models shows that model 2 and 3 provide adequate descriptions of the experimental data.

4.7.5.2 Discrimination of the model

The R^2 and adjusted R^2 of all models was calculated (Table 4.19). The result confirms that model 2 has the highest R-squared. Model 2 presents also the highest adjusted R-squared, indicating that the 3 variables introduced are useful variables, comparing to model 1.

Table 4.19 – Discrimination of waste ABS models.

Model/Parameter	SSE	SS_{yy}	R^2	n	K	R^2 adjusted
Model 1	3.63×10^{10}	5.03×10^{13}	0.99927817	27271	3	0.99927812
Model 2	7.79×10^{9}	5.03×10^{13}	0.99984520	27271	6	0.99984517
Model 3	1.31×10^{10}	5.03×10^{13}	0.99973898	27271	6	0.99973893

4.7.5.3 Validation of the model for the different heating rates

The best fitting model, model 2, was applied for different heating rates for the same reasons as for waste PS (see Chapter 4.7.4.3). The results present in Figure 4.27 show that the model fits for the heating rates of 5, 10 and 20 ºC/min. At 50 ºC/min and for higher heating rates a deviation between the model and the experimental data appears (see Annex IV.2,Figure I 3). This result may be related with limitation to mass and heat transfer at higher heating rates [44] and the model doesn't have these limitations into account. It should also be noted that at higher heating rates a shoulder starts to appear after the main peak, which may indicate a process that might not have been fully taken into consideration in the model, as this behaviour is also observed in the model but not with the same intensity.

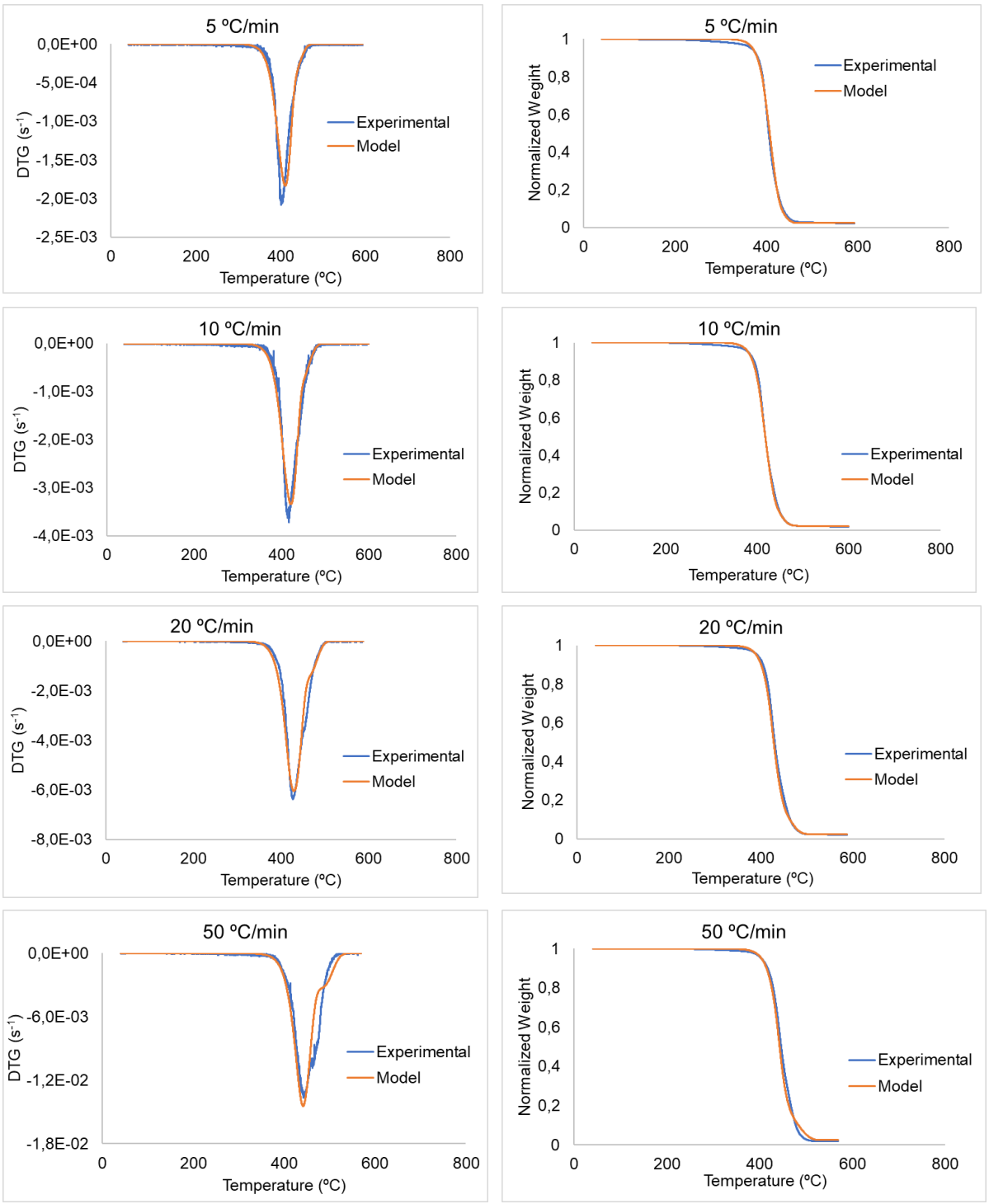

Figure 4.27 - Application of the model to different heating rates (for ABS).

4.7.5.4 Validation of the model with isothermal experiments

Model 2 was applied for the different isothermals to understand the behaviour of the model at these conditions. The same set of kinetic parameters obtained in dynamic conditions is maintained. The results present in Figure 4.28 show that the model describes the experimental data at 420 ºC to 500 ºC. At lower temperatures the model deviates somewhat from the experimental data.

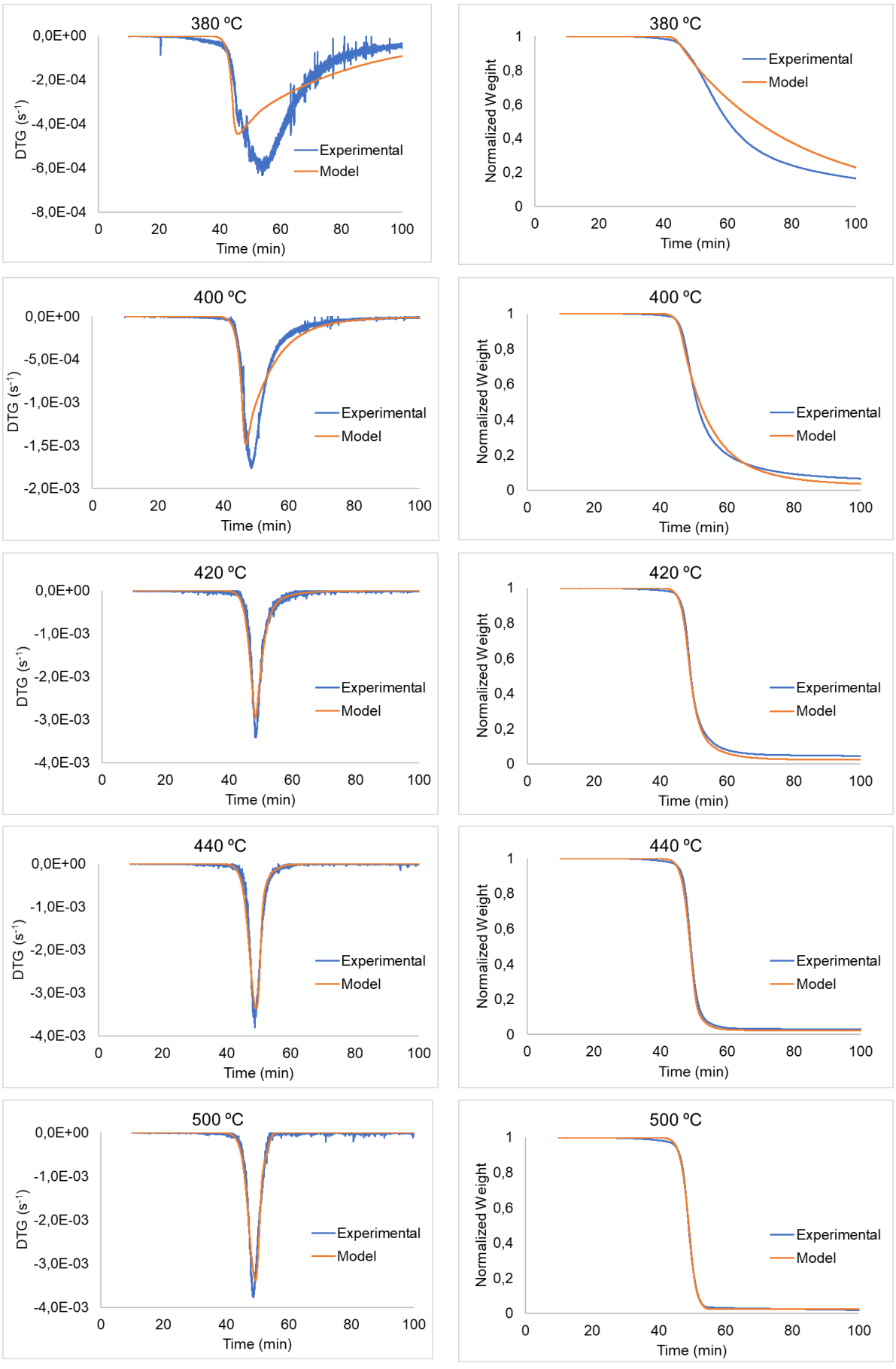

Figure 4.28 - Application of model 2 to different isothermals (for ABS).

4.7.5.5 Kinetic parameters

The kinetic parameters were estimated by making an overall fit to the experimental data at dynamic conditions as explained for waste PS (see Chapter 4.7.4.5).

The bootstrapping method, explained in Chapter 4.7.2, was also used to estimate the standard deviation of the estimated variables. Table 4.20 presents the average kinetic parameters obtained and their standard deviation. Waste ABS has a first activation energy of 255.43 ± 3.26 kJ/mol and a second of 193.34 ± 4.52 kJ/mol.

Table 4.20 - Average kinetic parameters obtained for waste ABS. W= fractioned weight, n=reaction order, kref= reference kinetic constant (s^{-1}), Ea=activation energy (kJ/mol).

	Waste ABS
$\boldsymbol{W_{C1}}$	0.69 ± 0.03
$\boldsymbol{W_{C2}}$	0.29 ± 0.03
$\boldsymbol{W_{residue}}$	0.02 ± 0.00
$\boldsymbol{n_1}$	1.00
$\boldsymbol{k_{ref,1}}$ **(s^{-1})**	$3.19\ x\ 10^{-3} \pm 9.10x\ 10^{-5}$
$\boldsymbol{E_{a,1}}$ **(kJ/mol)**	255.43 ± 3.26
$\boldsymbol{n_2}$	1.00
$\boldsymbol{k_{ref,2}}$ **(s^{-1})**	$1.11\ x\ 10^{-3} \pm 5.45x\ 10^{-5}$
$\boldsymbol{E_{a,2}}$ **(kJ/mol)**	193.34 ± 4.52

4.8 Bench-Scale Reactor Pyrolysis[2]

For comparison with the results obtained in the TG kinetic analysis, experiments using a bench-sclae reactor were conducted to study the pyrolysis of virgin and waste polystyrene. The experiments conditions, such as temperature, heating rate and residence time, were based on the TG analysis.

4.8.1 Yield

Experiments at three different set point temperatures (400, 450 and 500 ºC) were performed to study the effect of temperature on the product yields for virgin PS1 and waste PS pyrolysis. The product distributions (liquid, solid and gas) of virgin and waste PS are represented in Figure 4.29 and Figure 4.30, respectively. Virgin PS yields 31 % liquid at 400 ºC and 86 % at 500 ºC, while waste PS produces 21 % liquid at 400 ºC and 59 % ate 500 ºC. Both results show that as the temperature increases, the liquid yield increases, while the solid yield decreases. The gas yield is approximately constant and low.

At 500 ºC (with a isothermal of 90 minutes), waste PS produces 59 % liquid and 3 % gas. The TG results (see Chapter 4.5.1) have shown that at 500 ºC (with a isothermal of 60 minutes) the conversion is 96 %. The lower conversion obtained in the reactor may be due to the reflux that occurs inside the reactor. As explained below (Chapter 4.8.1.1), the inside temperature of the reactor is always lower than the set point, due to heat losses, endothermicity of the reaction and inside reflux. The temperature profile also shows that the average internal temperature of the reactor for waste PS is always lower than of virgin PS, and this may be due to the presence of additives that influence the kinetics and thus the reaction. In fact, virgin PS produces more liquid at all the set point temperatures (Figure 4.29 and Figure 4.30).

The yields obtained are different from the ones found in literature, which might be related with the sample itself, operational conditions and type of reactor. The liquid yield reported in literature for virgin PS, at around 500 ºC is 91.8 %[41] and 92 %[43]. However, both obtained as well a very low quantity of gas (2.5 %[41] and 1 %[43]). For waste PS, Sogancioglu *et al*. obtained for waste PS between 67.23 % at 500 ºC using a fixed bed reactor.[42] However, Sogancioglu *et al.* obtained a very low quantity of solid (6.21 %) [42] and a higher quantity of gas (26.59 %) [42] comparing to the results obtained in this Thesis. Other authors obtained for waste PS from MSW more than 70 % of liquid yield. [33,41,45,46]

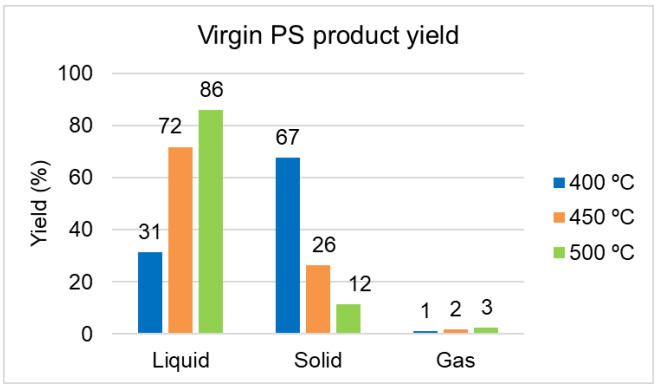

Figure 4.29 - Product distribution of the thermal pyrolysis of virgin PS at different temperatures.

[2] Bench-scale experiments and product analysis were done with Dr. Bruna Rijo.

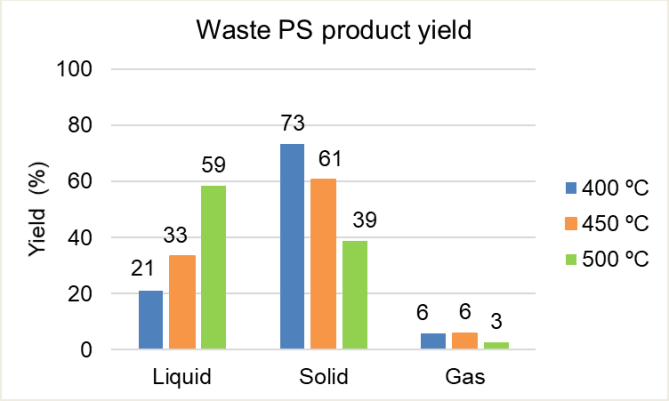

Figure 4.30 - Product distribution of the thermal pyrolysis of waste PS at different temperatures.

4.8.1.1. Temperature Profile of the Reactor

Both the temperature of the furnace (set point temperature) and the internal temperature of the reactor were recorded. Figure 4.31 presents the temperature profile of the furnace and of the reactor for an experiment without sample, for virgin PS and for waste PS. The internal temperature of the reactor is always lower than the set point temperature, which is associated with heat losses. The degradation of the plastic is an endothermic reaction and thus it absorbs heat, lowering the temperature reached inside the reactor, comparing to an experiment without sample, which has been observed by Singh *et al,* too. [33] Additionally to the endothermicity of reaction, the temperature inside the reactor is influenced by the existent reflux that is associated with the compounds that are volatilized but do not leave the reactor and condense.

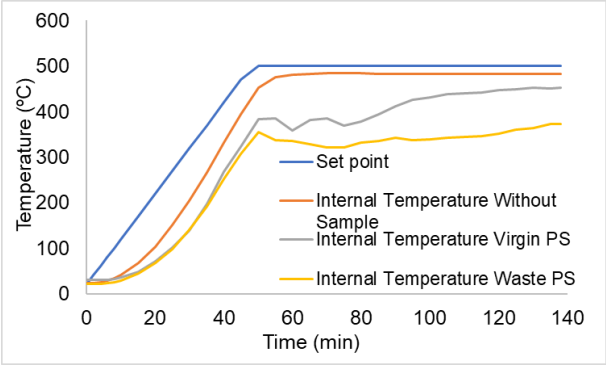

Figure 4.31 - Temperature Profile of the reactor with and without sample.

Figure 4.32 and Figure 4.33 present the temperature profile for virgin and waste PS, respectively, for different set points.

At a set point of 400 ºC, the temperature inside the reactor for virgin PS reaches a maximum of around 380 ºC at 60 minutes. At a higher set points (450 and 500 ºC) the temperature inside the reactor reaches a maximum of around 390 ºC.

The degradation of waste PS starts at lower temperature than virgin PS (350 ºC for all the set point temperatures), which is likely related with the presence of additives, as it has been observed in the TG results.

The average internal temperature during the isothermal was calculated, Table 4.21. The results show that the average internal temperature of the reactor for virgin PS increases with the increase of the set point from 340.65 ºC (at 400 ºC) to 414.92 ºC (at 500 ºC). The results for waste PS show that an

increase of the set point temperature from 400 ºC to 450 ºC doesn't change the average internal temperature, which is approximately of 316 ºC. At 500 ºC the average internal temperature of the reactor is 344.19 ºC. The average internal temperature of the reactor for virgin PS is always higher than of waste PS, and this may be related with the presence of additives that influence the kinetics and thus the reaction.

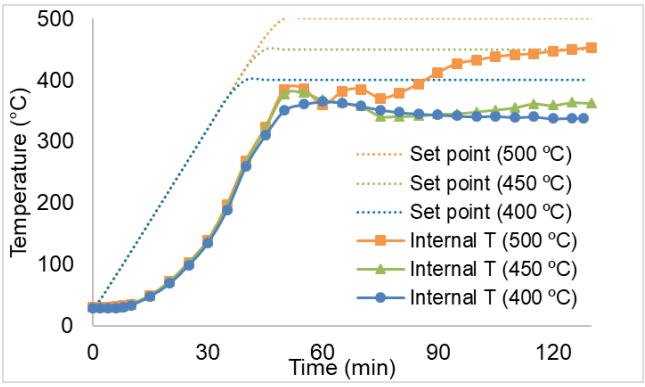

Figure 4.32 - Temperature profile for thermal pyrolysis of virgin PS.

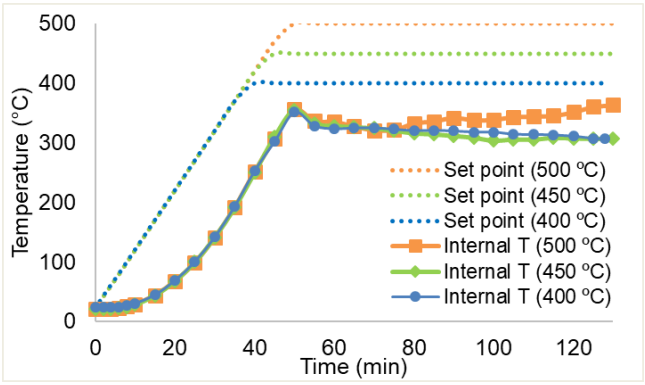

Figure 4.33 - Temperature profile for thermal pyrolysis of WEEE PS.

Table 4.21 - Average of the internal temperature of the reactor in the thermal pyrolysis of waste and virgin PS during the isothermal.

Set point temperature (ºC)	Average Internal Temperature (ºC) - Virgin PS	Average Internal Temperature (ºC) - Waste PS
400	340.65	315.58
450	355.24	315.81
500	414.92	344.19

4.8.2 Gas phase products

Figure 4.34 presents the gaseous composition of waste PS as function of temperature. For virgin polystyrene the quantity of gas produced was very low, making it impossible to analyse the gas.

The results show that the gas products of waste PS are within the range of C_2 and C_6 hydrocarbons. As the reaction temperature increases the formation of C_2 hydrocarbons is promoted and the formation of C_3 -C_6 hydrocarbons decrease, with complete disappearance of hydrocarbons in C_5 and C_6 range. Williams and Williams reported the same hydrocarbons range for the gaseous products.[46] The

composition of the gaseous products in terms of specific compounds was difficult to estimate due to the low resolution of the chromatogram and low quantity that is formed.

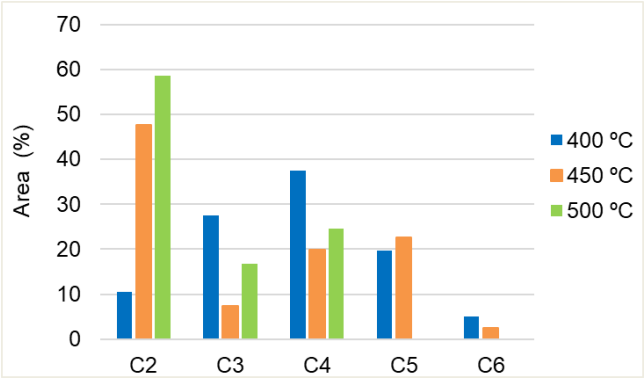

Figure 4.34 - Gas composition of waste PS pyrolysis at different temperatures.

4.8.3 Liquid phase products

The composition of the liquid derived from the pyrolysis of virgin and waste PS is shown in Figure 4.35 and Figure 4.36, respectively.

Virgin PS leads in higher quantity to the formation of C_8 hydrocarbons, which might comprehend in majority styrene, followed by ethylbenzene. C_7 and C_9 hydrocarbons products are obtained as well, which are in majority toluene and possibly α-methylstyrene, respectively. These results are concordant with Singh *et al.*[33]., Wu *et al.*[36], Zhang *et al.*[47] and Lee *et al.* [48]

Waste PS produces hydrocarbons in the range of C_7 to above C_{10}. See Annex III, Figure I 1 for an example of a chromatogram. C_8 hydrocarbons are produced in majority, however, in lower amount than virgin PS. The results show that styrene is the main compound and ethylbenzene is not produced. The waste plastic produces more C_9, C_{10} and $>C_{10}$ hydrocarbons than virgin PS. Thus, the pyrolysis of waste PS produces high-value hydrocarbons that may be used as feedstock as well as gasoline-range hydrocarbons (C_5 to C_8) [96].

The increase in temperature causes a small increase of the amount of heavier hydrocarbons, in particular of C_{10} and compounds higher than C_{10}. With the increase in temperature there is a more extensive cracking [97], lowering the amount of solid yield (Figure 4.30).

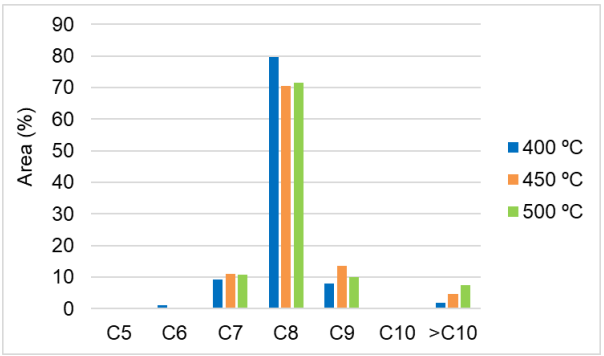

Figure 4.35 - Liquid composition of virgin PS pyrolysis at different temperatures.

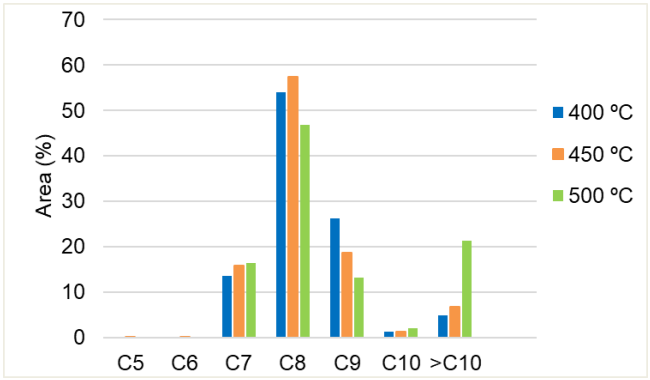

Figure 4.36 - Liquid composition of waste PS pyrolysis at different temperatures.

4.8.4 Solid analysis

The solid products were analysed as described in Chapter 3.4.3. Figure 4.37 and Figure 4.38 present the results of the DTG and DSC curve of the solid obtained by the thermal degradation of virgin and waste PS, respectively. The results show that the pyrolysis produces solids with compositions and different degradation temperatures. For the solid of virgin PS, the DTG curves for the set point temperatures of 400 and 450 ºC show a degradation peak at around 415 ºC, which is related with an endothermic peak in the DSC curve. This might be indicative of unreacted polymer, indicating that the degradation of the polymer may be incomplete in the reactor. [42,43] For waste PS, the same observation can be made but only for a set point temperature of 400 ºC. For higher temperature it can be seen that there are mass losses at lower temperature, which indicates that the solid obtained is probably already partially converted. The lower temperature also indicates that the solid compounds are, at least, partially volatile.

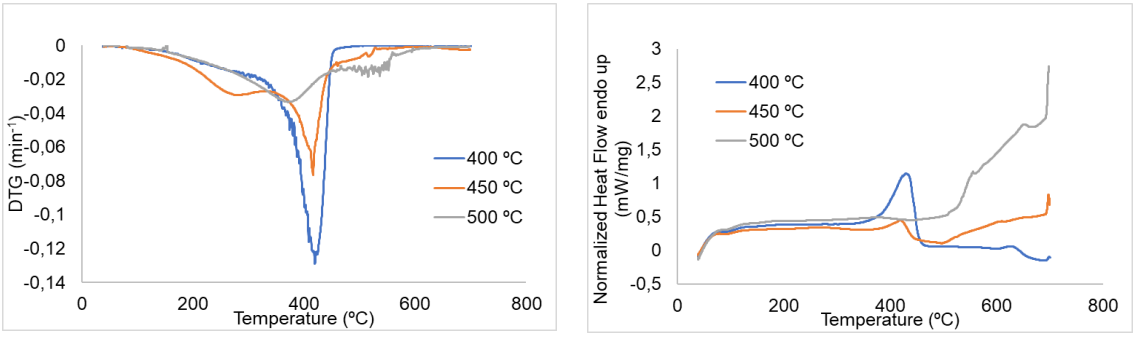

Figure 4.37 – DTG and DSC curve for the solid from virgin PS pyrolysis.

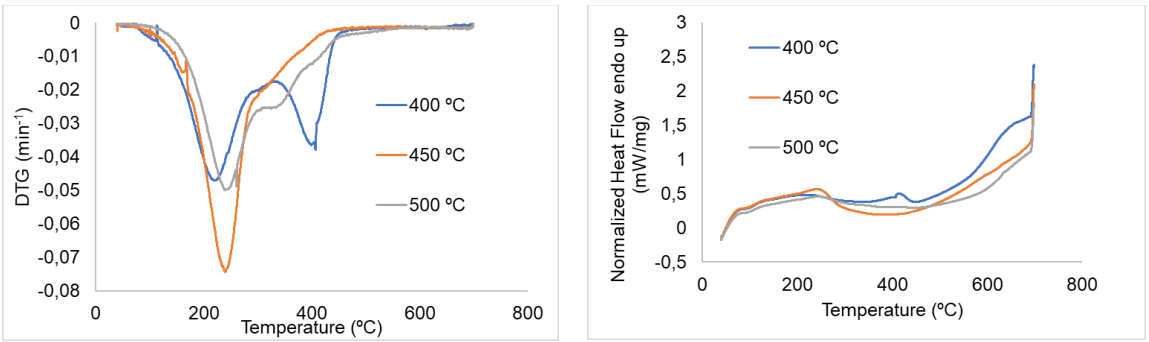

Figure 4.38 – DTG and DSC curve for the solid from waste PS pyrolysis.

[This page was left in blank.]

5. Conclusion

5.1 General Conclusion

The TG/DSC analysis was used to study the thermal behaviour of polystyrene (PS) and acrylonitrile-butadiene-styrene (ABS) from WEEE. Experiments under dynamic and isothermal conditions in inert atmosphere were performed to study the influence of the heating rate and of the temperature on the degradation behaviour of both plastics. The thermal degradation under air was studied as well.

For waste PS the results were compared to virgin PS. Waste PS showed two degradation peaks, while both virgin PS samples presented one degradation peak. The first degradation peak of waste PS is likely related with the degradation of additives, while the second with the degradation of polystyrene itself. As the heating rate increases, the onset temperature and maximum degradation temperatures increases. This behaviour is likely related with kinetic effects and possible heat transfer limitations. With the increase of the heating rate, the sample has less time to uniformly distribute the heat, which will lead to a decomposition at higher temperatures.

Waste ABS presented two degradation peaks and the observation and conclusion of the influence of the heating rate and temperature is the same as for PS.

The degradation under air performed for both waste plastic showed an extra degradation peak, when compared to degradation under nitrogen. This extra degradation peak is associated with an exothermic peak, which is indicative of an oxidative degradation. The final remaining residue at the end was less than 1 % for both plastics, meaning that both have less than 1 % of inorganic material.

Two virgin polystyrene samples, with different molecular weight, were studied and the TG results showed that the molecular weight of the polymer doesn't affect significantly the thermal decomposition of the polymer.

Analysing the data extracted from the TG/DSC results, it is possible to estimate the kinetic parameters using mechanistic models. A one-component degradation model adequately describes the decomposition of both virgin polystyrenes. Virgin PS with lower molecular weight (PS1) showed an activation energy of 282.09 ± 0.05 kJ/mol. It is lower than the value obtained for virgin PS2, which is of 375.01 ± 0.10 kJ/mol. These results indicate that the molecular weight has some influence on the kinetics. A two pseudo-component degradation model with a presence of a fixed quantity of residue fits the experimental data for waste PS. A single set of kinetic parameters, with a first activation energy of 814.73 ± 1.96 kJ/mol and a second of 128.14 ± 0.75 kJ/mol, provides an adequate description of the experimental data for different heating rates and isothermals.

The degradation of waste ABS is also well described by a two pseudo-component degradation model with the presence of a fixed quantity of residue. As for waste PS, a single set of kinetic parameters describes the ensemble of data, with a first activation energy of 255.43 ± 3.26 kJ/mol and a second one of 193.34 ± 4.52 kJ/mol.

The pyrolysis of waste polystyrene was also carried-out in a bench-scale reactor at different set point temperatures (400, 450 and 500 ºC) and compared to virgin PS. For both waste and virgin PS, as the temperature increases, the liquid yield increases, while the solid yield decreases. The gas yield is approximately constant and very low.

At 500 ºC (with a isothermal of 90 minutes), waste PS produces 59 % liquid and 3 % gas. The TG results have shown that at 500 ºC (with a isothermal of 60 minutes) the conversion of waste PS is 96 %. The lower conversion obtained in the reactor may be due to the reflux that occurs inside the reactor. The temperature inside the reactor is always lower than the set point, due to heat losses, the endothermicity of the reaction and occurrence of reflux conditions. The temperature profile also shows that the average internal temperature of the reactor for waste PS is always lower than of virgin PS, and this may be due to the presence of additives that influence the kinetics, and thus the reaction, but also the heat generation and consumption, as these additives may be predominantly flame retardants. In fact, virgin PS produces at 500 ºC yields more liquid and gas than waste PS, namely of 86 % and 1 % gas.

The DTG curve of the solid obtained by the thermal pyrolysis at 400 ºC of virgin and waste PS shows a degradation peak that might correspond to unreacted polymer, indicating that at a set point of 400 ºC, under the conditions used, the reaction is likely to be incomplete.

The products obtained from the pyrolysis were analysed by gas chromatography. Virgin polystyrene produced a very small quantity of gas making it impossible to analyse. The gas products of waste PS are within the range of C_2 and C_6 hydrocarbons. As the reaction temperature increases the formation of C_2 hydrocarbons is promoted and the formation of C_3 -C_6 hydrocarbons decrease, eventually with the complete disappearance of hydrocarbons in C_5 and C_6 range.

In terms of liquid yield, both virgin and waste PS produce in majority hydrocarbons in the range of C_7 to C_9. The C_7 hydrocarbons probably correspond to toluene. Both produce in higher quantity C_8 hydrocarbons, which might correspond in majority to styrene. The C_9 hydrocarbons might correspond to alpha-methylstyrene.

Thus, the pyrolysis of waste PS produces high-value hydrocarbons that might be used as feedstock for the petrochemical industry. Therefore, waste PS may be adequate for feedstock recycling in the chemical industry plus possibly introduced in a Circular Economy approach as it generates the monomers that can be used to produce new polystyrene.

5.2 Future perspective

As a future perspective it would be interesting to complement this Thesis research with the following development:

- Improve the kinetic models by introducing heat and mass transfer phenomena.
- Confirmation of the pyrolysis products by use of patterns in GC or by use of mass spectrometry.
- Co-pyrolysis of PS and ABS with different ratios and/or with another WEEE plastics.
- Study of the pyrolysis of ABS in the reactor.
- Optimization of the conditions of the bench-scale reactor.
- Large – scale reactor.
- Study of the economic feasibility of the process.
- Reactor modelling.

Bibliography

1. Eurostat,. Waste Electrical and Electronic Equipment (WEEE) - Eurostat. https://ec.europa.eu/eurostat/web/waste/key-waste-streams/weee. Accessed February 20, 2019.
2. EERA,. EERAs comments and proposals for the EU Plastics Strategy 2017. (2017).
3. Carrasco F, Santana OO, Cailloux J, Sánchez-soto M, Maspoch ML,. Thermochimica Acta Thermal degradation of poly (lactic acid) and acrylonitrile-butadiene-styrene bioblends : Elucidation of reaction mechanisms. *Thermochim Acta*, 654 (2017) 157-167.
4. Scheirs J, Kaminsky K, eds.,. *Feedstock Recycling and Pyrolysis of Waste Plastics*. UK: John Wiley & Sons; 2006.
5. Feedstock recycling - Circular Economy Guide. https://www.ceguide.org/Strategies-and-examples/Dispose/Feedstock-recycling. Accessed February 25, 2019.
6. Brydson J,. *Plastics Materials*. Vol 7. UK: Butterworth Heinemann; 1999.
7. *Plastics-the Facts 2018 An Analysis of European Plastics Production, Demand and Waste Data*. https://www.plasticseurope.org/en. Accessed February 25, 2019.
8. Geyer R, Jambeck JR, Law KL,. Production, use, and fate of all plastics ever made. *Sci Adv*, 3 (2017) e1700782.
9. Yang X, Sun L, Xiang J, Hu S, Su S,. Pyrolysis and dehalogenation of plastics from waste electrical and electronic equipment (WEEE): A review. *Waste Manag*, 33 (2013) 462-473.
10. Singh RK, Ruj B,. Plasticwaste management and disposal techniques - Indian scenario. *Int J Plast Technol*, 19 (2016) 211-226.
11. Zhou X, Broadbelt LJ, Vinu R,. Mechanistic Understanding of Thermochemical Conversion of Polymers and Lignocellulosic Biomass. *Adv Chem Eng*, 49 (2016) 95-198.
12. Riess M, Ernst T, Popp R, et al.,. Analysis of flame retarded polymers and recycling materials. *Chemosphere*, 40 (2003) 937-941.
13. Altwaiq A, Wolf M, Van Eldik R,. Extraction of brominated flame retardants from polymeric waste material using different solvents and supercritical carbon dioxide. *Anal Chim Acta*, 491 (2003) 111-123.
14. Smith S, *Master Thesis in Chemistry:* Extraction of Additives from Polystyrene and Subsequent Analysis. Faculty of Virginia (1998).
15. Martinho G, Pires A, Saraiva L, Ribeiro R,. Composition of plastics from waste electrical and electronic equipment (WEEE) by direct sampling. *Waste Manag*, 32 (2012) 1213-1217.
16. Dimitrakakis E, Janz A, Bilitewski B, Gidarakos E,. Small WEEE: Determining recyclables and hazardous substances in plastics. *J Hazard Mater*, 161 (2009) 913-919.
17. Mark JE, ed.,. *Polymer Data Handbook*. University of Cincinnati; 1999.
18. Everything You Need To Know About Polystyrene (PS). https://www.creativemechanisms.com/blog/polystyrene-ps-plastic. Accessed March 8, 2019.
19. Jakab E, Uddin MA, Bhaskar T, Sakata Y,. Thermal decomposition of flame-retarded high-impact polystyrene. *J Anal Appl Pyrolysis*, 68-69 (2003) 83-99.
20. Peng S, Chen L, Li L, Xie M, Huang H, Liu X,. Debromination of flame-retarded TV housing plastic waste. *J Mater Cycles Waste Manag*, 12 (2010) 103-107.
21. Liu G, Liao Y, Ma X,. Thermal behavior of vehicle plastic blends contained acrylonitrile-butadiene-styrene (ABS) in pyrolysis using TG-FTIR. *Waste Manag*, 61 (2017) 315-326.
22. Mariano Domingues da Silva C, Silva ALA, Pacheco R, Rocco AM,. Conductivity and Thermal Behaviour of Sulfonated ABS Membranes for Fuel Cell Applications. *ECS Trans*, 25 (2009) 881-889.
23. Yousefi M, Salavati-Niasari M, Gholamian F, Ghanbari D, Aminifazl A,. Polymeric nanocomposite materials: Synthesis and thermal degradation of acrylonitrile-butadiene-styrene/tin sulfide (ABS/SnS). *Inorganica Chim Acta*, 371 (2011) 1-5.
24. Feng J, Carpanese C, Fina A,. Thermal decomposition investigation of ABS containing Lewis-acid type metal salts. *Polym Degrad Stab*, 129 (2016) 319-327.
25. ABS 9 Resin. https://www.shutterstock.com/image-vector/plastic-recycling-symbol-abs-9-resin-1065919076. Accessed May 3, 2019.
26. Properties of Polystyrene. http://www.matweb.com/search/DataSheet.aspx?MatGUID=df6b1ef50ce84e7995bdd1f6fd1b04c9. Accessed March 3, 2019.
27. Specific Heat of common Substances. https://www.engineeringtoolbox.com/specific-heat-capacity-d_391.html. Accessed June 4, 2019.
28. Propertires of Acrylonitrile Butadiene Styrene (ABS).

http://www.matweb.com/search/DataSheet.aspx?MatGUID=eb7a78f5948d481c9493a67f0d089646. Accessed March 3, 2019.
29. Chemical Recycling | Plastics Recyclers Europe. https://www.plasticsrecyclers.eu/chemical-recycling. Accessed March 8, 2019.
30. Blanco I, Bottino FA,. Kinetics of degradation and thermal behaviour of branched hepta phenyl POSS / PS nanocomposites. *Polym Degrad Stab*, 129 (2016) 374-379.
31. Blanco I, Abate L, Bottino FA, Bottino P,. Thermal degradation of hepta cyclopentyl, mono phenyl-polyhedral oligomeric silsesquioxane (hcp-POSS)/polystyrene (PS) nanocomposites. *Polym Degrad Stab*, 97 (2012) 849-855.
32. Blanco I, Abate L, Bottino FA, Bottino P,. Thermal behaviour of a series of novel aliphatic bridged polyhedral oligomeric silsesquioxanes (POSSs)/polystyrene (PS) nanocomposites: The influence of the bridge length on the resistance to thermal degradation. *Polym Degrad Stab*, 102 (2014) 132-137.
33. Singh RK, Ruj B, Sadhukhan AK, Gupta P,. Thermal degradation of waste plastics under non-sweeping atmosphere: Part 1: Effect of temperature, product optimization, and degradation mechanism. *J Environ Manage*, 239 (2019) 395-406.
34. Kiran N, Ekinci E, Snape CE,. Recyling of plastic wastes via pyrolysis. *Resour Conserv Recycl*, 29 (2000) 273-283.
35. Katančić Z, Grčić I, Hrnjak-Murgić Z,. High-impact Polystyrene Nanocomposites with. *Croat Chem Acta*, 90 (2017) 401-411.
36. Wu J, Chen T, Luo X, Han D, Wang Z, Wu J,. TG/FTIR analysis on co-pyrolysis behavior of PE, PVC and PS. *Waste Manag*, 34 (2014) 676-682.
37. Dong D, Tasaka S, Inagaki N,. Thermal degradation of monodisperse polystyrene in bean oil. *Polym Degrad Stab*, 72 (2001) 345-351.
38. Faravelli T, Pinciroli M, Pisano F, Bozzano G, Dente M, Ranzi E,. Thermal degradation of polystyrene. *J Anal Appl Pyrolysis*, 60 (2001) 103-121.
39. McNeill IC,. Thermal degradation of polystyrene in different environments. *Polymer (Guildf)*, 247 (1997) 179-195.
40. Jang BN, Costache M, Wilkie CA,. The relationship between thermal degradation behavior of polymer and the fire retardancy of polymer/clay nanocomposites. *Polymer (Guildf)*, 46 (2005) 10678-10687.
41. Achilias DS, Kanellopoulou I, Megalokonomos P, Antonakou E, Lappas AA,. Chemical recycling of polystyrene by pyrolysis: Potential use of the liquid product for the reproduction of polymer. *Macromol Mater Eng*, 292 (2007) 923-934.
42. Sogancioglu M, Yel E, Ahmetli G,. Investigation of the Effect of Polystyrene (PS) Waste Washing Process and Pyrolysis Temperature on (PS) Pyrolysis Product Quality. *Energy Procedia*, 118 (2017) 189-194.
43. Audisio G, Bertini F,. Catalytic Degradation of Polymers: Part III Degradation of Polystyrene. *Polym Degrad Stab*, 29 (1990) 191-200.
44. Encinar JM, González JF,. Pyrolysis of synthetic polymers and plastic wastes. Kinetic study. *Fuel Process Technol*, 89 (2008) 678-686.
45. Williams PT, Slaney E,. Analysis of products from the pyrolysis and liquefaction of single plastics and waste plastic mixtures. *Resour Conserv Recycl*, 51 (2007) 754-769.
46. Williams PT, Williams EA,. Interaction of plastics in mixed-plastics pyrolysis. *Energy and Fuels*, 13 (1999) 188-196.
47. Zhang Z, Hirose T, Nishio S, et al.,. Chemical Recycling of Waste Polystyrene into Styrene over Solid Acids and Bases. *Ind Eng Chem Res*, 34 (1995) 4514-4519.
48. Lee SY, Yoon JH, Kim JR, Park DW,. Catalytic degradation of polystyrene over natural clinoptilolite zeolite. *Polym Degrad Stab*, 74 (2001) 297-305.
49. Deacon C, Wilkie CA,. Graft copolymerization of acrylic acid on to acrylonitrile-butadiene-styrene terpolymer and thermal analysis of the copolymers. *Eur Polym J*, 32 (1996) 451-455.
50. Du AK, Zhou Q, Van Kasteren JMN, Wang YZ,. Fuel oil from ABS using a tandem PEG-enhanced denitrogenation-pyrolysis method: Thermal degradation of denitrogenated ABS. *J Anal Appl Pyrolysis*, 92 (2011) 267-272.
51. Song P, Cao Z, Fu S, Fang Z, Wu Q, Ye J,. Thermal degradation and flame retardancy properties of ABS/lignin: Effects of lignin content and reactive compatibilization. *Thermochim Acta*, 518 (2011) 59-65.
52. Suzuki M, Wilkie CA,. The thermal degradation of ABS terpolymer as studied by TGA/IFR. *Polym Degrad Stab*, 47 (1995) 217-221.
53. Jung SH, Kim SJ, Kim JS,. Thermal degradation of acrylonitrile-butadiene-styrene (ABS) containing flame retardants using a fluidized bed reactor: The effects of Ca-based additives on halogen removal. *Fuel*

Process Technol, 96 (2012) 265-270.
54. Fatu D, Geambas G, Segal E,. On the thermal decomposition of the copolymer ABS and of nylon polyamide. *Thermochim Acta*, 149 (1989) 181-187.
55. Yang S, Rafael J, Barrera E V, Lozano K,. Thermal analysis of an acrylonitrile – butadiene – styrene / SWNT composite. *Polym Degrad Stab*, 83 (2004) 383-388.
56. Czégény Z, Jakab E, Blazsó M, Bhaskar T, Sakata Y,. Thermal decomposition of polymer mixtures of PVC, PET and ABS containing brominated flame retardant: Formation of chlorinated and brominated organic compounds. *J Anal Appl Pyrolysis*, 96 (2012) 69-77.
57. Bhaskar T, Murai K, Matsui T, et al.,. Studies on thermal degradation of acrylonitrile-butadiene-styrene copolymer (ABS-Br) containing brominated flame retardant. *J Anal Appl Pyrolysis*, 70 (2003) 369-381.
58. Jang J, Kim J, Bae JY,. Effects of Lewis acid-type transition metal chloride additives on the thermal degradation of ABS. *Polym Degrad Stab*, 88 (2005) 324-332.
59. Dewon D, Tasaka S, Aikawa S, Kamiya S, Inagaki N, Inoue Y,. Thermal degradation of ABS terpolymer in bean oil. *Polym Degrad Stab*, 73 (2001) 319-326.
60. Brebu M, Azhar Uddin M, Muto A, Sakata Y, Vasile C,. Composition of nitrogen-containing compounds in oil obtained from acrylonitrile-butadiene-styrène thermal degradation. *Energy and Fuels*, 14 (2000) 920-928.
61. Munteanu BS, Brebu M, Vasile C,. Thermal behaviour of binary and ternary copolymers containing acrylonitrile. *Polym Degrad Stab*, 98 (2013) 1889-1897.
62. Brebu M, Bhaskar T, Murai K, Muto A, Sakata Y, Uddin MA,. The individual and cumulative effect of brominated flame retardant and polyvinylchloride (PVC) on thermal degradation of acrylonitrile-butadiene- styrene (ABS) copolymer. *Chemosphere*, 56 (2004) 433-440.
63. Zhou Q, Yang JW, Du AK, Wang YZ, Van Kasteren JMN,. Fuel Oil from Acrylonitrile–Butadiene–Styrene Copolymers Using a Tandem PEG-Enhanced Denitrogenation–Pyrolysis Method. *AIChE J*, 55 (2009) 3294-3297.
64. Mitan NMM, Brebu M, Bhaskar T, Muto A, Sakata Y,. Individual and simultaneous degradation of brominated high impact polystyrene and brominated acrylonitrile-butadiene-styrene and removal of heteroelements (Br, N, and O) from degradation oil by multiphase catalytic systems. *J Mater Cycles Waste Manag*, 9 (2007) 56-61.
65. Rutkowski J V, Levin B,. Pyrolysis and Combustion Products and their Toxicity-A Review of the Literature. *Fire Mater*, 10 (1986) 93-105.
66. Bozi J, Czégény Z, Blazsó M,. Conversion of the volatile thermal decomposition products of polyamide-6,6 and ABS over Y zeolites. *Thermochim Acta*, 472 (2008) 84-94.
67. Muhammad C, Onwudili JA, Williams PT,. Catalytic pyrolysis of waste plastic from electrical and electronic equipment. *J Anal Appl Pyrolysis*, 113 (2015) 332-339.
68. PerkinElmer,. *Thermogravimetric Analysis (TGA)*.; 2010.
69. Abate L, Blanco I, Cicala G, Recca A, Restuccia CL,. Thermal and rheological behaviours of some random aromatic amino-ended polyethersulfone/polyetherethersulfone copolymers. *Polym Degrad Stab*, 91 (2006) 3230-3236.
70. Blanco I, Oliveri L, Cicala G, Recca A,. Effects of novel reactive toughening agent on thermal stability of epoxy resin. *J Therm Anal Calorim*, 108 (2012) 685-693.
71. TGA e DSC - Análise Térmica. http://www.analisestermicas.com.br/como-interpretar-curvas-de-tga-e-dsc/. Accessed February 15, 2019.
72. Siddiqui MN, Antonakou E V., Redhwi HH, Achilias DS,. Kinetic analysis of thermal and catalytic degradation of polymers found in waste electric and electronic equipment. *Thermochim Acta*, 675 (2019) 69-76.
73. Zeng W., Chow W., Yao B,. Chemical Kinetics and Mechanism of Polystyrene Thermal Decomposition. *Fire Saf Sci*, 7 (2007) 128–128.
74. Marcilla,A, Beltrán, M,. Kinetic study of the thermal decomposition of polystyrene and polyehylene-vinyl acetate graft copolymers by thermogravimetric analysis. *Quim Ing*, 3910 (1995) 117-124.
75. Majoni S, Chaparadza A,. Thermal degradation kinetic study of polystyrene/organophosphate composite. *Thermochim Acta*, 662 (2018) 8-15.
76. Jellinek HHG,. Thermal degradation of polystyrene and polyethylene. Part III. *J Polym Sci*, 4 (2003) 13-36.
77. Funt J., Magill J.,. Thermal Decomposition of Polystyrene: Effect of Molecular Weight. *J Polym Sci*, 12 (1974) 217-220.
78. Wu C, Chang C, Hor J, Shih S, Chen L,. On the thermal treatment of plastic mixtures of MSW: Pyrolysis Kinetics. *Waste Manag*, 13 (1993) 221-235.

79. Kumar D, Vinu R,. Journal of Analytical and Applied Pyrolysis Resource recovery via catalytic fast pyrolysis of polystyrene using zeolites. *J Anal Appl Pyrolysis*, 113 (2015) 349-359.
80. Chemical profile: US toluene - ICIS Explore. https://www.icis.com/explore/resources/news/2017/11/13/10044187/chemical-profile-us-toluene/. Accessed June 20, 2019.
81. Toluene - Chemical Economics Handbook (CEH) | IHS Markit. https://ihsmarkit.com/products/toluene-chemical-economics-handbook.html. Accessed June 20, 2019.
82. Styrene - Chemical Economics Handbook (CEH) | IHS Markit. https://ihsmarkit.com/products/styrene-chemical-economics-handbook.html. Accessed June 18, 2019.
83. Alpha Methyl Styrene Market: Global Industry Analysis and Forecast 2016 - 2026. https://www.persistencemarketresearch.com/market-research/alpha-methyl-styrene-market.asp. Accessed June 20, 2019.
84. Coats J., Redfern JP,. Thermogravimetric Analysis. *Analyst*, 88 (1963) 906-924.
85. Kumar S, Singh RK,. Pyrolysis kinetics of waste high-density polyethylene using thermogravimetric analysis. *Int J ChemTech Res*, 6 (2014) 131-137.
86. Sandler SR, Karo W, Bonesteel J-A, Pearce EM,. Thermogravimetric analysis. *Polym Synth Charact*, 1 (2007) 108-119.
87. Camino G, Costa L, Luda di Cortemiglia MP,. Overview of fire retardant mechanisms. *Polym Degrad Stab*, 33 (1991) 131-154.
88. R squared. http://www.wardsystems.com/manuals/neuroshell2/index.html?rsquared.htm.
89. Adjusted R squared. https://www.graphpad.com/guides/prism/8/curve-fitting/reg_adjusted-r-squared.htm. Accessed May 3, 2019.
90. Adjusted R2 / Adjusted R-Squared. https://www.statisticshowto.datasciencecentral.com/adjusted-r2/. Accessed May 3, 2019.
91. Pottel H,. Bootstrapping , permutation tests and simulation in Excel Resampling methods. (2015).
92. Efron B,. *An Introduction to the Bootstrap*.; 1993. http://www.hms.harvard.edu/bss/neuro/bornlab/nb204/statistics/bootstrap.pdf. Accessed April 8, 2019.
93. Westerhout RWJ, Waanders J, Kuipers JAM, Van Swaaij WPM,. Kinetics of the low-temperature pyrolysis of polyethene, polypropene, and polystyrene modeling, experimental determination, and comparison with literature models and data. *Ind Eng Chem Res*, 36 (1997) 1955-1964.
94. Kruse TM, Woo OS, Wong HW, Khan SS, Broadbelt LJ,. Mechanistic modeling of polymer degradation: A comprehensive study of polystyrene. *Macromolecules*, 35 (2002) 7830-7844.
95. Kruse TM, Sang Woo O, Broadbelt LJ,. Detailed mechanistic modeling of polymer degradation: Application to polystyrene. *Chem Eng Sci*, 56 (2001) 971-979.
96. Buekens AG, Huang H,. Catalytic plastics cracking for recovery of gasoline-range hydrocarbons from municipal plastic wastes. *Resour Conserv Recycl*, 23 (1998) 163-181.
97. Pütün E,. Catalytic pyrolysis of biomass : Effects of pyrolysis temperature , sweeping gas fl ow rate and MgO catalyst. *Energy*, 35 (2010) 2761-2766.

Annexes

I - Gas chromatography

Table I. 1 – Gas chromatography.

	Gas chromatography Shimadzu	Gas chromatography Perkin-Elmer
Column	PLOT (KCl/Al2Cl3)	BPI
Column Length	50m x 320 µm	30m x 250 µm
Carrier Gas	N_2	N_2
Flow rate/Pressure	2 bar	0.5 mL/min
Split	120 mL/min	50 mL/min
Injection Temp.	250 ºC	250 ºC
Detector Temp.	250 ºC	250 ºC
Injection Volume of Sample	200 µL	0.1 µL

II- Calibration of Gas Chromatography

Shimadzu GC-9A

Table I. 2 – Pattern samples – Shimadzu GC-9A.

Pattern Samples	Chemical Formula	Retention Time (min)
n-Pentane	C_5H_{12}	3.058
1-Pentene	C_5H_{10}	4.342
n-Hexane	C_6H_{14}	5.777
1-Hexene	C_6H_{12}	6.312
n-Heptane	C_7H_{16}	8.283
1-Heptene	C_7H_{14}	8.807

Perkin Elmer – Clarus 680

Table I. 3 - Pattern samples - Perkin Elmer -Clarus 680.

Pattern Samples	Chemical Formula	Retention Time (min)
1-Pentene	C_5H_{10}	2.300
n-Pentane	C_5H_{12}	2.352
1-Hexene	C_6H_{12}	2.773
n-Hexane	C_6H_{14}	2.859
1-Heptene	C_7H_{14}	3.661
n-Heptane	C_7H_{16}	3.809
Toluene	C_7H_8	4.695
n-Octane	C_8H_{18}	5.332
1-Nonene	C_9H_{18}	6.751
1-Decene	$C_{10}H_{20}$	8.461
n-Decane	$C_{10}H_{22}$	8.569

III – Example of a chromatogram

Liquid of waste polystyrene at a set point of 450 ºC

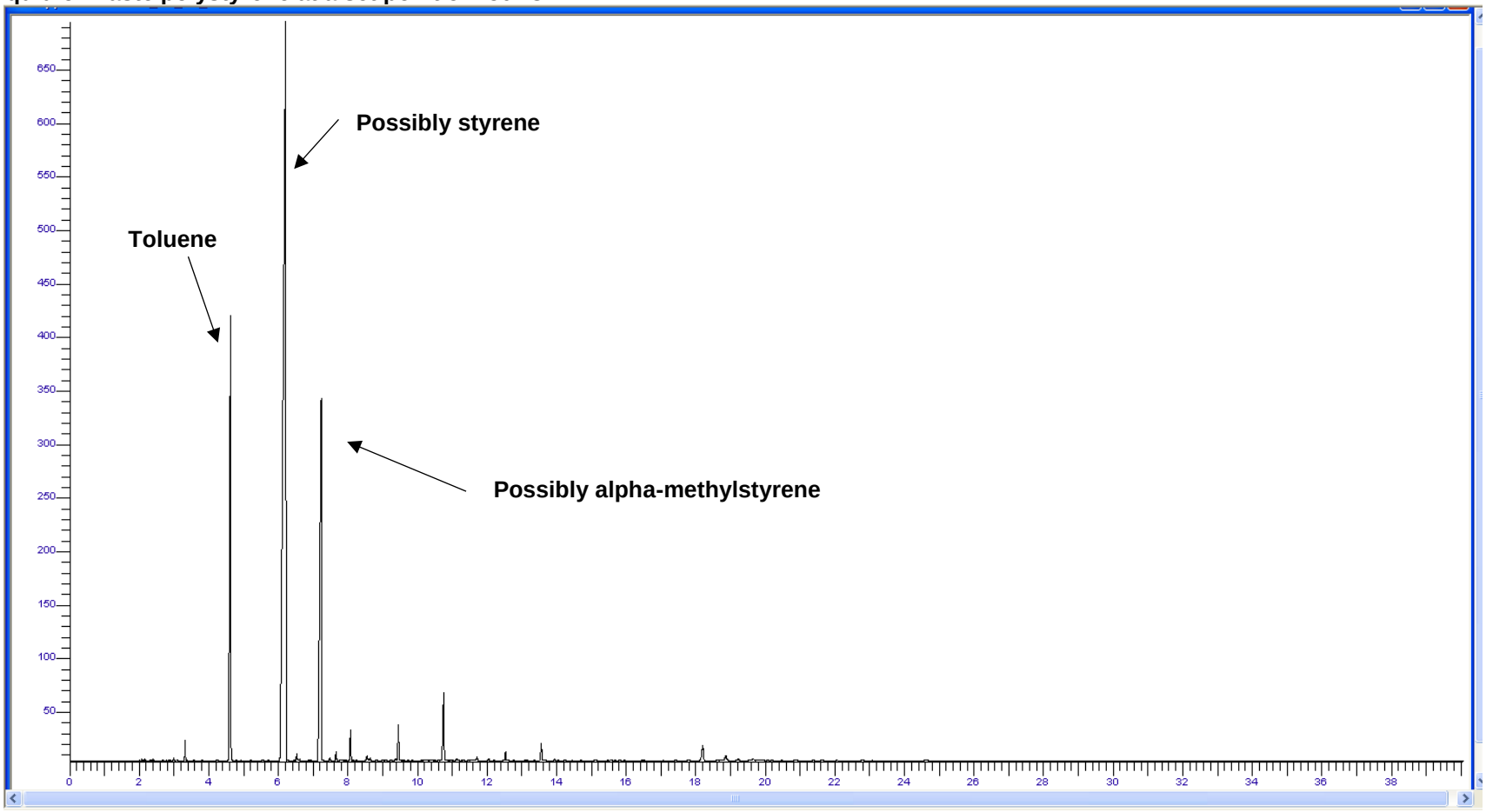

Figure I 1 - Example of a chromatogram. Legend: y-axis: Height (mV) and x-axis: Time (min).

IV – Kinetic model - dynamic conditions

IV.1 Waste Polystyrene

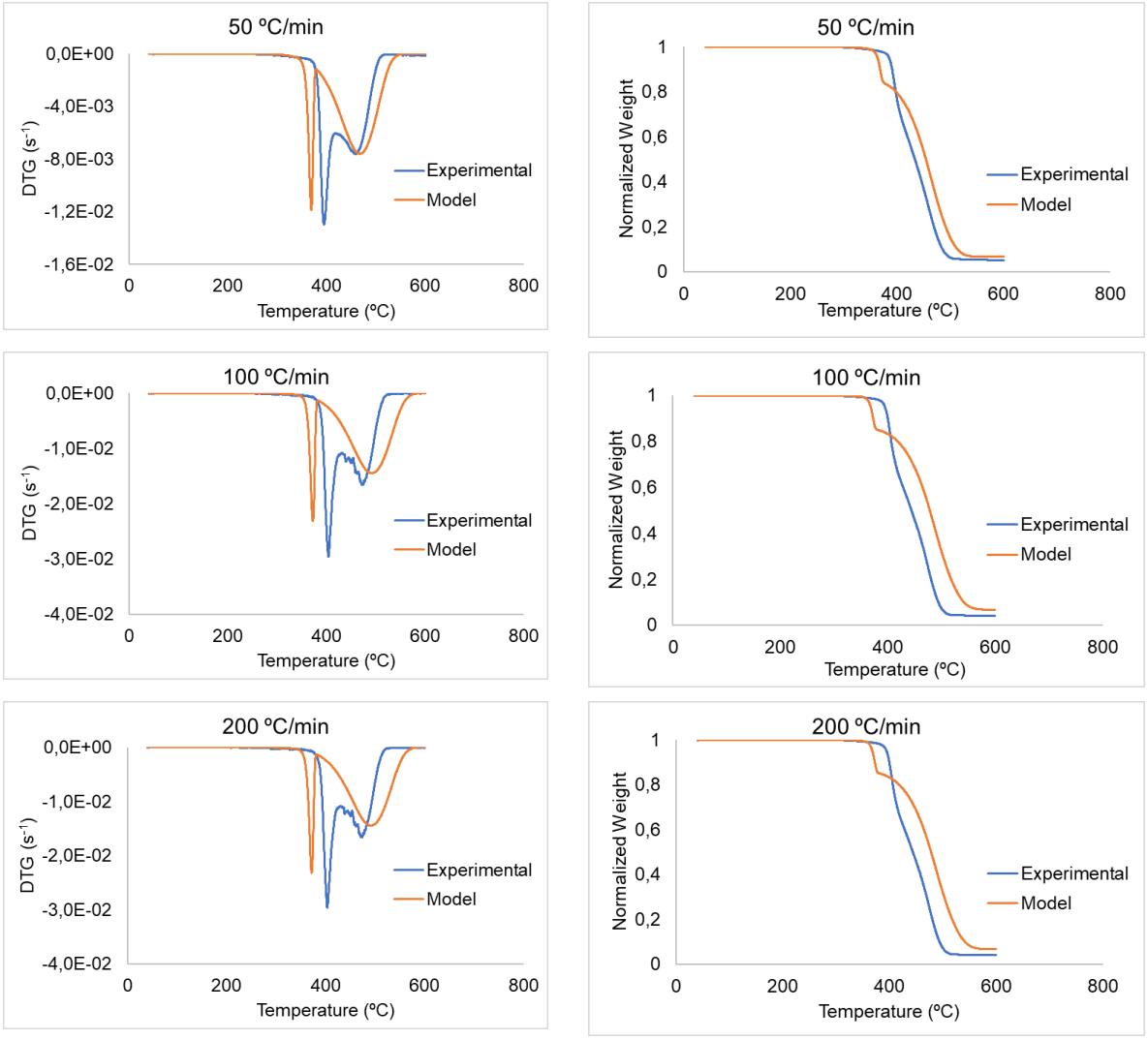

Figure I 2 - Fitting of model 2 for waste PS to higher heating rates (50,100 and 200 ºC/min).

IV.2 Waste ABS

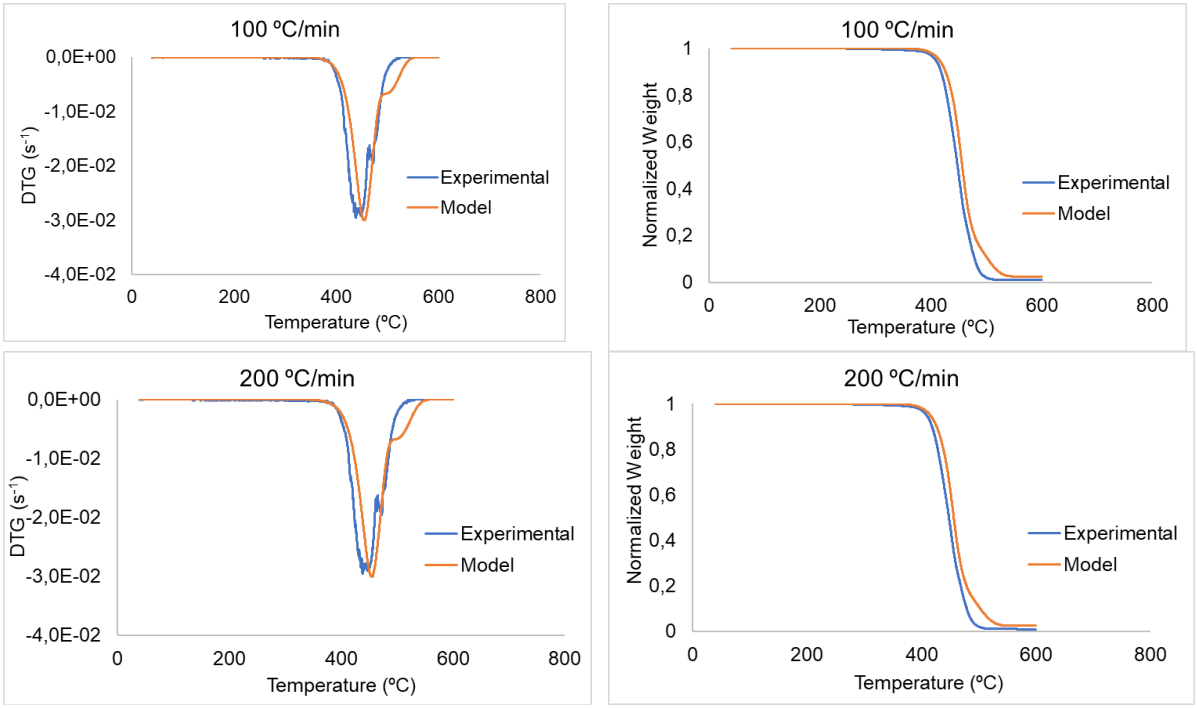

Figure I 3 - Fitting of model 2 for waste ABS for higher heating rates (100 and 200 ºC/min).